GENERALIZED PREDICTIVE CONTROL OF DC-DC BUCK CONVERTER

Kamakshi Manjari

GENERALIZED PREDICTIVE CONTROL OF DC-DC BUCK CONVERTER

A
Thesis Submitted
in Partial Fulfillment of the Requirements
for the Degree of

DOCTOR OF PHILOSOPHY

by

KAMAKSHI MANJARI

Department of Electronics and Electrical Engineering
Indian Institute of Technology Guwahati
Guwahati-781039, Assam, INDIA
January, 2020

Certificate

This is to certify that the thesis entitled "**Generalized Predictive Control of DC-DC Buck Converter**", submitted by **Kamakshi Manjari** (146102017), a research scholar in the *Department of Electronics and Electrical Engineering, Indian Institute of Technology Guwahati*, for the award of the degree of **Doctor of Philosophy**, is a record of an original research work carried out by her under my supervision and guidance. The thesis has fulfilled all requirements as per the regulations of the institute and in my opinion has reached the standard needed for submission. The results embodied in this thesis have not been submitted to any other University or Institute for the award of any degree or diploma.

Prof. Somanath Majhi
Dept. of Electronics and Electrical Engg.,
Indian Institute of Technology Guwahati,
Guwahati - 781039, Assam, India.

Date:

Place: Guwahati.

To my family ...

Acknowledgment

I take this opportunity to offer my heartfelt thanks and genuine gratitude to my thesis supervisor, Dr. Somanath Majhi. Words are inadequate to express my appreciation and gratitude to Dr. Majhi for his immense patience and guidance in correcting this thesis.

I am thankful to my doctoral committee chairperson Dr. Indrani Kar for all the useful suggestions to improve this thesis. I also thank my doctoral committee members Dr. S. K. Nayak and Dr. K. Srinivasan, for devoting their precious time in evaluating my work and providing useful inputs on my work.

I am also very thankful to my friends in the Control and Instrumentation Laboratory in the Indian Institute of Technology Guwahati, for providing me with a lively student life throughout my academic work in the research laboratory. I can not think of my research journey without the love and support of Gargi Ba, Gautam, Gayatri, Jitendra, Mriganka, Nama, Niladri, Protima, Ramyani, Sreeram, Suman Da, Sumi, Tarique, Trusna, Uddipana, and Vivek. I am forever indebted to my senior Dr. Kasi V. Ramana, for his support in my research work.

Last but definitely not the least, I would like to thank my family and parents for giving me the moral support and encouragement to complete my thesis. This would not have been possible without my parents' love and sacrifice. My twin sister Dr. Lepakshi has been my constant support and motivation throughout this journey. My sincere thanks go to my beloved husband Manish for his patience and belief in my worthiness.

(*Kamakshi Manjari*)

Abstract

Predictive control has gained much popularity since its introduction in the 1960s. Till now, it is a widely researched topic in the control research community as well as in industrial application. There are a number of predictive control laws available which work on the same principle but with a different name and with minor modifications, such as dynamic matrix control (DMC), receding horizon control (RHC), model predictive control (MPC), and generalized predictive control (GPC) to name just a few. The popularity of these controllers is mainly due to its easy handling of constraints, multi-input multi-output (MIMO) system and control of non-linear plants which are usually properties of an actual industrial plant. In this thesis, a class of predictive controller, i.e. GPC, is considered. Despite several successful implementations of GPC in industry, there is a lack of theoretical result for robustness and stability analysis of GPC as well as properties of GPC are also not well defined. In this thesis, modeling, design and tuning of GPC are presented for the DC-DC buck converter. As implementation of the advanced controller is usually limited to process control industry and robotics, it is rarely implemented in power electronics devices. GPC has been designed and validated in simulation and hardware for a single output DC-DC buck converter. Control of a DC-DC Buck converter using GPC is achieved by approximating plant model to a stable first-order plus dead time (FOPDT) model. The controller design procedure is then verified by implementing voltage mode control (VMC) of DC-DC Buck converter in case of inactive constraints. The implemented algorithm is then verified using numerical simulation in MATLAB as well as hardware implementation of the pre-computed control algorithm. A modified GPC has improved the tracking error

during load and input variation by an outer loop PI control. To tune the FOPDT model of the converter, a tuning formula has been derived explicitly for FOPDT plant model. Performance of observer-based GPC has been verified in numerical simulation result for dual output DC-DC buck converter.

Contents

List of Figures

List of Tables

List of Abbreviations

CARIMA	Controlled auto-regressive integrated moving average
CCM	Continuous conduction mode
DMC	Dynamic matrix control
ePWM	Enhanced pulse width modulation
FIR	Finite impulse response
FOPDT	First-order plus dead time
GPC	Generalized predictive control
LTI	Linear time invariant
MPC	Model predictive control
MIMO	Multi-input multi-output
PID	Proportional-integral-derivative
RHC	Receding horizon control
QP	Quadratic programming
SISO	Single input single output
SOPDT	Second-order plus dead time
SIDO	Single-inductor dual-output
SIMO	Single-inductor multi-output
VMC	Voltage mode control

List of Symbols

$w(k)$	Reference trajectory
$\zeta(k)$	Zero mean Gaussian white noise
$y(k)$	Output of plant model
$u(k)$	Control input of plant model
Δ	Difference operator
$\|\|(.)\|\|$	Norm of a vector
N	Prediction horizon
M	Control horizon
$\mathbf{Q}$	Error weight matrix
$\mathbf{R}$	Control weight matrix
L_o	Observer gain matrix

CHAPTER 1

INTRODUCTION

As technology is advancing at a faster pace, the need for an efficient machine is also increasing day by day. Product quality and production rate are mainly dependent on the implemented control techniques. This increase in demand for a better functioning of the product has increased focus in designing of better control strategy, which results in improved plant performance. Generalized predictive control (GPC) is one of the particular class of model predictive control (MPC), which is very popular in industrial application [1–4]. Over the past decade, predictive controller has gained wide recognition as one of the most significant control algorithms. GPC algorithm uses an input-output model of the plant to predict future output response. GPC is not designed for a specific kind of plant; instead, it is defined for a wide range of processes in which internal model of the plant is explicitly used to obtain the most suitable predicted plant output. Introduction of minimum time optimization in linear programming by Zadeh and Whalen [5] in the 1960s and moving horizon concept by Propoi [6] in optimal control are considered as the foundation of predictive control algorithm. Any model-based predictive controller works on the principle of receding horizon control (RHC) principle. In RHC, the manipulated control sequence is evaluated at each instant of sampled

time. As mentioned, MPC has been implemented for a wide variety of applications [7–12] such as chemical and process control industry, oil refining industry, robotics, aerospace, automotive, and power electronics drives system [13, 14] applications to name a few, because of its effectiveness and robustness.

Many improvements and modifications were adopted for the core idea of MPC, and several versions of MPC were introduced. This evolution of the predictive controller led to the emergence of the GPC strategy in the late 1980s, which consolidate all significant features of the predictive controllers in a unified structure. Although usage of the predictive controller has increased rapidly, still proportional-integral-derivative (PID) controllers are preferred in many processes instead of any other advanced controller. In the PID controller, the gain parameters are tuned by comparing the set-point with the output feedback signal instead of using optimizing a cost function. This comparison with the set-point continues until the closed-loop plant model tracks the desired reference trajectory. Whereas in predictive control, a finite time cost function is optimized at each sampled instant which increases mathematical complexity. Another major criticism of the predictive control algorithm is the absence of a general-purpose closed-loop stability theory based on tuning parameters of the controllers. MPC stability analysis has been guaranteed for cost function having terminal constraint and adding constraints to cost function for some cases [15, 16]. In MPC, the optimization problem is formulated by specifying a cost function along with input and output constraints if needed. But in a conventional controller, gains are set manually to incorporate limitations or constraints of a system. To simplify the optimization burden usually convex cost function and convex constraints are considered. This optimization problem is known as a convex optimization problem [17]. Mostly a linear dynamics of a plant can accurately represent a plant model in most of the cases, and it can be easily extended for non-linear dynamics; hence a linear structure of the plant model is

preferred. But in many cases, a plant model is expressed by non-linear dynamics. Nonlinear MPC (NMPC) has also been proposed [18, 19] for non-linear models and constraints for which an online solver is required to solve the optimization problem. Solvers have been developed to tackle the online optimization problem as it is a hectic task to obtain a fast and optimized control input in real-time control of a plant.

1.1 DC-DC buck converter

Electrical energy is the main reason behind many incredible inventions of modern devices like television, computers, robots and several other useful pieces of equipment. Use of electricity has revolutionized transportation and medical facility as well. The electrical signal can be categorized into two forms, namely alternating current (AC) and direct current (DC). Most of the electrical appliances, power generation, transmission and distribution are usually operated in AC power. Still, the use of DC power and DC appliances have never been obsolete; instead, it plays a significant role in the current generation. DC is gaining popularity as use of photo voltaic (PV) cells, battery-operated vehicle, portable devices or any device which operates by battery supply; all run on DC power. Transferring AC voltage levels to higher voltages is preferred as it reduces transmission loss. Since DC power is more stable compared to AC, research is going on to find different ways to equip high voltage direct current (HVDC) in power transmission with higher efficiency.

As DC-DC power conversion plays an essential role in a considerable number of electrical equipment, new techniques are developed for efficient conversion of DC voltage level. Before the development of power semiconductors, DC voltage conversion was a highly inefficient and expensive procedure to be carried out. Either DC was converted to AC or linear regulators were used to regulate voltage

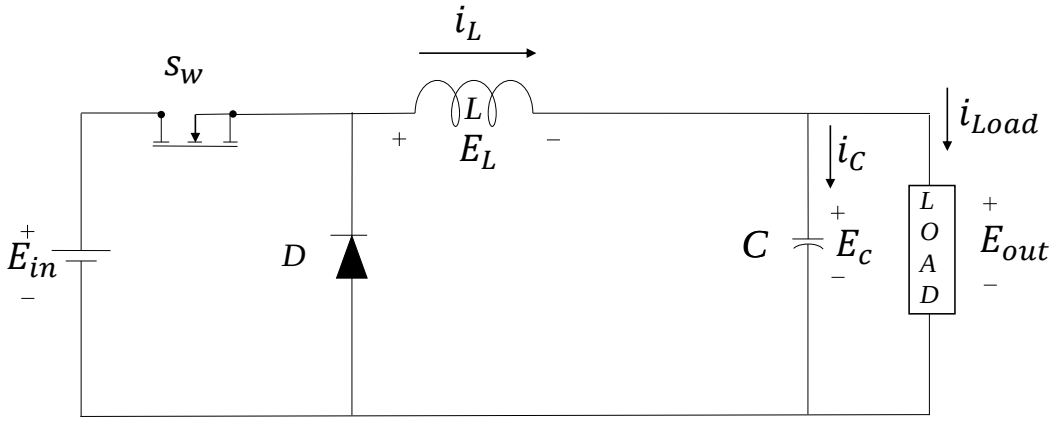

Figure 1.1: An ideal DC-DC Buck converter circuit diagram with an unspecified type of load

levels of DC power. Linear regulators use the principle of voltage divider circuit, in which a variable resistor is connected in series with a constant load resistance to obtain the desired output voltage level. It generates a pure DC signal, but because of the use of a passive device to regulate the voltage level, the efficiency was very poor. Development of robust semiconductor devices during the late 1980s was the period when switched-mode power supply (SMPS) started to replace linear voltage regulators. The DC-DC converter is a type of SMPS in which, primarily input DC power supply voltage is converted to different output DC voltage levels. In SMPS, the switching cycle of an active device is controlled, to control the output voltage level. By the use of active devices, the efficiency of SMPS improved significantly and soon after SMPS replaced voltage regulators. Although efficiency increases in SMPS the voltage obtained at the output is not a pure DC signal; instead, it is a pulsating output. Hence LC filter circuit is used along with a load. Using these circuit elements of SMPS, different topologies of DC-DC converter are modeled according to the user's requirement. The three basic topologies are buck, boost

and buck-boost. A basic circuit diagram of a DC-DC buck converter is shown in Figure 1.1. From the circuit diagram of the buck converter, it can be observed that the output voltage waveform is varied according to the type of load. A load can be resistive, capacitive or inductive load according to the requirement. Details of this circuit with resistive load is explained in Chapter 4, in which GPC is designed for a DC-DC buck converter having a constant resistive load.

A converter is usually operated along with a controller in a closed-loop mechanism to obtain a stable desired regulated output voltage. The controller tracks the set-point or minimizes the voltage regulation during load change or parameter uncertainties for a converter operation. The constrained control algorithm can also regulate factors like the reduction of ripple in capacitor voltage or ripple in inductor current effectively. In many cases, the input supply is fluctuating in nature, but the desired output is a steady constant voltage. This fluctuation in input supply results in a fluctuating output voltage which needs to be regulated by a controller. Modeling error and uncertainties in the parameter is another challenge while operating a converter. Usually, a higher switching frequency is preferred for a circuit having inductor in operation as it determines the size of the inductor. Increase in switching frequency also helps in minimizing the ripple in converter signals. As more and more digitalization is adopted for every field of science, controllers are also implemented in interface with computer installation. But, controller implementation in the digital platform restricts the switching frequency as compared to analog interfacing. Digitally implemented controllers are easy to operate as the tuning parameters need not be changed manually unlike analog controller. The limitation in switching frequency is not an issue nowadays as very high-speed operating controllers are available. While digital controllers result in improved performance of the closed-loop system but it is costlier as compared to analog controller.

1.2 Research motivation

Performance of a closed-loop system output depends on the plant model and characteristics of the implemented control algorithm in the feedback or feed-forward path. All the derived controller algorithm in the literature can be classified into four different levels. The first level of the controller deals with some ancillary systems, in which a PID controller could be an excellent choice. The second level controllers are for the issues occurring in a multi-variable dynamic process, which is interfered by some unmeasured perturbations or saturation. The third level controllers are for the optimization problems based on minimization of cost functions; GPC is also at this level. The fourth level controllers consist of those time and space scheduling production problems that include a feasible solution for an optimization-based problem formulation and have the best performance benefits of the closed-loop dynamics. Because of the simple structure, low cost, easy and convenient manipulation of the tuning parameters and simple understanding of the control, PID has become one of the significant controller used in the family of level one. Even though advance control algorithms have been proposed but still PID is most reliable by most control engineering practitioners only because of its simple tuning algorithm. However, the economic benefits induced by tier one and two are usually negligible. In contrast, the optimization concept in level three controller such as GPC can bring many improvements in the performance of the system. It can efficiently deal with the multi-variable case and also can be used to control processes with constraints and delays. While it has been argued that the PID controller can also be used for a multi-output system by using multiple PID controllers [20], but it is a difficult task to synchronize all the controllers. Instead, it increases the overall system complexity as the number of tuning parameters also increase. To incorporate constraints for a plant signal, a PID is modified by using

saturation for the signal to be limited [21]. But achieving the desired plant performance using these methods for PID controller makes the designing and tuning procedure equally complicated as any advanced controller.

The predictive control algorithm has a long history of its gradual evolution since the introduction of optimal and adaptive control theory. Linear quadratic Gaussian (LQG) controller [22] and linear quadratic regulator (LQR) [23] are the foundation for developing a predictive controller. Early LQG controller was very rarely used in the process control industry due to its limitation in handling constraints, disturbance, non-linearities and calculation burden. Newly developed predictive controllers during late 1980s, such as dynamic matrix control (DMC) [24], model predictive heuristic control (MPHC) [25] and model algorithmic control (MAC) [26] solved few shortcomings of LQG. Later on, these became trade names for commercially available software programs for different companies, but collectively these controllers are called model-based predictive control or predictive control in general. Richalet et al. [25] did one of the significant development in predictive control by proposing MPHC. GPC was introduced in [27, 28], which is considered to be a gradual development from the generalized minimum-variance (GMV) control [29] algorithm. GPC was developed to offer an alternate solution for self-tuning regulators for transfer function plant model and improved robustness feature. Traditional GPC is a class of MPC in which transfer function model of the process is used to predict the future output. In general, the term GPC or MPC are used interchangeably in the literature. Even though GPC is an excellent choice for the process control industry, it went largely unnoticed due to its similarity with stochastic control theory which also uses the transfer function of the model. Although advance control strategy yields better performance compared to a PID controller, still its application is limited to theoretical research rather than an actual real-time implementation for a plant.

In recent years, the use of advanced control for power electronics drives system has increased a lot because of its efficiency, robustness for load and input variation, and strategy for easy constraint handling. Nowadays, power converters are used in every field of technology. Converters are used in micro-grid, portable devices, HVDC transmission, storage devices and several other application in the electronics industry. Importance of power converter makes the design of an advanced controller for electric drives an exciting research area. Usually, for a converter circuit, the controller is designed by specifying frequency-domain specifications such as gain margin (GM) and phase margin (PM) [30]. But due to complex mathematics involved in GPC for computing the control input, frequency domain parameter specifications are seldom used in GPC to regulate the power electronics and drives circuit.

Figure 1.2 shows a block diagram representation of a general predictive controller for a predefined reference tracking problem. It shows the basic structure of predictive control, in which input to the plant and model is an optimized control sequence obtained by optimization. The optimization procedure continues till the tracking error is minimized. To formulate the optimization problem, the prediction of output signal is necessary for a predictive control. These advanced controllers helped in achieving desired user specifications but due to design complexity tuning of these controllers is very complicated. The designer has to tune a number of horizons and weights of the chosen cost function. An efficient tuning method is required to achieve the best performance of any controller. Tuning techniques of GPC is classified into two types [31], either it can be formula-based [32, 33], or it can be range on the tuning parameters [34, 35] based on plant dynamics. Tuning of GPC starts with the model of the plant. GPC has more number of tuning parameters as compared to PID, which include prediction horizon, control horizon and cost function weights. Tuning of these parameters determines the closed-

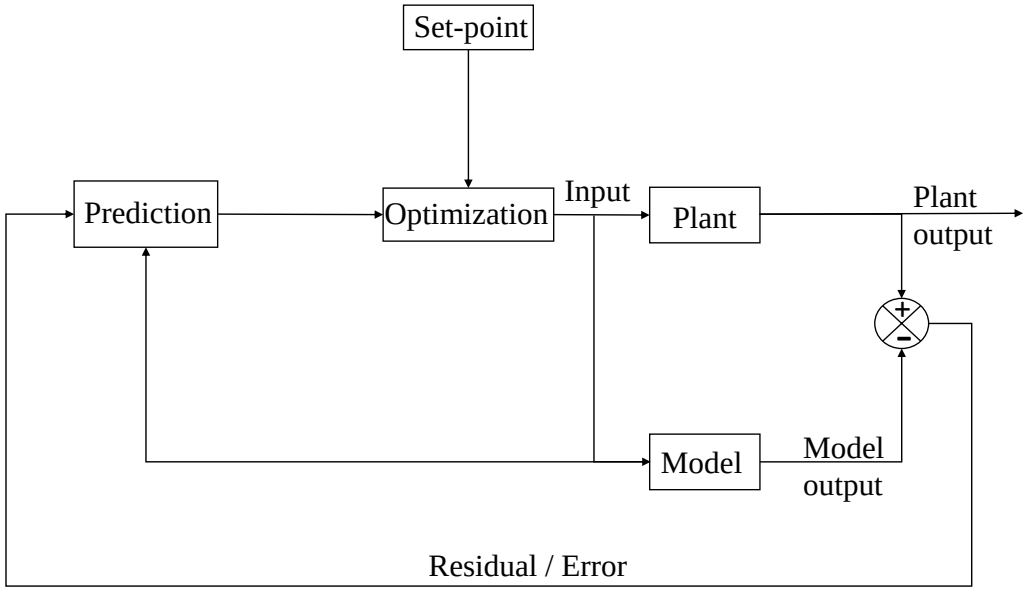

Figure 1.2: Closed-loop block diagram of a predictive controller for reference tracking problem

loop stability of the whole system. Tuning of prediction and control horizons are straight forward and available in the literature. However, tuning of weights is not direct as there exists a very complicated relationship between system parameters and weights of the cost function, which require experience and based mainly on extensive simulation. Tuning of an optimal control cost function weights has always been a heuristic approach. Hence, different tuning methods have also been proposed to achieve a direct tuning of weights in the predictive controller instead heuristic approach. In [36], tuning of MPC weight matrices is achieved by using reverse optimization in which MPC is matched with an already available desired linear time-invariant (LTI) controller. The matching problem is formulated as a convex optimization problem in which exact matching is guaranteed for a com-

pletely observable system. Authors in [37] discussed the condition where all the states of the system are not available, and the loop shaping technique is used to overcome the drawbacks of the earlier proposed controller matching technique of MPC tuning. In [38], the authors have achieved an exact matching of GPC with LTI controller, which needs to satisfy a specific rank condition. The optimization problem for tuning of weighting matrix is complicated for active constraints. Although tuning of MPC or GPC in a closed-loop is well explained in [39, 40] still tuning of predictive control for some given specification with robustness is still a very challenging research topic. However, the fact that GPC is an input-output model-based controller and minimizes a finite time receding horizon cost function has been an obstacle in searching the stability properties of GPC. There were several attempts [41–47] to prove the stability properties of GPC. But due to its finite time optimization based control law, the closed-loop stability is not guaranteed. To ensure stability for finite-time optimal control, usually, a constraint is added for the final state. This addition of terminal constraint might guarantee the controller stability, but it limits the usability of the controller along with added complexity.

Motivated by these challenges in the GPC design procedure to control a DC-DC buck converter, research in this thesis have been carried out to analyze the design and tuning procedure of GPC for the buck converter. This strategy can be extended to other converter topologies as well with necessary modification in the plant model. This thesis mainly deals with modeling and tuning of GPC for single input single output (SISO) and multi-input multi-output (MIMO) system of the linear plant model. Formulation and designing of GPC are analyzed, and performance is explained for a better understanding of the controller. An analytical expression is derived for first-order plus dead time (FOPDT) system. Derivation of GPC along with stability analysis of the derived control law is also presented.

1.3 Contributions of the thesis

In this thesis, modeling and tuning algorithm of GPC for SISO and MIMO system is presented in a detailed way. The derived algorithm has resulted in an easy tuning strategy for GPC cost function weight matrix. A GPC tuning algorithm for first-order plus dead time (FOPDT) plant model has been proposed in this thesis. In this proposed tuning rule, a direct relationship between the weight matrix of the cost function and plant parameters has been proposed. The tuning is based on the pole placement method, given that the plant dynamics are represented in a stable FOPDT form. This analytical tuning strategy is based on weight tuning of a cost function, assuming a constant control horizon to reduce the computational burden of the high value of the control horizon. In earlier research work of GPC, it was mainly limited to the SISO system. A transfer function model of the plant is used to obtain the output prediction model, which limits its applicability to the MIMO system. In this thesis design of GPC is explored for a dual output plant model. GPC designing and tuning guideline for a specific case MIMO system is explored in this thesis. Another main contribution of this thesis is the experimental analysis of GPC for DC-DC buck converter. A detailed hardware implementation using DSP micro-controller for SISO buck converter is presented in this thesis. The converter is represented in an FOPDT transfer function, and the tuning method proposed in this thesis is implemented to check the stability and robustness of the proposed tuning algorithm. A modified GPC has been proposed to have an error free reference tracking during disturbance in either load or input side.

Single inductor multi-output (SIMO) converter is very popular in low power devices. The behavior of GPC for a specific two outputs DC-DC buck converter is presented in a detailed manner. A detailed derivation of the plant dynamics of the dual output buck converter is presented in this thesis. The plant model has

been formed in the form of a two input two output (TITO) system using the time-averaging method to design GPC for a single inductor dual output (SIDO) DC-DC buck converter. A Lyapunov based stability analysis of the cost function is also presented in this thesis. In this analysis, uniqueness of the optimization problem is not guaranteed; only stability of the control law is proved. The cost function is assumed to be a Lyapunov function, and then a detailed stability analysis is provided for finite time optimization. Effect of prediction horizon on stability is presented to understand the role of the horizon for stable closed-loop control. To control the unobservable plant model variables, an observer has been designed for GPC. Convergence of the observer has also been presented.

1.4 Thesis organization

The thesis is organized as follows.

- **Chapter 2:** In this chapter, GPC problem formulation has been explained in a detailed manner. Formulation of the predicted output model from plant model is explained in this chapter along with the effect of variation of tuning parameters on the performance of the closed-loop plant dynamics. GPC is modeled in transfer function form to study the closed-loop sensitivity for the effect of disturbance and noise on control input and output. Effect of filter polynomial is presented in simulation results.

- **Chapter 3:** In this chapter, a generalized tuning rule for first-order plus dead time system (FOPDT) is derived in terms of plant model parameters. As most of the industrial plants can be approximated to an FOPDT model, GPC weight tuning procedure is provided for this model. In this method, the weights of the chosen cost function are obtained from the derived analytical expressions. Simulation results are provided to show the efficacy of the

controller.

- **Chapter 4:** The obtained tuning algorithm is implemented by designing a hardware lab set up of a SISO DC-DC buck converter in Chapter 4. To implement the obtained tuning rule for GPC, a micro-controller is used to generate the switching pulse. Instead of an online optimization-based controller, pre-computed GPC control law is preferred for the linear plant model. The converter is controlled in voltage control mode. Both simulation and hardware experimental results are provided to show the effect of pre-computed GPC on load and input variation.

- **Chapter 5:** In this chapter, the design of GPC is presented for a MIMO system. Specifically, GPC is designed for a dual output buck converter system. The chosen plant is a SIDO DC-DC buck converter, which is a low power device. The main challenge in controlling this plant is, outputs are dependent on each other, which makes the system a coupled device. Stability analysis of GPC control law and the designed observer has been presented using the Lyapunov function method. MATLAB numerical simulation results are provided to present output responses of the closed-loop system.

- **Chapter 6:** In this chapter, conclusion of the research work is presented along with suggested improvements and the future scope of this work.

CHAPTER 2

PRELIMINARY

2.1 Introduction

The success of predictive control is because of its easy understanding of the working principle and the ability to handle multi-variable systems with input and output constraints effectively. It is more of an idea, instead of a distinct controller. As this is a model-based predictive controller, the system model is expressly employed in this class of the controller to predict the output response so that the receding horizon technique generates the specified input sequence for the plant. There are different versions of the initial proposed predictive control algorithm accessible within the literature, with all having its own limitations. An extensive review of the recent developments and achievements of the predictive controller is obtainable within the survey paper by Mayne [48]. Among current areas of interest in the control theory domain, the embedded predictive controller is considered as one of the most impressive promises of the future, due to the interest in several areas of engineering. The critical limitation for the embedded controller is to control those plant dynamics with a fast plant response when operating on controller processors with lower computational power. This formulation is widely used because it leads

to a quadratic programming (QP) problem, for which several memory and computationally efficient solvers exist. Formulations based on linear parameter varying systems are chosen as well, but due to the need to build the QP problem at each iteration, this type of controllers are more challenging to be used in embedded control.

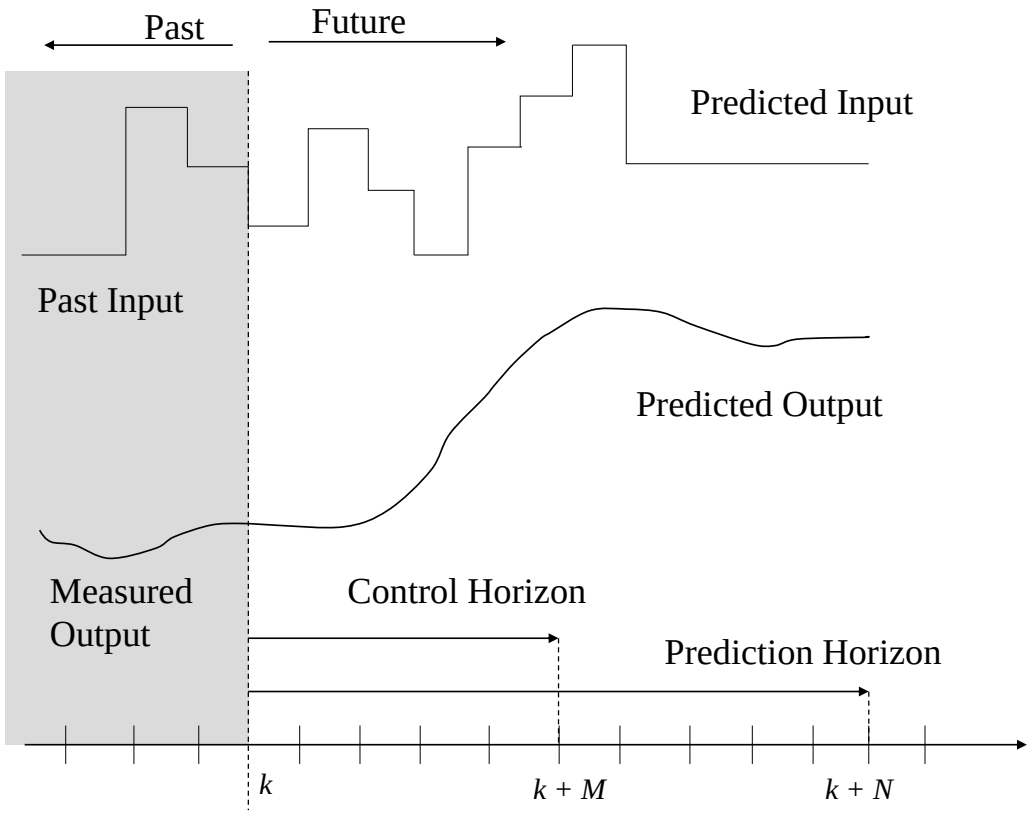

Figure 2.1: Pictorial representation of moving horizon principle in GPC

Clarke et al. [27,28] proposed GPC in 1987, and since then, it has become one of the popular model-based predictive control algorithms. The fundamental element of GPC consists of an optimizer which minimizes a defined cost function over a

predefined prediction horizon to obtain a series of future optimized control input. The defined cost function is a weighted sum of squares of the predicted tracking error and control effort. GPC can be designed for a wide range of processes including unstable and non-minimum phase plants, given the plant model is known to the designer. It shows desirable performance and acceptable robustness for unknown delays or poorly identified models. Basically, all the predictive controllers are based on the same concept of optimization of predicted error that is why GPC is similar with the other available predictive controllers, but it is different in terms of the model used for prediction. It is a class of control strategy, in which the auto-regressive model of internal plant model is used to predict the plant output. Figure 2.1 shows the principle of receding horizon incorporated in a GPC at sampling instant k. The predicted input sequence is computed by optimizing a chosen cost function of the control performances, such as the tracking error, change in control effort and the control variable. The performance index or cost function is optimized subject to the feasibility of the constraint imposed by the requirement of the system, i.e. the LTI model, and constraints on states, inputs and outputs. Conventionally, through the use of the Diophantine equation, an N-step ahead predictor model has been extracted using the polynomial method in GPC. In the literature, an analogous version of the predictor in a state-space model is also available. However, it was not clearly mentioned why these equations are used.

In this chapter, components of GPC are explained in a detailed manner. A brief introduction to various plant models implemented in predictive control is given. The basic methodology for the GPC design is presented in a comprehensive way. In the simulation study, details are presented about the GPC tuning parameters and the impact of tuning parameter variance. The optimized control law is modeled in a closed-loop transfer function type, and GPC sensitivity for noise and disturbance

is also analyzed. Simulation findings are also presented to show the effect of GPC with and without a filter polynomial in the plant model.

2.2 Elements of GPC

A predictive control strategy usually consists of similar elements, so different forms of the model can be selected, which results in different control algorithms. Three main elements of the GPC are

1. Model of the plant
2. Cost function or performance index
3. Optimized control law

2.2.1 Plant model

A model is chosen, which gives a relatively accurate output as the original plant to obtain output prediction. For a model-based control, if the manipulated variable is not yielding the desired plant response then it is assumed that the model chosen is having a large plant mismatch or the optimal control problem is an ill-posed one. While selecting a model for the plant, it should be kept in mind to chose a relatively easy representation of the model which relates the plant inputs and outputs in a simple mathematical expression. The commonly used models are as follows.

1. *Finite impulse response (FIR) model:* An FIR model can be represented by an impulse response and step response of the model. Impulse response models are used in MPHC [49], EPSAC [50] and DMC [24]. An impulse response of output in terms of input u_k and disturbance d_k is represented as

in (2.1).

$$y_k = \sum_{i=0}^{\infty} G_i z^{-i} u_k + d_k \tag{2.1}$$

Similarly, a step response model is also defined for stable systems which is represented as in (2.2)

$$y_k = \sum_{i=0}^{N} G_i z^{-i} \Delta u_k + d_k \tag{2.2}$$

where G_i is the truncated representation in FIR and $\Delta u_k = u_k - u_{k-1}$. These models were widely used because of its simple structure and easy identification scheme. However, it can only be represented for stable systems. Another disadvantage is that large data is required to identify an accurate enough plant model.

2. *Transfer function model:* A transfer function model usually represented by a controlled auto-regressive integrated moving average (CARIMA) model, which is used in GPC, predictive functional control (PFC) [51], and multipredictor receding horizon adaptive control (MURHAC) [52]. This model for the SISO system is represented as

$$A(z^{-1})y_k = B(z^{-1})u_k + \frac{F(z^{-1})}{\Delta(z^{-1})}\zeta_k \tag{2.3}$$

where $A(z^{-1})$, $B(z^{-1})$ and $F(z^{-1})$ are plant parameters but $F(z^{-1})$ is usually considered as a design parameter as it affects the closed-loop sensitivity. ζ_k is the zero-mean Gaussian noise. For a MIMO system, this transfer function model is expressed as a matrix fraction description (MFD) form, where the parameters are represented as matrix polynomial. Δ is the difference opera-

tor defined as $\Delta(z^{-1}) = 1 - z^{-1}$. The inclusion of integrated noise $\frac{1}{\Delta(z^{-1})}\zeta_k$ results in disturbance rejection and off-set free output tracking as input is represented as Δu_k in the predicted model.

$$\lim_{k\to\infty} \Delta u_k = 0 \tag{2.4}$$

$$\{y_k = w_k; \quad \Delta u_k = 0\} \quad \forall \quad k \tag{2.5}$$

where w_k is the reference set point at k^{th} sample instant and $u_k = u_{ss}$ at steady state.

3. *State-space model:* A state-space model for a real process without instantaneous output, $D = 0$ is represented as

$$x_k = Ax_{k-1} + Bu_k \tag{2.6}$$

$$y_k = Cx_{k-1} \tag{2.7}$$

where $x_k \in \mathbb{R}^n$ is the state vector, $y_k \in \mathbb{R}^l$ and $u_k \in \mathbb{R}^m$ are the plant output and input respectively. It is usually represented for MIMO processes. Insertion of an observer for inaccessible states, makes the controller design process complicated for a state-space model. Disturbance in this model can be incorporated as output disturbance or state disturbance. Output equation is modified as

$$y_k = Cx_{k-1} + d_k \tag{2.8}$$

where $d_k = d_{k-1} + \zeta_k$.

Output disturbance model is represented as

$$\begin{bmatrix} x_k \\ d_k \end{bmatrix} = \begin{bmatrix} A & 0 \\ 0 & I \end{bmatrix} \begin{bmatrix} x_{k-1} \\ d_{k-1} \end{bmatrix} + \begin{bmatrix} B \\ 0 \end{bmatrix} u_k + \begin{bmatrix} 0 \\ I \end{bmatrix} \zeta_k \tag{2.9}$$

$$y_k = \begin{bmatrix} C & I \end{bmatrix} \begin{bmatrix} x_{k-1} \\ d_{k-1} \end{bmatrix} + \zeta_{k-1} \tag{2.10}$$

Similarly, for a state disturbance model, state equation (2.6) is modified as (2.11).

$$x_k = Ax_{k-1} + Bu_k + Fd_k \tag{2.11}$$

Finally, the modified state-space equations are represented as in (2.12) and (2.13).

$$\begin{bmatrix} x_k \\ d_k \end{bmatrix} = \begin{bmatrix} A & F \\ 0 & I \end{bmatrix} \begin{bmatrix} x_{k-1} \\ d_{k-1} \end{bmatrix} + \begin{bmatrix} B \\ 0 \end{bmatrix} u_k + \begin{bmatrix} F \\ I \end{bmatrix} \zeta_k \tag{2.12}$$

$$y_k = \begin{bmatrix} C & 0 \end{bmatrix} \begin{bmatrix} x_{k-1} \\ d_{k-1} \end{bmatrix} \tag{2.13}$$

Inclusion of an integrator is necessary as the regular state feedback, $u_k = -Kx_k$ will not be resulting in an off-set free control in the presence of disturbance, where K is the feedback gain matrix.

4. *Non-linear model:* As many plant dynamics can not be linearized, non-linear models are chosen as plant model. Representing plant dynamics by a non-

linear function complicates the controller design procedure, and optimization value does not guarantee the global optimal solution for the chosen non-linear model.

2.2.2 Cost function

A simple quadratic cost function is chosen for optimization. There are two main reasons for choosing a quadratic cost function. Firstly, a global optimum solution is obtained for a quadratic problem assuming all the constraint criteria are satisfied. Secondly, a quadratic cost function is a Lyapunov function which will guarantee the stability of the control law. Stability of a predictive control mainly depends on the stability of the obtained control input. The obtained control input determines the closed-loop poles of the system. A typical expression of the cost function is expressed as

$$J(N_1, N_2, M) = \sum_{i=N_1}^{N_2} \delta(i)[\hat{y}_{k+i|k} - w_{k+i}]^2 + \sum_{i=0}^{M-1} \lambda(i)[\Delta u_{k+i}]^2 \tag{2.14}$$

where $\hat{y}_{k+i}$ is the predicted output, N_1, N_2 are minimum, and maximum prediction horizon and M is control horizon. $\delta(i)$ and $\lambda(i)$ are weights which penalizes tracking error and change in control input. The cost function (2.14) is minimized with respect to Δu_{k+i} at every sampling instant and results in an off-set free reference tracking. Any predictive control technique is based on a unique time frame known as the horizon. The output is predicted for a certain span of sampled time, which is called a prediction horizon and the number of obtained input control sequence for a chosen control horizon. Stability of the controller is also dependent on the chosen prediction horizon. When an infinite time quadratic cost function is considered, the stability of the obtained control input is inherently proved by

assuming the cost function to be a Lyapunov function. However, choosing an infinite horizon cost function increase the mathematical computational complexity for a fast system. Also, there is no significant improvement for a high value of the prediction horizon. Similarly, the control horizon is also kept at a minimum value it can be. A high value of the control horizon increases the computational burden of the controller. A predictive control usually follows moving horizon principle. At k^{th} sample instant, the cost function is optimized for a horizon of $\{(k+1),(k+N)\}$ which moves one step ahead for optimization of a cost function for next sample time to $\{(k+2),(k+N+1)\}$. Constraints can be included while optimizing the cost function as to limit input, change in input, state or output, but it increases complexity to obtain an optimized control law, and it also affects the feasibility of the optimization problem.

$$u_{k_{min}} \leq u_k \leq u_{k_{max}} \tag{2.15}$$

$$\Delta u_{k_{min}} \leq \Delta u_k \leq \Delta u_{k_{max}} \tag{2.16}$$

$$x_{k_{min}} \leq x_k \leq x_{k_{max}} \tag{2.17}$$

$$y_{k_{min}} \leq y_k \leq y_{k_{max}} \tag{2.18}$$

2.2.3 Optimized control law

To generate the optimized control law, the first step is to obtain an output prediction ($\hat{y}_{k+1}$) model from the plant model. The cost function optimizes the tracking error and control effort. Using RHC only first element of optimized control is implemented at that sampling instant, and rest are discarded. For a set value of control horizon M, the optimized control law is defined as

$$\Delta u_{k+i-1} = 0 \qquad i > M \tag{2.19}$$

2.3 Formulation of GPC for transfer function model

The model chosen to formulate GPC in a transfer function form is expressed in a CARIMA model

$$a(z^{-1})y_k = B(z^{-1})u_k + F(z^{-1})\frac{\zeta_k}{\Delta(z^{-1})} \tag{2.20}$$

where $y_k \in \mathbb{R}^l$, $u_k \in \mathbb{R}^m$ are the output and input of the plant at the k^{th} instant of sample time respectively. When $l = m = 1$, model (2.20) is generalizeed for SISO plant dynamics. $a(z^{-1})$ and $b(z^{-1})$ are plant model transfer function parameters. $F(z^{-1})\frac{\zeta_k}{\Delta(z^{-1})}$ improves plant robustness in rejecting noise and disturbance. Model parameters $a(z^{-1})$ and $b(z^{-1})$ are expressed as

$$a(z^{-1}) = 1 + a_1 z^{-1} + a_2 z^{-2} + ... + a_{nl+1} z^{-nl} \tag{2.21}$$

$$B(z^{-1}) = b_0 + b_1 z^{-1} + b_2 z^{-2} + ... + b_{nm} z^{-nm} \tag{2.22}$$

where nl and nm are the order of the transfer function polynomial of the plant model. To obtain output prediction for model (2.20) the corresponding difference equation is obtained from the model by rearranging (2.20) is as follows.

$$a(z^{-1})\Delta\frac{y_k}{F(z^{-1})} = B(z^{-1})\frac{\Delta u_k}{F(z^{-1})} + \zeta_k \tag{2.23}$$

$$\Rightarrow A(z^{-1})\tilde{y}_k = B(z^{-1})\Delta\tilde{u}_k + \zeta_k \tag{2.24}$$

where $\tilde{y}_k$ and $\Delta\tilde{u}_k$ are filtered variables and $a(z^{-1})\Delta = A(z^{-1})$. Basically, $\frac{1}{F(z^{-1})}$ is a low-pass filter. Prediction equation can also be obtained by assuming an expected value of zero for the term $F(z^{-1})\zeta_k$. Certainly, this assumption is not satisfactory as past values of ζ_k can be extrapolated. By representing the model

in (2.24) accuracy of the prediction is improved as the bias due to past values of ζ_k is removed. The diophantine equations used in [27, 28] are

$$1 = E_k(z^{-1})A(z^{-1}) + z^{-k}F_k(z^{-1}) \tag{2.25}$$

$$E_k(z^{-1})b(z^{-1}) = R_k(z^{-1}) + z^{-k}S_k(z^{-1}) \tag{2.26}$$

By using (2.25) and (2.26), output prediction equation is obtained. To have a unique solution of the diophantine equation, polynomials E an F are chosen to be of the degree equal to $k-1$ and nl respectively and polynomials R an S are chosen to be of the degree equal to $k-1$ and nm respectively. The predicted output is expressed in a free and forced response. Use of diophantine equation as in [27, 28] to obtain the prediction model increases computation time, so matrix method is used which is computationally easy to obtain the prediction equation.

2.3.1 Prediction and optimization

As per receding horizon theory $\Delta\tilde{u}_{k+M-1} = 0$ for $M \geq 0$ and for a feasible optimization problem, prediction horizon is always greater than or equal to control horizon $N \geq M$. For N prediction horizon and M control horizon, output prediction equation is obtained from one step ahead prediction equation to N step ahead prediction equation, which is expressed as follows

$$\tilde{y}_{k+1} + a_1\tilde{y}_k + \cdots + a_{nl+1}\tilde{y}_{k-nl} = b_0\Delta\tilde{u}_k + b_1\Delta\tilde{u}_{k-1} + \cdots + b_{nm}\Delta\tilde{u}_{k-nm+1} \tag{2.27}$$

$$\tilde{y}_{k+2} + a_1\tilde{y}_{k+1} + \cdots + a_{nl+1}\tilde{y}_{k-nl+1} = b_0\Delta\tilde{u}_{k+1} + b_1\Delta\tilde{u}_k + \cdots + b_{nm}\Delta\tilde{u}_{k-nm+2} \tag{2.28}$$

$$\vdots$$

$$\tilde{y}_{k+N} + a_1\tilde{y}_{k+N-1} + \cdots + a_{nl+1}\tilde{y}_{k+N-nl-1} = b_0\Delta\tilde{u}_{k+N-1} + b_1\Delta\tilde{u}_{k+N-2} + \cdots + b_{nm}\Delta\tilde{u}_{k+N-nm} \tag{2.29}$$

The above set of prediction equations which can be expressed in a generalized matrix form as

$$C_a \underbrace{\begin{bmatrix} \tilde{y}_{k+1} \\ \tilde{y}_{k+2} \\ \vdots \\ \tilde{y}_{k+N} \end{bmatrix}}_{\tilde{y}_p} + H_a \underbrace{\begin{bmatrix} \tilde{y}_k \\ \tilde{y}_{k-1} \\ \vdots \\ \tilde{y}_{k-nl} \end{bmatrix}}_{\tilde{y}} = C_b \underbrace{\begin{bmatrix} \Delta\tilde{u}_k \\ \Delta\tilde{u}_{k+1} \\ \vdots \\ \Delta\tilde{u}_{k+M-1} \end{bmatrix}}_{\Delta\tilde{u}_p} + H_b \underbrace{\begin{bmatrix} \Delta\tilde{u}_{k-1} \\ \Delta\tilde{u}_{k-2} \\ \vdots \\ \Delta\tilde{u}_{k-nm+1} \end{bmatrix}}_{\Delta\tilde{u}} \tag{2.30}$$

where C_a, C_b are Toeplitz matrices and H_a, H_b are Hankel matrices, $\tilde{y}_p$ and $\Delta\tilde{u}_p$ are the future output and input of the prediction model, $\tilde{y}$ and $\Delta\tilde{u}$ are the past values of output and input respectively. Properties of Toeplitz and Hankel matrices are used in further simplification of output expression and easy calculation.

$$C_a = \begin{bmatrix} 1 & 0 & \dots & 0 \\ a_1 & 1 & \dots & 0 \\ a_2 & a_1 & \dots & 0 \\ \vdots & \vdots & \vdots & \vdots \end{bmatrix}; \qquad H_a = \begin{bmatrix} a_1 & a_2 & \dots & a_{nl+1} \\ a_2 & a_3 & \dots & 0 \\ a_3 & a_4 & \dots & 0 \\ \vdots & \vdots & \vdots & \vdots \end{bmatrix};$$

$$C_b = \begin{bmatrix} b_0 & 0 & \dots & 0 \\ b_1 & b_0 & \dots & 0 \\ b_2 & b_1 & \dots & 0 \\ \vdots & \vdots & \vdots & \vdots \end{bmatrix}; \qquad H_b = \begin{bmatrix} b_1 & b_2 & \dots & b_{nm} \\ b_2 & b_3 & \dots & 0 \\ b_3 & b_4 & \dots & 0 \\ \vdots & \vdots & \vdots & \vdots \end{bmatrix} \tag{2.31}$$

Final predicted output equation in filtered form is given as

$$\tilde{y}_p = P\Delta\tilde{u}_p + Q\Delta\tilde{u} + R\tilde{y} \tag{2.32}$$

where $P = C_a^{-1}C_b$, $Q = C_a^{-1}H_b$ and $R = -C_a^{-1}H_a$. Output prediction $\hat{y}_p$ must be represented as an unfiltered future signal Δu_p. $\hat{y}_p$ is obtained from $\tilde{y}_p$ as follows

$$C_{F_y}\tilde{y}_p + H_{F_y}\tilde{y} = \hat{y}_p \tag{2.33}$$

$$C_{F_u}\Delta\tilde{u}_p + H_{F_u}\Delta\tilde{u} = \Delta u_p \tag{2.34}$$

where the coefficient matrices in (2.33) and (2.34) are obtained similarly as (2.30). Substituting (2.33) and (2.34) in (2.32) final unfiltered output prediction is expressed as

$$\hat{y}_p = \tilde{P}\Delta u_p + \tilde{Q}\Delta\tilde{u} + \tilde{R}\tilde{y} \tag{2.35}$$

where

$$\tilde{P} = C_{F_y}PC_{F_u} \tag{2.36}$$

$$\tilde{Q} = C_{F_y}Q - C_{F_y}PC_{F_u}^{-1}H_{F_u} \tag{2.37}$$

$$\tilde{R} = H_{F_y} + C_{F_y}R \tag{2.38}$$

If $nl = nm$, then $C_{F_y} = C_{F_u} = C_F$ and $H_{F_y} = H_{F_u} = H_F$ in (2.33) and (2.34). Similarly, final unfiltered output equation is modified accordingly. By using the commutative property (e.g. $C_aC_F^{-1} = C_F^{-1}C_a$) of toeplitz matrices for SISO system the unfiltered output prediction is expressed as

$$\hat{y}_p = P\Delta u_p + \tilde{Q}\Delta\tilde{u} + \tilde{R}\tilde{y} \tag{2.39}$$

where coefficient matrices are evaluated as

$$\tilde{Q} = C_FQ - PH_F \tag{2.40}$$

$$\tilde{R} = H_F + C_FR \tag{2.41}$$

Remark 2.3.1 *If* $F(z^{-1}) = 1$, *then* $H_{F_y} = H_{F_u} = 0$, $C_{F_y} = C_{F_u} = I$. *Hence,* (2.35) *and* (2.39) *will have the output prediction model as in* (2.32).

Remark 2.3.2 *To represent output predicted model in terms of explicit model parameters,* (2.33) *and* (2.34) *can be substituted in* (2.30).

Optimal control input is obtained once predicted output is expressed in unfiltered form. The cost function to obtain optimized control input is defined as

$$J(\Delta u) = \mathbf{Q}\sum_{i=1}^{N} \|(w_{p+i} - \hat{y}_{p+i})\|_2^2 + \mathbf{R}\sum_{i=0}^{M} \|\Delta u_{p+i}\|_2^2 \tag{2.42}$$

where w_p is the reference sequence and $\mathbf{Q}$ is the tracking error weight and $\mathbf{R}$ is the control error weight, which are chosen to be positive definite constant diagonal matrices $\mathbf{Q} = \text{diagonal}(\delta(i))$ and $\mathbf{R} = \text{diagonal}(\lambda(i))$. Now substituting the predicted output model in cost function (2.42)

$$J(\Delta u) = \mathbf{Q}\left\|(w_p - P\Delta u_p + \tilde{Q}\Delta\tilde{u} + \tilde{R}\tilde{y}\right\|_2^2 + \mathbf{R}\,\|\Delta u_p\|_2^2 \tag{2.43}$$

As the cost function is quadratic in nature a unique optimal solution can be obtained by first derivative of (2.42). Current optimal control input is obtained by minimising the cost function with respect to the control increment Δu_p.

$$\frac{dJ}{d\Delta u_p} = 0 \tag{2.44}$$

$$\Rightarrow \frac{dJ}{d\Delta u_p} = 2(P^T\mathbf{Q}P + \mathbf{R})\Delta u_p + 2P^T\mathbf{Q}[\tilde{Q}\Delta\tilde{u} + \tilde{R}\tilde{y} - w_p] \tag{2.45}$$

$$\Rightarrow \Delta u_p = (P^T\mathbf{Q}P + \mathbf{R})^{-1}P^T\mathbf{Q}[w_p - \tilde{Q}\Delta\tilde{u} - \tilde{R}\tilde{y}] \tag{2.46}$$

As RHC is incorporated in GPC, the first element of (2.46) is used at that sample instant and rest are discarded hence Ψ is defined as $\Psi = \begin{bmatrix}1 & 0 & \dots & 0\end{bmatrix}$. The optimized control input is recalculated at every step of sampling instant. Hence,

control law is obtained as

$$\Delta u_p = P_k w_p - \tilde{N}_k \tilde{y} - \hat{D}_k \Delta \tilde{u} \tag{2.47}$$

Coefficients are defined as

$$P_k = \Psi(P^T \mathbf{Q} P + \mathbf{R})^{-1} P^T \mathbf{Q} \tag{2.48}$$

$$N_k = P_k \tilde{R} \Rightarrow \Psi(P^T \mathbf{Q} P + \mathbf{R})^{-1} P^T \mathbf{Q} \tilde{R} \tag{2.49}$$

$$\hat{D}_k = P_k \tilde{Q} \Rightarrow \Psi(P^T \mathbf{Q} P + \mathbf{R})^{-1} P^T \mathbf{Q} \tilde{Q} \tag{2.50}$$

Remark 2.3.3 *An unconstrained minimization of cost function results in a linear feedback control law with feed forward term as in* (2.46)

2.4 Closed-loop analysis of GPC

Closed-loop analysis is done to check sensitivity of the system output and control input with respect to noise and disturbance. The coefficient of GPC control law without filter and constraint is defined as transfer function expressed as

$$D_k(z^{-1}) \Delta u_p = P_k(z^{-1}) w_p - N_k(z^{-1}) y \tag{2.51}$$

For closed-loop analysis the polynomial of (2.51) are given as

$$D_k(z^{-1}) = 1 + z^{-1} \hat{D}_k(z^{-1}) \tag{2.52}$$

$$P_k(z^{-1}) = P_k[z \;\; z^2 \;\; z^3 \cdots \;\; z^{nr}]^T \tag{2.53}$$

$$N_k(z^{-1}) = N_k[1 \;\; z^{-1} \;\; z^{-2} \;\; \cdots \;\; z^{-nl}]^T \tag{2.54}$$

Substituting (2.51) by using matrix property $\bar{B}\bar{A}^{-1} = A^{-1}B$ in (2.51) yields

$$u_p = \bar{A}(z^{-1})[D_k(z^{-1})\Delta\bar{A}(z^{-1}) + N_k(z^{-1})\bar{B}(z^{-1})]^{-1}P_k(z^{-1})w \tag{2.55}$$

$$y = \bar{B}(z^{-1})[D_k(z^{-1})\Delta\bar{A}(z^{-1}) + N_k(z^{-1})\bar{B}(z^{-1})]^{-1}P_k(z^{-1})w \tag{2.56}$$

Similarly (2.47) can be modified to (2.57) for GPC with a filter $F(z^{-1})$ as

$$\frac{\tilde{D}_k(z^{-1})}{F(z^{-1})}\Delta u_p = P_k(z^{-1})w - \frac{\tilde{N}_k(z^{-1})}{F(z^{-1})}y \tag{2.57}$$

where the coefficient $\tilde{D}_k = F(z^{-1}) + z^{-1}D_k$ and the closed-loop form is modeled similar to (2.58) and (2.59) as

$$u_p = \bar{A}(z^{-1})F(z^{-1})[\tilde{D}_k(z^{-1})\Delta\bar{A}(z^{-1}) + \tilde{N}_k(z^{-1})\bar{B}(z^{-1})]^{-1}P_k(z^{-1})w \tag{2.58}$$

$$y = \bar{B}(z^{-1})F(z^{-1})[\tilde{D}_k(z^{-1})\Delta\bar{A}(z^{-1}) + \tilde{N}_k(z^{-1})\bar{B}(z^{-1})]^{-1}P_k(z^{-1})w \tag{2.59}$$

Pole and control law of GPC and GPCF (GPC with filter) are available in Table 2.1. For readability purpose notation $A(z^{-1})$ is denoted as A. The expressions are referred to present sample instant k.

Table 2.1: GPCF and GPC pole and control law

	Polynomial pole	Control law
GPCF	$\frac{\tilde{D}_k}{F}\Delta u_p = P_k w - \frac{\tilde{N}_k}{F}y$	$\tilde{P}_{cl} = \tilde{D}_k\Delta\bar{A} + \tilde{N}_k\bar{B}$
GPC	$\frac{D_k}{F}\Delta u_p = P_k w - \frac{N_k}{F}y$	$P_{cl} = D_k\Delta\bar{A} + N_k\bar{B}$

2.5 Effect of variation in tuning parameters

In this section, the effect of different tuning parameters of GPC is presented in the simulation result for reference tracking problem. The parameters of GPC are tuned heuristically in this chapter to show the system response for various tuning parameters.

2.5.1 Example 1

Consider the model

$$G_1(z^{-1}) = \frac{z^{-1} - 0.63z^{-2}}{1 - 1.2z^{-1} + 0.32z^{-2}} \tag{2.60}$$

In Figure 2.2, $G_1(z^{-1})$ is tuned for desired output (y) response for different values of error weights with other tuning parameters set at constant value. To penalize the control error the weights are set at higher value $\lambda = 100$. Control horizon is set at $M = 2$ and prediction horizon at $N = 10$.

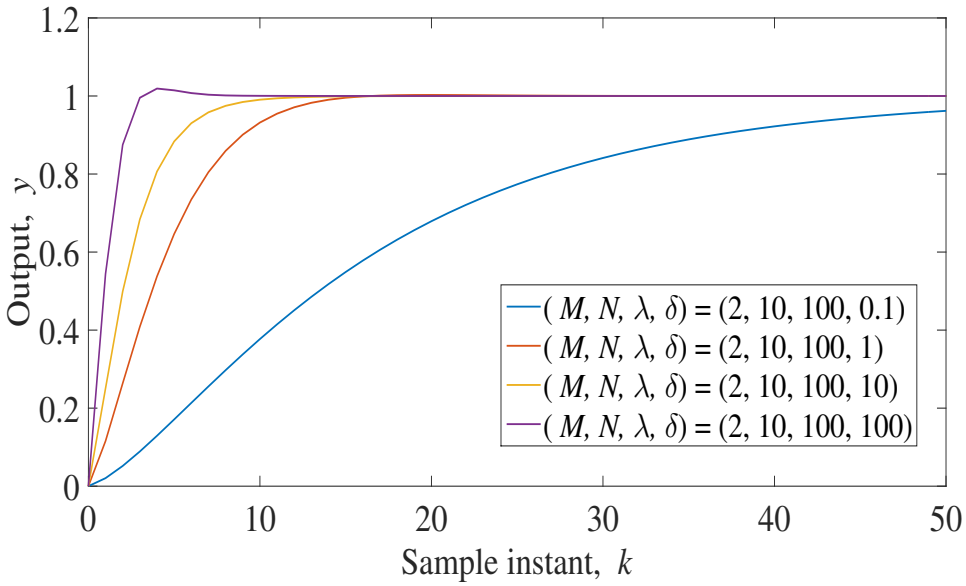

Figure 2.2: Output response of $G_1(z^{-1})$ for different values of δ

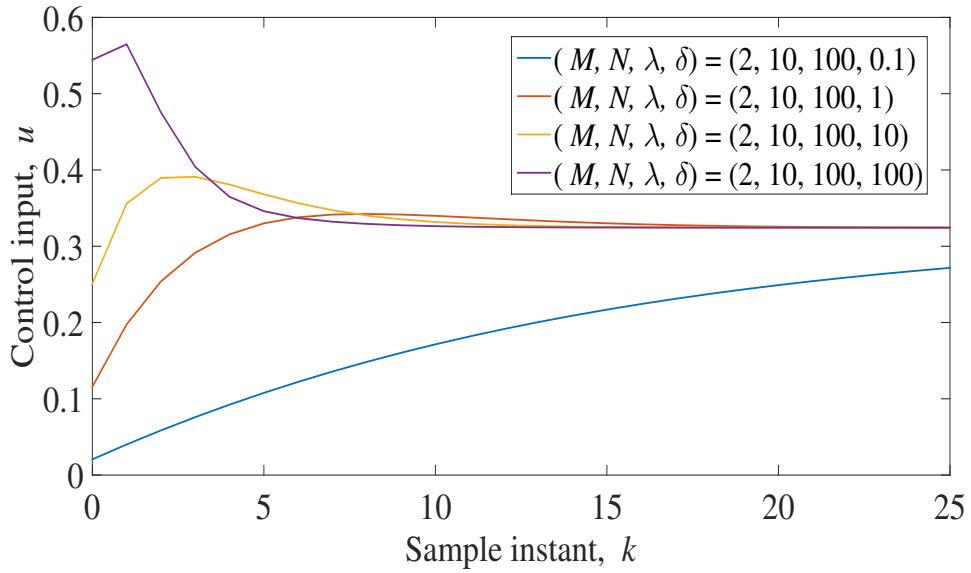

Figure 2.3: Control input response of $G_1(z^{-1})$ for different values of δ

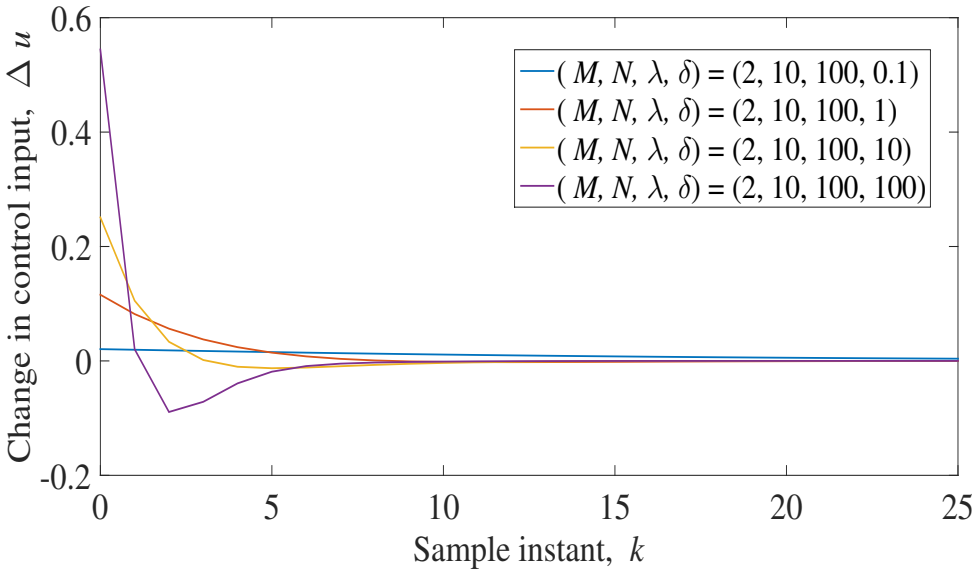

Figure 2.4: Change in control input response of $G_1(z^{-1})$ for different values of δ

Similarly in Figure 2.3 and 2.4, optimized control input (u) and change in control input (Δu) responses are presented for GPC without filter polynomial. From the numerical simulation results presented, weight can be set at $\lambda = 100$ which gives desired output response in Figure 2.2. Effect of variation in control horizon for y, u and Δu are presented in Figure 2.5, 2.6 and 2.7 respectively. For a feasible solution in GPC control horizon is always less than or equal to the chosen prediction horizon.

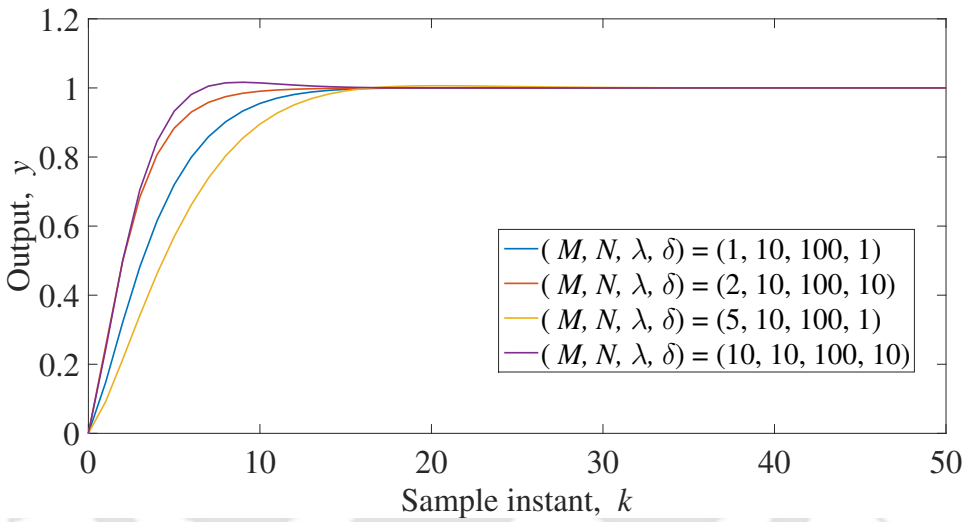

Figure 2.5: Output response of $G_1(z^{-1})$ for different values of control horizon, M

In Figure 2.8, 2.9 and 2.10 effect of higher value of prediction is shown . It is observed that the performance does not change significantly for a higher value of prediction horizon or control horizon. Instead it increases the computation time of the controller. Hence, an optimal tuning criteria should be followed for tuning of parameters in GPC. In Figure 2.11, the closed-loop output response (y_{cl}) is compared with the open-loop response (y_{op}). Along with the output response, control response is also presented in Figure 2.11.

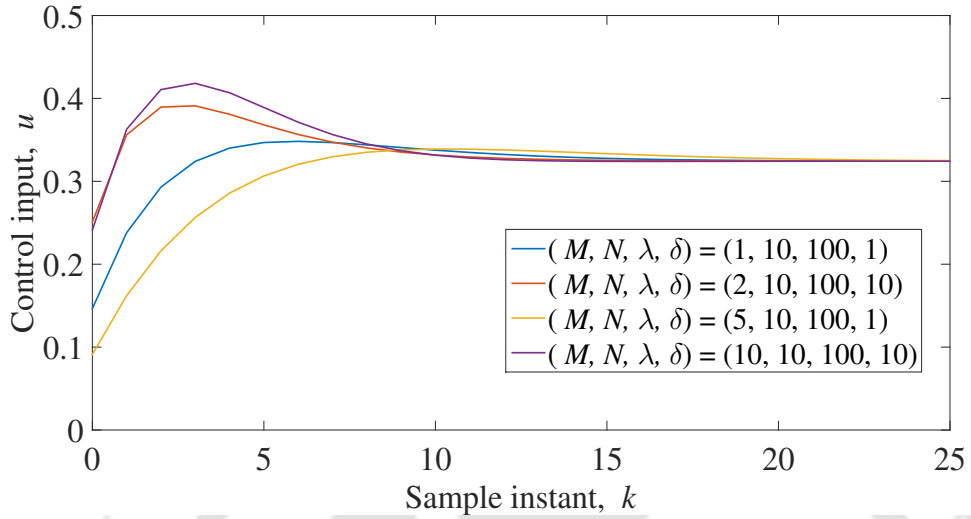

Figure 2.6: Control input response of $G_1(z^{-1})$ for different values of control horizon, M

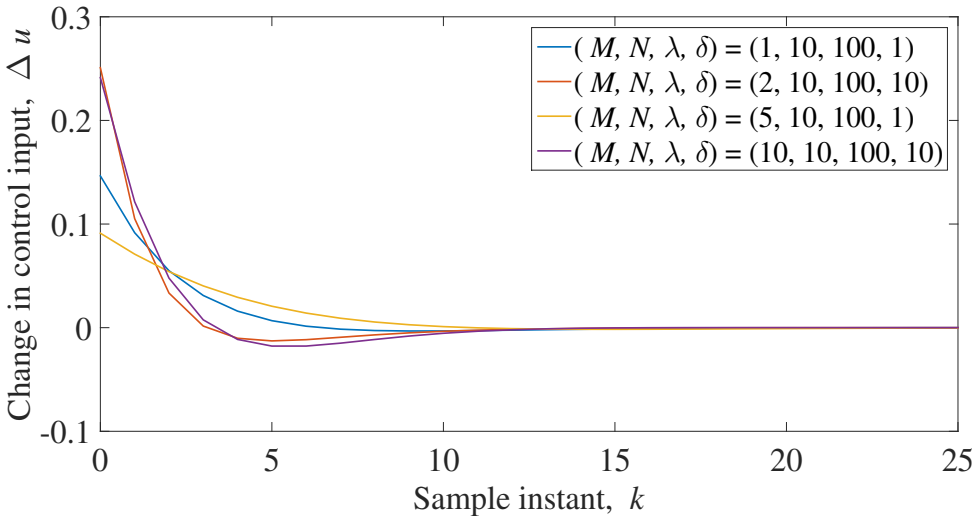

Figure 2.7: Change in control input response of $G_1(z^{-1})$ for different values of control horizon, M

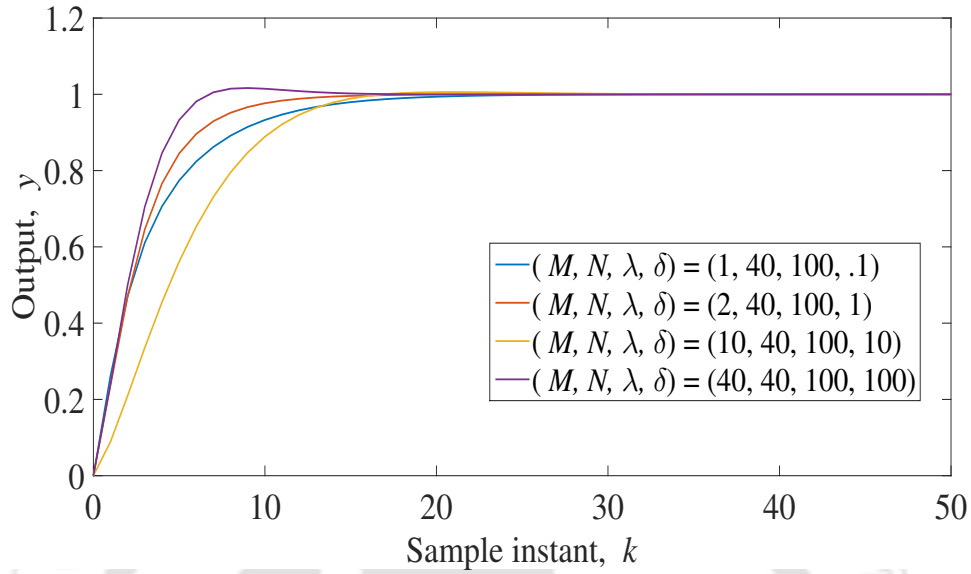

Figure 2.8: Output response of $G_1(z^{-1})$ for different values of control horizon, M with high prediction horizon, N

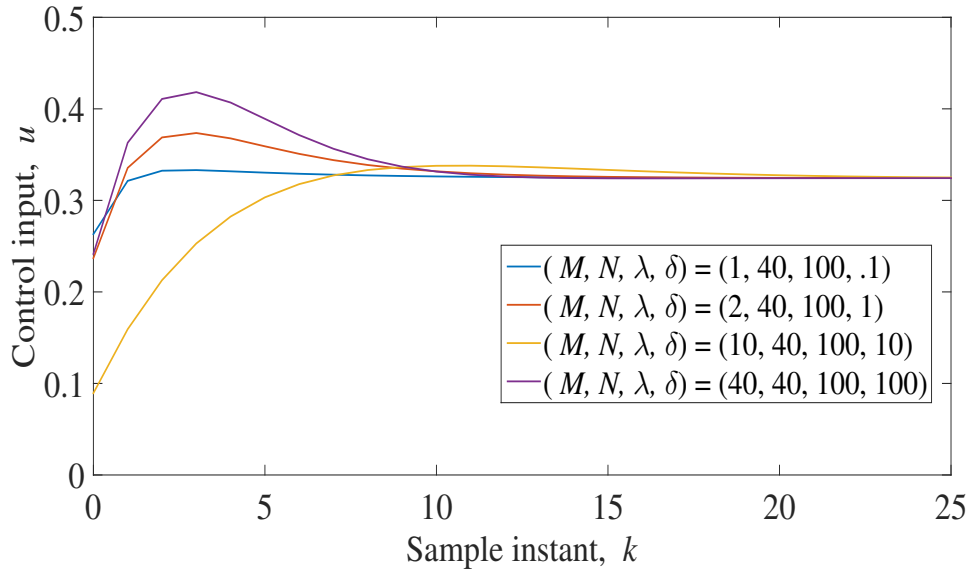

Figure 2.9: Control input response of $G_1(z^{-1})$ for different values of control horizon, M with high prediction horizon, N

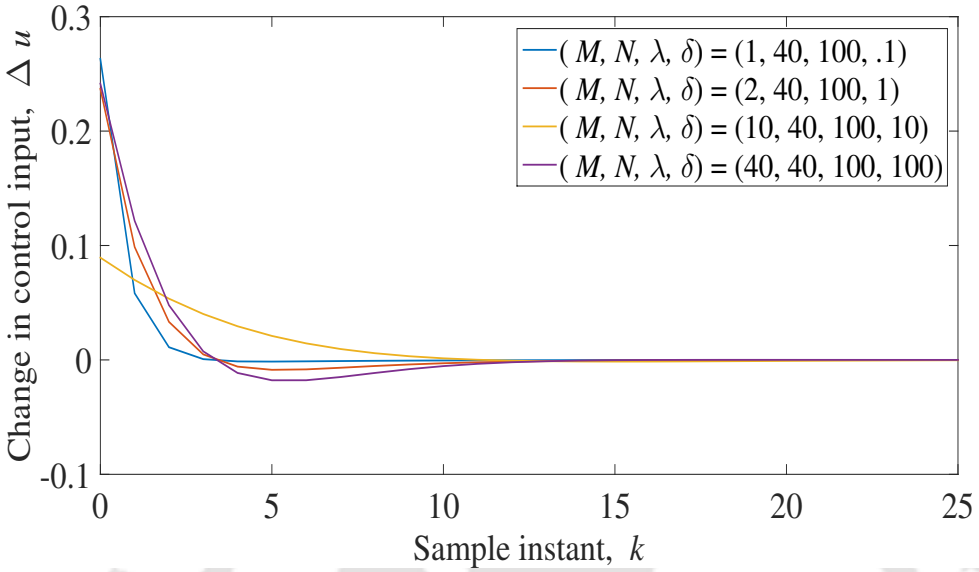

Figure 2.10: Change in control input response of $G_1(z^{-1})$ for different values of control horizon, M with high prediction horizon, N

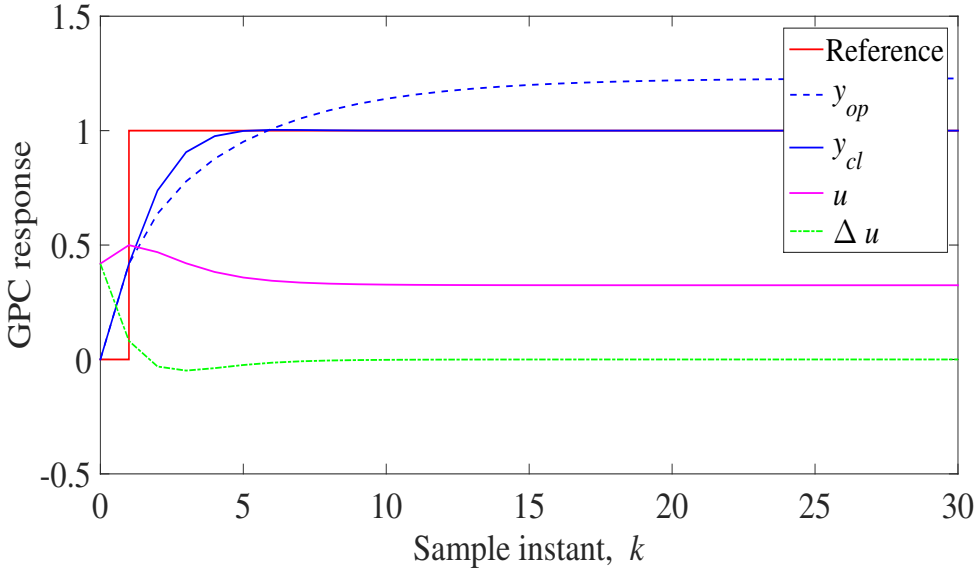

Figure 2.11: Closed-loop and open loop response of $G_1(z^{-1})$

2.6 Sensitivity functions of GPC

Let the plant be modeled with disturbance and noise be expressed as

$$Ay_k = Bu_k + F_d\frac{\zeta_d}{\Delta} + F_n\zeta_n \tag{2.61}$$

where $F_n\zeta_n$ is the noise component and $F_d\frac{\zeta_d}{\Delta}$ is the model of the disturbance. Sensitivity of output and input with respect to disturbance and noise are obtained and listed in Table 2.2.

Table 2.2: Sensitivity of output and input for disturbance and noise

	Disturbance	Noise	Uncertainty
Output sensitivity	$S_{yd} = \frac{\bar{B}D_kB^{-1}F_d}{\Delta P_{cl}}$	$S_{yn} = \frac{\bar{B}D_kB^{-1}F_n}{P_{cl}}$	$S_u = \frac{\bar{B}N_k}{P_{cl}}$
Input sensitivity	$S_{ud} = \frac{\bar{A}N_kA^{-1}F_d}{P_{cl}}$	$S_{un} = \frac{\bar{A}N_kA^{-1}F_n}{P_{cl}}$	

Remark 2.6.1 *The sensitivity functions available in Table 2.2 are for GPC without including filter (F). When sensitivity transfer functions for GPCF are derived, the expressions are modified accordingly by using Table 2.1 hence filter polynomial (F) is divided from the denominator of the transfer function.*

2.6.1 Example 2

Consider the model

$$G_2(z^{-1}) = \frac{z^{-1} + 1.2z^{-2}}{1 - 1.2z^{-1} + 0.3z^{-2}} \tag{2.62}$$

Variation in sensitivity functions are shown for GPC and GPCF. $F(z^{-1}) = 1$ and $F(z^{-1}) = 1 - 0.8z^{-1}$ for GPC and GPCF respectively. For this chosen model by including the filter, sensitivity of the model is improved at higher frequencies.

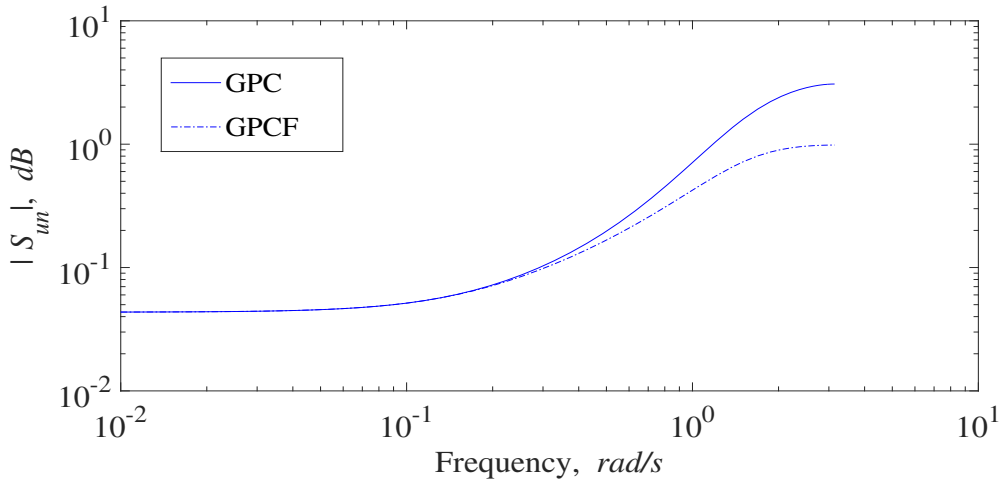

Figure 2.12: Input sensitivity with respect to noise, S_{un}

Performance of control input sensitivity for noise (S_{un}) and disturbance (S_{ud}) shown in Figure 2.12 and 2.13 are improved for GPCF. Similarly, the over all sensitivity function of plant with respect to uncertainty (S_u) is improved for the entire frequency range for GPCF as shown in Figure 2.16. Hence it can be concluded that the robustness of the closed-loop model is improved for this particular case. As shown in Figure 2.14 and 2.15 for lower frequencies, output responses S_{yn} and S_{yd} are less sensitive for GPC instead of GPCF.

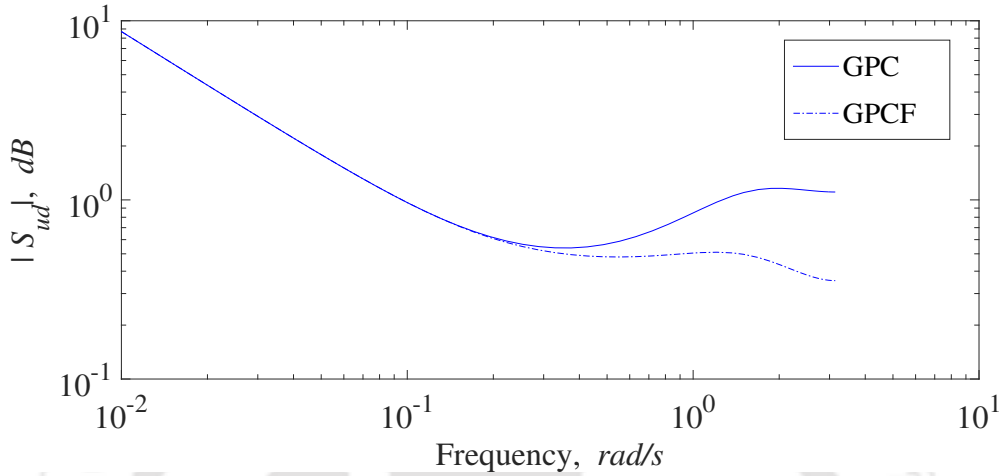

Figure 2.13: Input sensitivity with respect to disturbance, S_{ud}

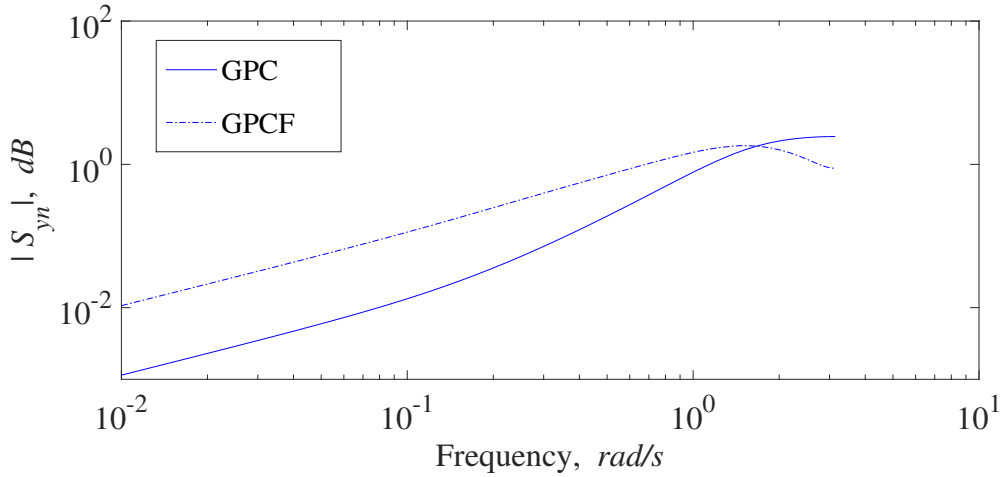

Figure 2.14: Output sensitivity with respect to noise, S_{yn}

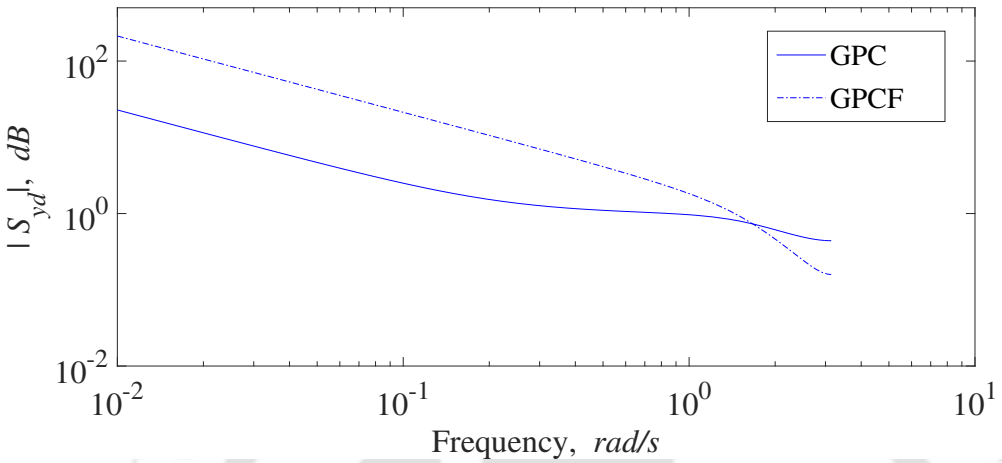

Figure 2.15: Output sensitivity with respect to disturbance, S_{yd}

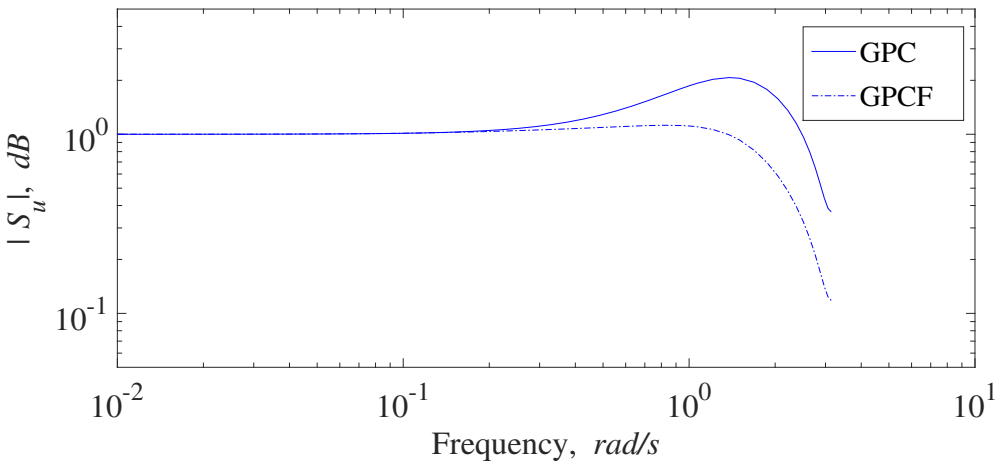

Figure 2.16: Overall sensitivity with respect to uncertainty, S_u

2.7 Effect of noise and disturbance

In this section, effect of random noise and step disturbance on reference tracking problem, control input and change in control input are presented in simulation results for GPC and GPCF. For the simulation result a model $G_3(z^{-1})$ is considered.

$$G_3(z^{-1}) = \frac{z^{-1} + 0.4z^{-2}}{1 - 1.2z^{-1} + 0.3z^{-2}} \tag{2.63}$$

The chosen values of filter polynomials are $F(z^{-1}) = 1$ and $F(z^{-1}) = 1 - 0.8z^{-1}$ for GPC and GPCF respectively.

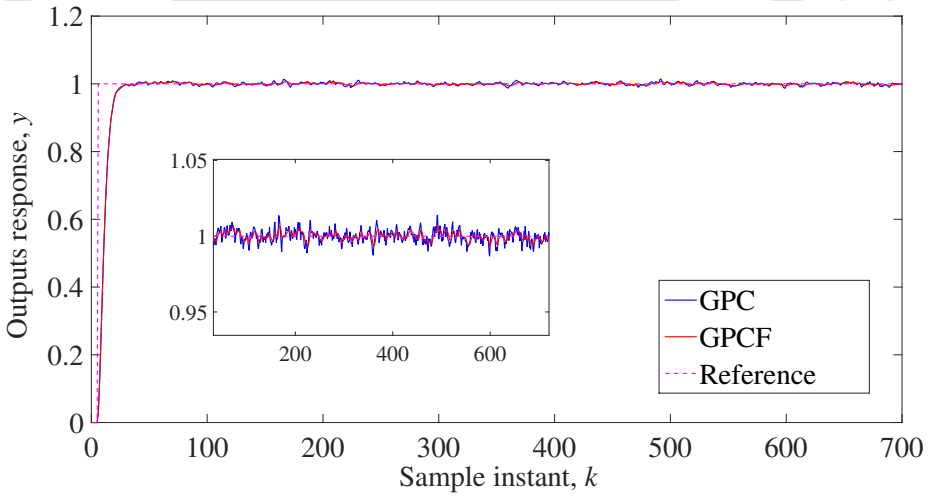

Figure 2.17: Reference tracking of GPC and GPCF for model $G_3(z^{-1})$ in presence of noise

In Figure 2.17, effect of random noise of $SNR = 50.5\ dB$ is considered for output response. The output responses of GPC and GPCF are shown for reference tracking problem. The control input and change in control input responses are shown in Figure 2.18 and 2.19 respectively.

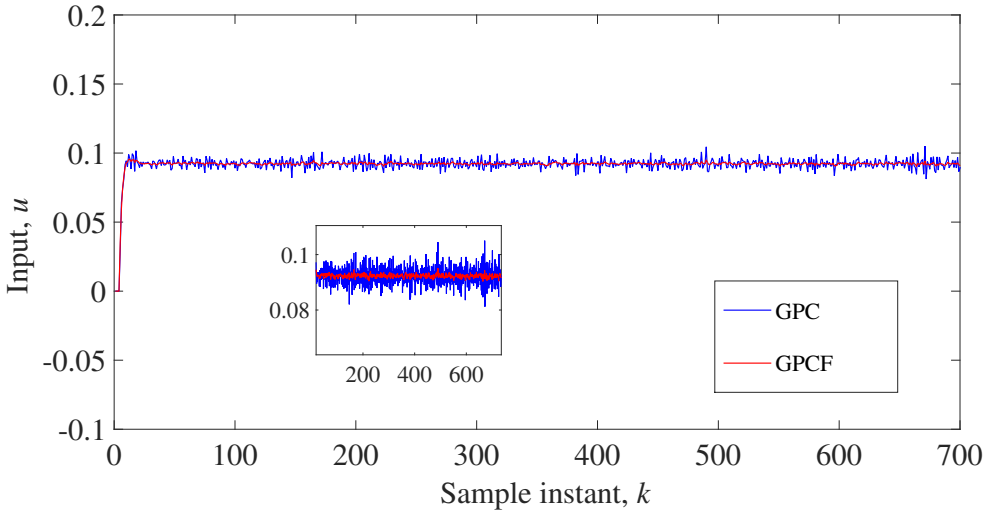

Figure 2.18: Control input response for model $G_3(z^{-1})$ in presence of noise

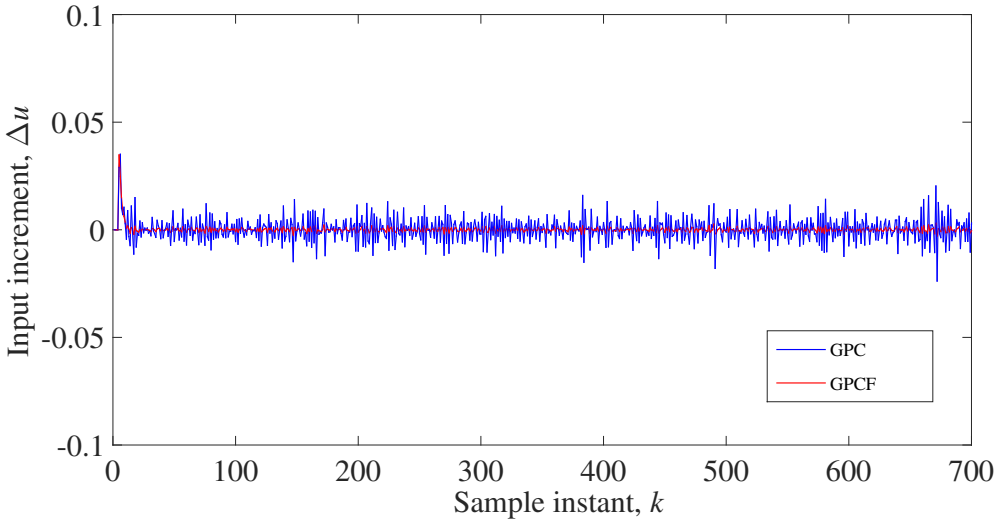

Figure 2.19: Change in control input response for model $G_3(z^{-1})$ in presence of noise

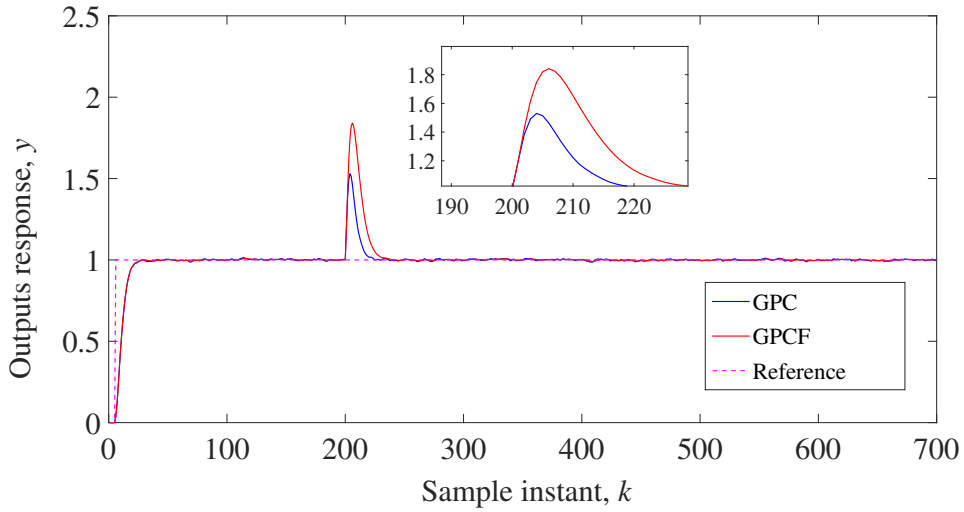

Figure 2.20: Reference tracking of GPC and GPCF for model $G_3(z^{-1})$ in presence of noise and disturbance

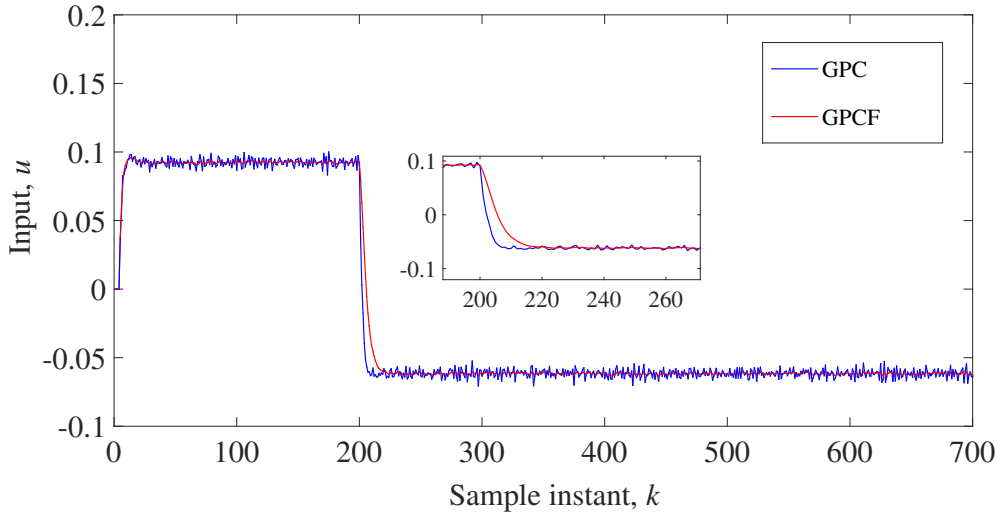

Figure 2.21: Control input response for model $G_3(z^{-1})$ in presence of noise and disturbance

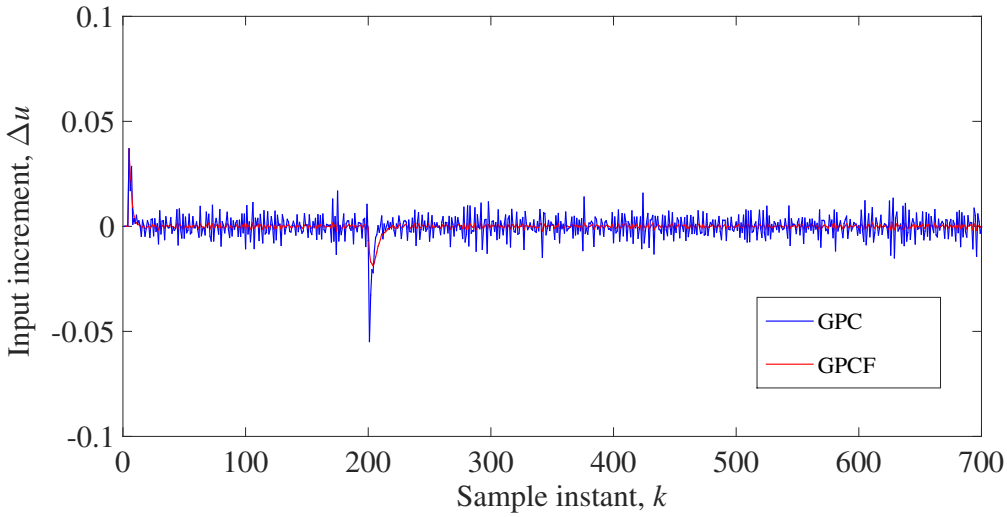

Figure 2.22: Change in control input response for model $G_3(z^{-1})$ in presence of noise and disturbance

Effect of random noise can be observed from these numerical simulation results. From these simulation results it can be observed that the variation in control input and consequently in change in control input is considerably high in GPC where as it has be significantly reduced in GPCF. Simulation results are shown in Figure 2.20 in presence of an input step disturbance for GPC and GPCF. It can be observed from the output responses in Figure 2.20 that the effect of disturbance in GPCF is prominent than the GPC. Similarly control input and change in control input responses are shown in Figure 2.21 and 2.22 respectively. Effect of step disturbance can be observed from these simulation results.

2.8 Summary

It can be concluded from these simulation results presented in this chapter, that by including a filter, the sensitivity might improve or degrade, which needs to be analyzed. Hence, filter in CARIMA model is considered as a design parameter.

Although sensitivity might improve, it makes the design procedure much more complicated as the number of tuning parameters also increase. Most of the tuning rules available in the literature are heuristic in nature or based on extensive simulations. Hence, a generalized expression for the FOPDT plant model is presented in the next chapter.

CHAPTER 3

PROPOSED ANALYTICAL TUNING RULE OF GPC FOR FOPDT SYSTEM

3.1 Introduction

An accurate analytical tuning methodology has its advantages over the heuristic method in its ability to evaluate the right controller parameters. As GPC is a model-based predictive control, the plant model plays a crucial role in determining the efficiency of the overall closed-loop system output. As the order of the model increases, so does the complexity of the tuning algorithm for the controller. This increase in the computational burden is the primary disincentive to the industrial and practicable application of predictive control. Many plant models can be approximated to an FOPDT model [53], which provide an accurate performance response as the higher-order plant model. The approximated plant model is therefore used in this chapter to obtain the weight tuning rule for the closed-loop FOPDT plant model. The tuning of the GPC is not as simple as the classical controller. One of the main limitation of GPC is that the number of design variables are more than any traditional controller. The GPC has the prediction horizon, the control horizon and the cost function weights typically as

the primary tuning parameters. The impact of these tuning parameters affect the efficiency and stability of the closed-loop system, which was provided in Chapter 2. Detailed analysis findings on many tuning parameters in the literature [31, 54] demonstrate that the heuristic nature of the tuning rule is often used to avoid complex derived formulas for higher and non-linear systems. Attempts have been made to derive an inter-relationship between GPC tuning parameters and plant model parameters for a low-order linear plant model to obtain the desired closed-loop specification, but this is not easy to formulate. Shreedhar and Cooper [32,33] have proposed a tuning system in which weights are calibrated for the DMC such that there is no singular value for the cost function. Therefore, trial and error as well as bound on constraints are mostly preferred for tuning of predictive control.

An analytical tuning rule derivation is usually a complicated process hence limited formula based tuning results are available for tuning of weights in GPC. In an optimization-based control technique, output or error weight in the cost function is incorporated to penalize tracking error signal or optimized control effort respectively, so that the desired plant performance is achieved with minimum input effort. One of the simple weight tuning algorithm proposed by Rowe and Maciejowski [55] in 1999 is based on infinite horizon LQG control, assuming weights on the rate of change of control input has a unity matrix. A state-space model is used for plant model, and output weights are tuned by using an obtained expression for a minimum phase system as C^TC, where C is the output matrix in a state-space representation of a model. In 2000, Rowe and Maciejowski [56] proposed tuning of the output weight matrix for non-minimum phase system by using H_∞ loop shaping method. Similarly, tuning rules for SOPDT plant models in GPC algorithm [57, 58] and non-minimum multi-variable plants have also been derived [59]. Lee and Yu [60] have proposed tuning of the FOPDT model using regression analysis for DMC. Sensitivity function of closed-loop MPC is used by

Shah and Engell [61] to tune MPC which satisfies closed-loop specifications. Other than output and error weight, the rate of change in control input is also penalized by input weight in the cost function. By penalizing the change in control input, the designer is limiting the variation in control input which might cause fatigue in a plant. The rate-of-change-of-input (Δu) weights can be used as a constraint to minimize control effort. The input weight helps in achieving a robust controller design at the cost of the slower or sluggish controller. Setting a small penalty gives a more aggressive controller that is less robust. Apart from analytical expression, numerical optimization method has also been proposed so that it gives an optimal solution for a constrained cost function which satisfies specifications for specified time-domain characteristic [62]. In [63, 64], a convex optimization method is implemented to tune the weight matrices of the cost function, which drives the plant to the desired closed-loop system. For a reverse engineering based convex optimization weight tuning method, it was assumed that the constraints are inactive to simplify this complicated numerical approach. The inverse optimization method is not widely implemented, as a solution is not guaranteed for an inverse optimization problem. Even though several analytical expressions have been formulated, the tuning guideline derived in most literature is challenging to understand; hence most control designers follow trial and error approach to tune GPC.

In this chapter, an analytical tuning formula of GPC has been derived for an FOPDT plant model which ensures stability and desired closed-loop performance for a SISO system. This tuning rule is derived for a stable SISO FOPDT plant model as most of the higher-order system can be approximated to an FOPDT plant model which gives accurate plant response for higher range of frequency. A generalized mathematical expression for tuning of weights has been proposed, which guarantees closed-loop stability of the controlled system. If the closed-loop

response is stable, then there exists a weight which guarantees the stability of the overall system.

3.2 Derivation of analytical expression

Predictive control is a model-based control strategy where the model of the actual plant is explicitly used only to obtain the output prediction. In GPC, the optimized control input is evaluated at each instant of sampled time, and only the first element of the obtained optimized control sequence is implemented as the manipulated variable for the plant. The target here is to predict future output response for a chosen prediction horizon so that it follows a given reference signal using an optimized control effort. To achieve such an objective, usual expression of the cost function is presented as in (3.1)

$$J = \sum_{i=0}^{N} \delta(i)[\hat{y}(k+i|k) - w(k+i)]^2 + \sum_{i=0}^{M-1} \lambda(i)[\Delta u(k+i)]^2 \tag{3.1}$$

where $\hat{y}(k+i|k)$ is the i-step ahead output prediction, $\Delta u(k+i)$ is the future optimized control input, Δ is the difference operator, $w(k+i)$ is the future reference, N is the prediction horizon, M is control horizon, and the weighting sequences are defined as $\delta(i)$ and $\lambda(i)$. Let the plant dynamics be represented by an FOPDT model

$$G_m(s) = \frac{K_p}{\tau s + 1} e^{-\theta_d s} \tag{3.2}$$

where θ_d is the delay time in the plant, K_p and τ are plant parameters. The corresponding discrete transfer function of the model with a sampling time T_s is obtained as

$$G_m(z^{-1}) = \frac{b}{1 - az^{-1}} z^{-d} \tag{3.3}$$

where $a = e^{-T_s/\tau}$, $b = K_p(1 - e^{-T_s/\tau})$ and $d = \theta_d/T_s + 1$ are the parameter of the discretized model (3.3). The first step of predictive control is to obtain the output prediction by using the model of the plant. The prediction equation in CARIMA model is represented as

$$(1 - az^{-1})y_k = bz^{-d}u_k + \frac{F(z^{-1})e_k}{\Delta(z^{-1})} \tag{3.4}$$

where $F(z^{-1})$ is the filter component which is assumed to be 1 in this chapter for simplicity. Equation (3.4) is rearranged to obtain the output prediction equations by successive recursion of one step ahead prediction of (3.4)

$$(1 - az^{-1})\Delta(z^{-1})y_{k+d} = b\Delta(z^{-1})u_k + e_{k+d} \tag{3.5}$$

By assuming zero-mean Gaussian noise, which makes the predicted value of e_k to be zero, the prediction model of the considered system is obtained by recursion of one step ahead prediction model, instead of using a diophantine equation. One step ahead output prediction model is written as

$$\hat{y}_{k+d+1} - (1 + a)\hat{y}_{k+d} + a\hat{y}_{k+d-1} = b\Delta u_k \tag{3.6}$$

where $\hat{y}$ representation is the predicted output sequence notation used in this chapter. By applying receding horizon control and $\Delta u_{k+M} = 0$ for $M \geq 1$ and assuming $N \geq M$, output prediction equations have been obtained. Similarly, the prediction equations for N prediction horizon and M control horizon are represented as

$$C_D\hat{y}_p = C_N u_p - H_D\hat{y}_1 \tag{3.7}$$

where

$$C_D = \begin{bmatrix} 1 & 0 & \dots & 0 \\ -(1+a) & 1 & \dots & 0 \\ a & -(1+a) & \dots & 0 \\ \vdots & \vdots & \dots & \vdots \end{bmatrix}; \quad H_D = \begin{bmatrix} -(1+a) & a \\ a & 0 \\ \vdots & \vdots \end{bmatrix};$$

$$C_N = \begin{bmatrix} b & 0 & \dots & 0 \\ 0 & b & \dots & 0 \\ \vdots & \vdots & \dots & \vdots \end{bmatrix}; \quad \hat{y}_p = \begin{bmatrix} \hat{y}_{k+d+1} \\ \hat{y}_{k+d+2} \\ \vdots \\ \hat{y}_{k+d+N} \end{bmatrix};$$

$$u_p = \begin{bmatrix} \Delta u_k \\ \Delta u_{k+1} \\ \vdots \\ \Delta u_{k+M-1} \end{bmatrix}; \quad \hat{y}_1 = \begin{bmatrix} \hat{y}_{k+d} \\ \hat{y}_{k+d-1} \end{bmatrix} \tag{3.8}$$

Equation (3.7) can be further simplified as

$$\hat{y}_p = Gu_p + S\hat{y}_1 \tag{3.9}$$

where the coefficient matrices are obtained $G = C_D^{-1}C_N$ and $S = -C_D^{-1}H_D$. Ele-

ments of matrices G and S are obtained as in (3.10)

$$G = \begin{bmatrix} b & 0 & \dots & 0 \\ (a+1)b & b & \dots & 0 \\ \vdots & \vdots & \ddots & \vdots \\ \sum_{i=0}^{N-1} a^i b & \sum_{i=0}^{N-2} a^i b & \dots & b \end{bmatrix}; \quad S = \begin{bmatrix} (a+1) & -a \\ (a^2+a+1) & -(a^2+a) \\ \vdots & \vdots \\ \sum_{i=0}^{N} a^i & -\sum_{i=1}^{N} a^i \end{bmatrix} \tag{3.10}$$

From (3.10), matrix S can be represented as two columns of entries S_1 and S_2 as in (3.11)

$$S = \begin{bmatrix} S_1 & -S_2 \end{bmatrix} \tag{3.11}$$

where S_1 and S_2 are column vectors whose sum gives a vector having all the elements 1. The second step of GPC is to obtain the optimal control input for the plant model. To obtain the optimal control input, (3.1) is the chosen cost function for this chapter. After solving this unconstrained optimal problem, obtained optimal control is represented as

$$u_p = (G^T Q_\delta G + Q_\lambda)^{-1} G^T Q_\delta [1_n w_k - S_2 \Delta \hat{y}_{k+d} - 1_n \hat{y}_{k+d}] \tag{3.12}$$

where weight matrices Q_δ and Q_λ are positive definite diagonal matrices having elements $\delta(i)$ and $\lambda(i)$ respectively. 1_n is a vector having all the elements 1. u_p is the optimized control input signal having dimension with respect to the control horizon of the GPC. So, using receding horizon algorithm only the first row of Δu_k value is computed in (3.13) , which is given by

$$\Delta u_k = K_{w_1}[w_k - \hat{y}_{k+d}] - K_{y_1} \Delta \hat{y}_{k+d} \tag{3.13}$$

where

$$\begin{bmatrix} K_{w_1} & K_{w_2} & \dots & K_{w_M} \end{bmatrix}^T = K_w = (G^T Q_\delta G + Q_\lambda)^{-1} G^T Q_\delta I_p \tag{3.14}$$

$$\begin{bmatrix} K_{y_1} & K_{y_2} & \dots & K_{y_M} \end{bmatrix}^T = K_y = (G^T Q_\delta G + Q_\lambda)^{-1} G^T Q_\delta S_2 \tag{3.15}$$

Block diagram of the obtained control strategy in (3.13) is shown in Figure 3.1. Assuming that there is no mismatch in CARIMA model and there is no filter used,

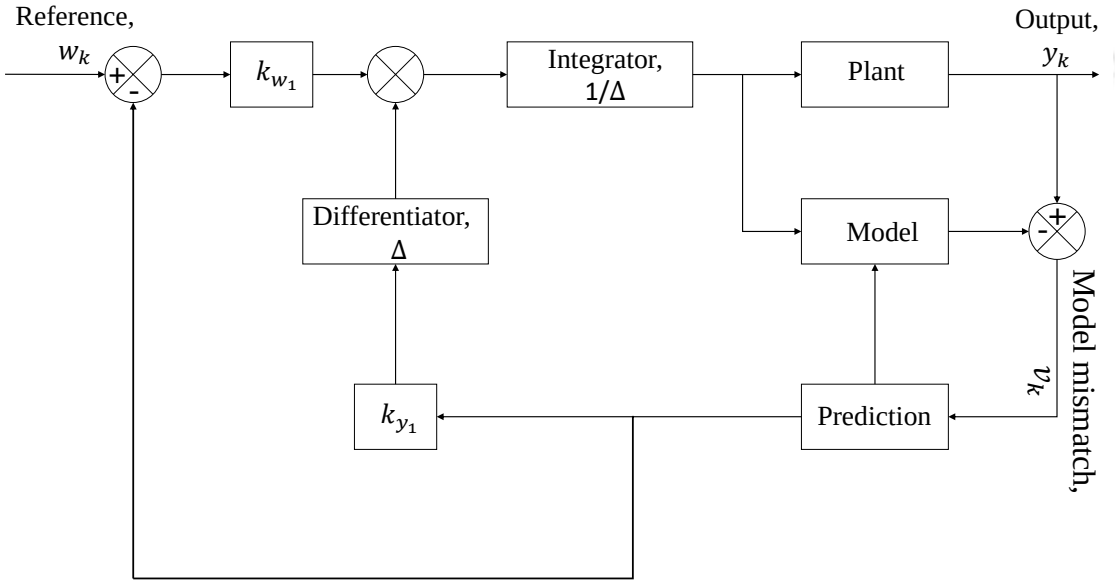

Figure 3.1: Block diagram representation of derived closed-loop model of GPC in Eq. (3.13)

(3.13) can be modified as the closed loop transfer function which is represented as

$$G_{cl} = \frac{bK_{w_1} z^{(1-d)}}{1 + (-1 - a + bK_{w_1} + bK_{y_1}) z^{-1} + (a - K_{y_1}) z^{-2}} \tag{3.16}$$

From (3.16), it can be observed that the GPC closed-loop transfer function of an

FOPDT plant model is actually an SOPDT model if the there is no model mismatch. By applying Jury's stability criteria [65] the stability conditions achieved are

$$K_{w_1}>0 \tag{3.17}$$

$$K_{w_1}>2(K_{y_1}-a-1) \tag{3.18}$$

$$(K_{w_1}+a+1)>K_{y_1}>(K_{w_1}+a-1) \tag{3.19}$$

3.2.1 Plant model mismatch

Let the exact predicted output for a model be represented as

$$\hat{y}_{k+d-1} = a^{d-1}y_k + b\left(a^{d-2}u_{k-d} + \cdots + au_{k-2} + u_{k-1}\right) + v_k \tag{3.20}$$

where v_k is the model prediction mismatch of output response defined as

$$v_k = \hat{y}_p - y_k \tag{3.21}$$

A plant of higher order can be represented as

$$\frac{y_k^p(z^{-1})}{u_k} = \frac{B(z^{-1})}{A(z^{-1})} \tag{3.22}$$

The approximated FOPDT model is denoted as in (3.3). To determine the plant model mismatch, (3.3) is substituted in (3.20) and it yields

$$\hat{y}_{k+d-1} = a^{d-1}y_k + \frac{b}{1-az^{-1}}z^{-d} + v_k \tag{3.23}$$

Hence the prediction mismatch can be obtained as

$$v_k = \left(\frac{B(z^{-1})}{A(z^{-1})} - \frac{b}{1 - az^{-1}} z^{-d} \right) u_k \tag{3.24}$$

which can be simplified to

$$\hat{y}_{k+d} = \left(1 + b \frac{z^{-1} - z^{-d}}{1 - az^{-1}} \frac{A(z^{-1})}{B(z^{-1})} \right) y_k^p \tag{3.25}$$

Once the prediction of the output is obtained, the optimized control input in (3.13) can be modified as

$$\Delta u_k = K_{w_1} w_k - \hat{y}_{k+d} \left(K_{w_1} + \Delta K_{y_1} \right) \tag{3.26}$$

Therefore, substituting the value of $\hat{y}_{k+d}$ in (3.26) it yields the optimized control input sequence expressed as

$$\Delta u_k = K_{w_1} w_k - \left(1 + b \frac{z^{-1} - z^{-d}}{1 - az^{-1}} \frac{A(z^{-1})}{B(z^{-1})} \right) \left(K_{w_1} + \Delta K_{y_1} \right) y_k^p \tag{3.27}$$

Hence the final closed-loop model of the system for higher order plant model is represented as

$$G_{cl} = \frac{K_{y_1}(1 - az^{-1}) N(z^{-1})}{P_{cl}} \tag{3.28}$$

where

$$P_{cl} = \Delta(1 - az^{-1}) D(z^{-1}) + \left((1 - az^{-1}) N(z^{-1}) + b(z^{-1} - z^{-d}) D(z^{-1}) \right) \times \left(K_{w_1} + \Delta K_{y_1} \right) \tag{3.29}$$

Roots of P_{cl} can be placed for a desired specified plant characteristic. As it can be observed from (3.29), roots of P_{cl} depends on the chosen weight matrix for the cost function. Hence, in the subsequent section an anlytical formula has been

derived to calculate the weight matrix of the cost function. So, the closed-loop system poles can be placed at a desired value, if the chosen specification satisfies the feasible gain criteria.

3.3 Tuning rule for GPC

In this section, generalized tuning formula for control horizon of one is obtained when there are no active constraints available. Using (3.16) and inequalities in Jury's stability criteria, the closed-loop poles can be placed at a desired location which can be solved analytically. However it is not guaranteed that the closed-loop poles with desired specification can be placed arbitrarily. To place the desired closed-loop poles in the feasible region which is obtained in (3.17), (3.18), and (3.19), the weight matrices are already defined in a pre-specified form.

3.3.1 Control horizon of one

A generalized expression for control horizon of one is formed by simplifying (3.14) and (3.15).

$$K_{w_1} = \frac{\delta(i)\sum_{i=0}^{l} a^i}{b\left(\left(\sum_{i=0}^{l} a^i\right)^2 \delta(i) + \lambda(i)\right)} \qquad l = 0, 1, ..., (N-1) \tag{3.30}$$

$$K_{y_1} = \frac{a\left(\delta(i)\left(\sum_{i=0}^{l} a^i\right)^2\right)}{b\left(\left(\sum_{i=0}^{l} a^i\right)^2 \delta(i) + \lambda(i)\right)} \qquad l = 0, 1, ..., (N-1) \tag{3.31}$$

As it has already been explained weights of the tuning matrices play a significant role in system performance than other tuning parameters of a GPC, the chosen

weight matrix form is represented as

$$Q_\delta = \begin{bmatrix} 1 & 0 & 0 & \dots & 0 \\ 0 & 1 & 0 & \dots & 0 \\ \vdots & \vdots & \vdots & \ddots & \vdots \\ 0 & 0 & 0 & \dots & q \end{bmatrix}_{N\times N} \quad , \quad Q_\lambda = b^2 \begin{bmatrix} r \end{bmatrix}_{1\times 1} \tag{3.32}$$

To simplify, new variables X_N and Y_N are defined as

$$X_N = \sum_{i=1}^{N} \left(\frac{1-a^i}{1-a}\right)^2, Y_N = \sum_{i=1}^{N} \left(\frac{1-a^i}{1-a}\right) \tag{3.33}$$

Considering an arbitrary prediction horizon which satisfies the inequalities (3.40), the weights to be tuned for GPC in (3.32) is obtained as

$$q = \frac{Y_b K_{yd_1} - aX_b K_{wd_1}}{X_a(aX_a K_{wd_1} - K_{yd_1})} \tag{3.34}$$

$$r = \frac{a - K_{yd_1}}{K_{yd_1}}(X_b + qX_a^2) \tag{3.35}$$

where r and q are chosen to be positive. Hence, it can be stated that

$$\frac{a - K_{yd_1}}{K_{yd_1}} > 0 \Rightarrow a > K_{yd_1} > 0 \tag{3.36}$$

Similarly,

$$\frac{Y_b K_{yd_1} - aX_b K_{wd_1}}{X_a(aX_a K_{wd_1} - K_{yd_1})} > 0 \tag{3.37}$$

$$\Rightarrow Y_b K_{yd_1} > aX_b K_{wd_1}$$

and (3.38)

$$\Rightarrow aX_a K_{wd_1} > K_{yd_1} \tag{3.39}$$

For weight matrix representation in (3.32), the desired feasible gains K_{wd_1} and

K_{yd_1} can be summarized for control horizon one by the inequality criteria as follow

$$K_{wd_1} > 0 \tag{3.40}$$

$$a > K_{yd_1} > 0 \tag{3.41}$$

$$aX_a > \frac{K_{yd_1}}{K_{xd_1}} > \frac{X_b}{Y_b} \tag{3.42}$$

where

$$X_a = 1 + a + ... + a^{N-1}$$
$$X_b = 1 + (1+a)^2 + (1+a+a^2)^2 + ... + (1+a+...+a^{N-1})^2$$
$$Y_b = 1 + (1+a) + (1+a+a^2) + ... + (1+a+...+a^{N-1})$$

The weight matrix can also be defined as a diagonal matrix, in which elements of the matrix is the scalar multiple of identity matrix. For a non diagonal matrix, formulation of a generalized tuning rule for every element of the weight matrix is quite difficult. Hence, Q_δ and Q_λ are defined as

$$Q_\delta = \begin{bmatrix} q & 0 & 0 & \dots & 0 \\ 0 & q & 0 & \dots & 0 \\ \vdots & \vdots & \vdots & \ddots & \vdots \\ 0 & 0 & 0 & \dots & q \end{bmatrix}_{N\times 1} \quad , \qquad Q_\lambda = b^2 \begin{bmatrix} r \end{bmatrix}_{1\times 1} \tag{3.43}$$

Similar to (3.36) and (3.37), the inequality conditions are defined as

$$\frac{1+a}{a} > K_{w_1} > \frac{1-a}{a} \tag{3.44}$$

$$K_{y_1} < \frac{2+2a}{1+2a} \tag{3.45}$$

for a feasible pole placement.

3.3.2 Control horizon of two

Considering control horizon of two, it can be represented as the gain matrices as

$$\begin{bmatrix} K_{w_1} \\ K_{w_2} \end{bmatrix} = K_w = (G^T Q_\delta G + Q_\lambda)^{-1} G^T Q_\delta I_p \tag{3.46}$$

$$\begin{bmatrix} K_{y_1} \\ K_{y_2} \end{bmatrix} = K_y = (G^T Q_\delta G + Q_\lambda)^{-1} G^T Q_\delta S_2 \tag{3.47}$$

With more simpler notation (3.46) and (3.47) are represented in matrix form as

$$\begin{bmatrix} X_{aa} + r_{aa} & X_{ab} \\ X_{ba} & X_{bb} + r_{bb} \end{bmatrix} \begin{bmatrix} K_{y_1} & K_{w_1} \\ K_{y_2} & K_{w_2} \end{bmatrix} = \begin{bmatrix} aX_{aa} & Y_{ab} \\ aX_{ba} & Y_{bb} \end{bmatrix} \tag{3.48}$$

where r_{aa} and r_{bb} are the input weight matrices and the matrix elements in (3.48) can be expressed in (3.33) as

$$X_{aa} = \delta(i) X_i \qquad i = 1, 2, ...N \tag{3.49}$$

$$X_{ab} = \delta(i) Y_{i-1} Y_i \qquad i = 2, 3, ...N \tag{3.50}$$

$$X_{bb} = \delta(i) X_{i-1} \qquad i = 2, 3, ...N \tag{3.51}$$

$$Y_{aa} = \delta(i) Y_i \qquad i = 1, 2, ...N \tag{3.52}$$

$$Y_{bb} = \delta(i) Y_{i-1} \qquad i = 2, 3, ...N \tag{3.53}$$

where these elements are derived from X_N and Y_N. Solving (3.48) for r_{aa} and r_{bb}

$$\begin{bmatrix} X_{aa}K_{y_1} + r_{aa}K_{y_1} + X_{ab}K_{y_2} & X_{aa}K_{w_1} + r_{aa}K_{w_1} + X_{ab}K_{w_2} \\ X_{ba}K_{y_1} + X_{bb}K_{y_2} + r_{bb}K_{y_2} & X_{ba}K_{w_1} + X_{bb}K_{w_2} + r_{bb}K_{w_2} \end{bmatrix} = \begin{bmatrix} aX_{aa} & Y_{ab} \\ aX_{ba} & Y_{bb} \end{bmatrix} \tag{3.54}$$

From (3.54), r_{aa} and r_{bb} can be obtained as

$$r_{aa} = \frac{1}{K_{y_1}} \left(aX_{aa} - X_{ab}K_{y_2} - X_{aa}K_{y_1} \right) \tag{3.55}$$

$$= \frac{1}{K_{w_1}} \left(Y_{ab} - X_{ab}K_{w_2} - X_{aa}K_{w_1} \right) \tag{3.56}$$

$$r_{bb} = \frac{1}{K_{y_2}} \left(aX_{ba} - X_{bb}K_{y_2} - X_{ba}K_{y_1} \right) \tag{3.57}$$

$$= \frac{1}{K_{w_2}} \left(Y_{bb} - X_{bb}K_{w_2} - X_{ba}K_{w_1} \right) \tag{3.58}$$

To achieve the desired performance which satisfies the required inequality criteria, weights are evaluated as follow

$$r_{aa} = \frac{(Y_{aa}X_{ab} - X_{aa}Y_{bb})(a - K_{y_1})}{aX_{ab}K_{w_1} - Y_{bb}K_{y_1}} \tag{3.59}$$

$$r_{bb} = \frac{(Y_{aa}X_{bb} - X_{ab}Y_{bb})(K_{y_1} - aK_{w_1})}{aX_{bb}K_{w_1} - Y_{11}K_{y_1}} \tag{3.60}$$

It can be observed that

$$X_{aa}X_{bb} - X_{ab}^2 = Y_{aa}X_{ab} - X_{aa}Y_{bb} \tag{3.61}$$

$$Y_{aa}X_{ab} - X_{aa}Y_{bb} > 0 \tag{3.62}$$

$$Y_{aa}X_{bb} - X_{ab}Y_{bb} > 0 \tag{3.63}$$

Similar to (3.36) and (3.37), inequality criteria can be obtained by choosing the cost function weights as positive value. For control horizon of two the feasible region for achieving desired gain is obtained similarly as in control horizon of one. The final inequality criteria for r_{aa} and r_{bb} are obtained as

$$K_{w_1} > 0 \tag{3.64}$$

$$a > K_{y_1} > 0 \tag{3.65}$$

$$\frac{aX_{aa}}{Y_{aa}} > \frac{K_{y_1}}{K_{w_1}} > a \tag{3.66}$$

Generalized expression for higher control horizon three, four etc. is not performed as the derivation and inequality criteria is very difficult to obtain. The desired performance can be achieved with the proposed tuning algorithm for control horizon of one and two for the chosen plant model instead of deriving complicated mathematical expression which is not only difficult to derive but also the performance does not improve significantly as compared to lower values of control horizon.

3.4 Stability analysis of cost function

A Lyapunov function is a scalar function defined on the phase space, which can be used to prove the stability of an equilibrium point. In this section stability of the chosen cost function has been proved.

Definition 1 Let a function $Z^o(x)$ be continuously differentiable in a neighborhood U of the origin. The function $Z^o(x)$ is called the Lyapunov function for an autonomous system $\dot{x} = f(x)$, if the following conditions are met:

1. $Z^o(x) > 0$ for all $x \neq 0$ and $x \in U$.
2. $Z^o(0) = 0$;
3. $\frac{dZ^o}{dt} \leq 0$ for all $x \in U$

If in a neighborhood U of the zero solution $x = 0$ of an autonomous system there is a Lyapunov function $Z^o(x)$, then the equilibrium point $x = 0$ of the system is stable in the sense of Lyapunov. The system is said to be asymptotically stable in the sense of Lyapunov, if $\frac{dZ^o}{dt} < 0$ for all $x \in U$.

The necessary condition for stability of a cost function is the feasibility of the chosen optimal cost function solution at each sample instant. For unique solution of the control law a convex cost function is chosen. A discrete Lyapunov function stability approach is considered as the derived control law is discrete in nature. Hence difference operator is used instead of derivative of a function. Stability of the cost function can be proved if the cost function satisfies the Lyapunov stability criteria. The minimum of the finite horizon cost function (J_{min}) is chosen as the Lyapunov function, $Z^o(e_i)$. $e_i = w_i - \hat{y}_i$ is defined as the tracking error in the cost function.

Theorem 3.1 *To show that $Z^o(e_i)$ is asymptotically stable these criteria are to be satisfied.*

1. $Z^o(f(e_i)) = 0 \quad \forall\ e_i = 0$
2. $Z^o(f(e_{i+1})) \leq Z^o(f(e_i)) \quad \forall\ i > 0$
3. $\Delta Z^o(f(e_{i+1})) \leq 0 \quad \forall\ i > 0$

Proof: The Lyapunov value function $Z^o(f(e_i)) = \min_{\Delta u}\{Z(e_i, \Delta u_i)\}$ is assumed to be the optimal value of the cost function. Stability of the cost function is proved by assuming terminal constraint on tracking error, i.e. $e_{i+N} = 0$. The chosen Lyapunov function, Z^o is quadratic in nature hence it can be stated that $Z^o(f(e_i)) \geq 0$ and $Z^o(f(e_i)) = 0$ only if $f(e_i) = 0$. To show that $z(f(e_i)) = 0$ $\forall\ e(0) = 0$ and $\Delta u(0) = 0$ a new vector $v = \begin{bmatrix} e_i & \Delta u_i \end{bmatrix}^T$ can be defined. It is assumed, $\exists v \neq 0$ for which $z = v^T \begin{bmatrix} Q_\delta & 0 \\ 0 & Q_\lambda \end{bmatrix} v = 0$. Matrices Q_δ and Q_λ are considered to be diagonal in nature, hence z is positive definite as $\begin{bmatrix} Q_\delta & 0 \\ 0 & Q_\lambda \end{bmatrix}$ is

positive definite. $z = 0$ when $v = 0$, which contradicts original assumption. The second condition can be proved by defining $Z^o(f(e_{i+1}))$ as

$$Z^o(f(e_{i+1})) = \min_{\Delta u}\{Z(e_{i+1}, \Delta u_{i+1})\} \quad \forall \quad i > 0 \tag{3.67}$$

$$= f(e_{N+i+1}, \Delta u_{M+i+1}) + Z^o(f(e_i)) - f(e_1, \Delta u_1) \tag{3.68}$$

$$\leq Z^o(f(e_i)) - f(e_1, \Delta u_1) \quad \forall \quad i > 0 \tag{3.69}$$

Assuming the final value of the tracking error to be zero i.e. $f(e_{N+i+1}, \Delta u_{M+i+1}) = 0$, (3.67) can be expressed as

$$Z^o(f(e_{i+1})) \leq Z^o(f(e_i)) \quad \forall \quad i > 0 \tag{3.70}$$

Next criteria to be satisfied is $\Delta Z^o(f(e_{i+1})) \leq 0, \forall i \geq 0$. Therefore, ΔZ^o is expressed as

$$\Delta Z^o(f(e_{i+1})) = Z^o(f(e_{i+1})) - Z^o(f(e_i)) \quad \forall \quad i > 0 \tag{3.71}$$

Hence, to obtain the difference of Lyapunov function $\Delta Z^o(f(e_{i+1})) \leq 0$, from (3.69) it can be obtained that

$$Z^o(f(e_{i+1})) \leq Z^o(f(e_i)) - f(e_1, \Delta u_1) \quad \forall \quad i > 0 \tag{3.72}$$

$$Z^o(f(e_{i+1})) - Z^o(f(e_i)) \leq -f(e_1, \Delta u_1) \quad \forall \quad i > 0 \tag{3.73}$$

$$\Delta Z^o(f(e_{i+1})) \leq 0 \quad \forall \quad i > 0 \tag{3.74}$$

Hence, it has been proved that the tracking error is converging in nature. Therefore, the error converges to zero as the chosen function is stable in the sense of Lyapunov.

3.5 Numerical simulation results

To verify the tuning guideline presented in this chapter, two examples are presented. As most of the industrial process and power converters are represented in lower order delayed plant model, first example is an FOPDT plant model and the second example is a second order time delay plant model. In both the examples the weights of cost function are evaluated based on desired specified closed-loop performance. From the discrete closed-loop transfer function prediction horizon, control horizon and gains of the control law are evaluated based on inequality criteria derived in this chapter.

3.5.1 Example 1

An FOPDT plant model [3] $G_{m1} = \dfrac{1.5e^{-4s}}{10s+1}$ is chosen to validate effectiveness of the proposed tuning rule. Selecting sampling time, $T_s = 1$ sec, the corresponding discretized transfer function model is $G_{d1}(z^{-1}) = \dfrac{0.14z^{-5}}{1-0.9z^{-1}}$. Let us design a GPC controller for the chosen plant model, which has a closed-loop performance of maximum overshoot of 10% and settling time of 25 sec. Optimal gains are selected to be $K_{w1} = 0.4$ and $K_{y1} = 0.2$, by comparing with the closed loop transfer function in (3.16). The chosen gain satisfies the inequality criteria in (3.17), (3.18), (3.19). Let us assume constraints on input and output as $u(n) \leq 0.8$, $\Delta u = 0.5$ and $y(n) \leq 1.5$ respectively to show the validity of derived tuning guideline even though this has been derived without considering active constraint. Prediction horizon is evaluated as $5 \leq N \leq 9$. Output response for desired closed-loop specification is shown in Figure 3.2 along with active constraint for reference tracking. Figure 3.3 shows optimized control input for the controlled plant model. From the obtained tuning guideline, optimal gain is chosen to be $K_{wd1} = 0.3$ and $K_{yd1} = 0.06$. Tuning parameters of G_{m1} is shown in Table 3.1. Weight matrices

are evaluated numerically for control horizon of one and two.

Table 3.1: Tuning parameters for G_{m1}

Model	$M = 1$	$M = 2$
$G_{m1} = \frac{1.5e^{-4s}}{10s+1}$	$q = 1.7$ $r = 150.76$	$Q_\lambda = \begin{bmatrix} 76.1 & 0 \\ 0 & 45.4 \end{bmatrix}$ $Q_\delta = I_N$

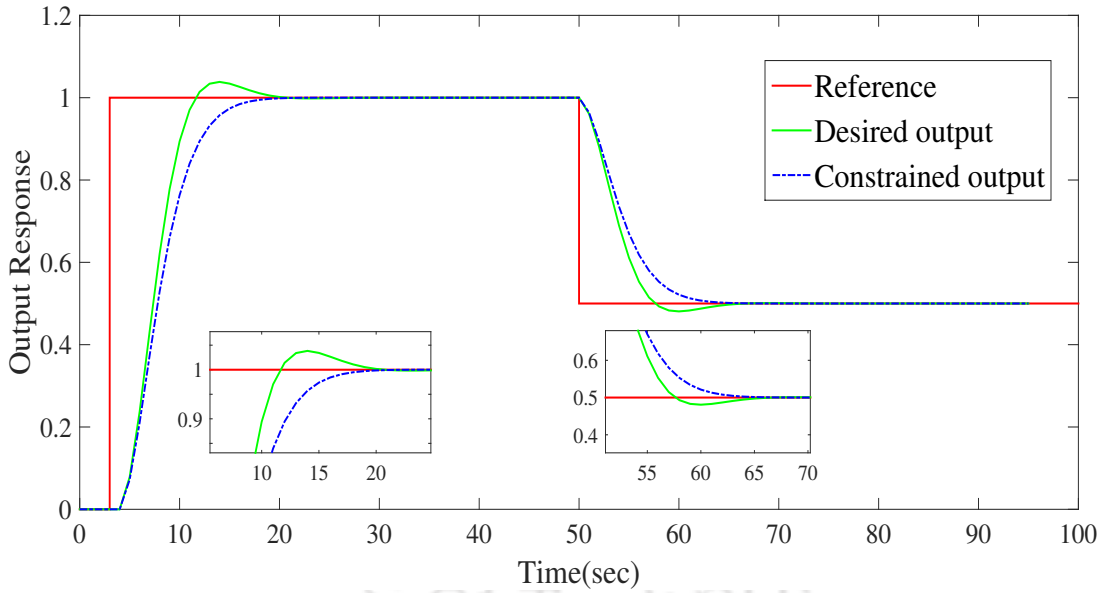

Figure 3.2: Closed-loop output response of G_{m1}

3.5.2 Example 2

In this example a second order time delay plant model is considered $G_{m2} = \frac{e^{-2s}}{(5s+1)(2s+1)}$. The approximated FOPDT model is represented as $\frac{e^{-3s}}{(6s+1)}$

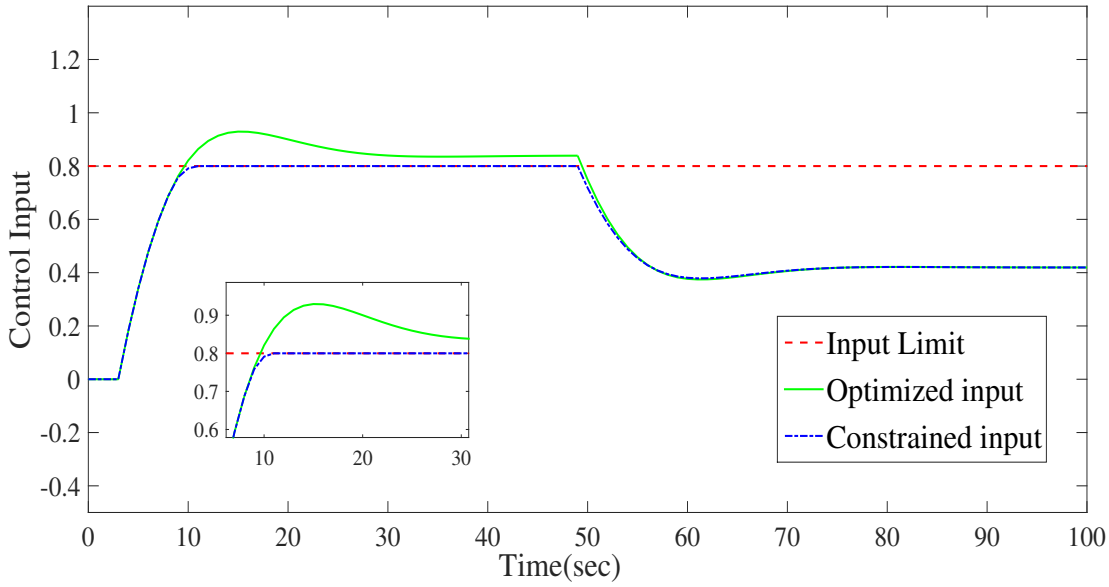

Figure 3.3: Optimized control input response of G_{m1}

The corresponding discretized first order plant model is represented as $G_{d2}(z^{-1}) = \frac{0.283z^{-4}}{1-0.726z^{-1}}$. After obtaining the discrete closed-loop transfer function, the range of feasible gain matrix is obtained. For this example a closed-loop output response with no overshoot is considered as desired specification with input constraint $u(n) \leq 2$. Figure 3.4 shows the desired closed-loop output response of plant model G_{m2}. can be observed. Note that, as per desired specification, the output responses with or without active constraints do not have overshoot. Similarly, the control input response is shown in Figure 3.5. From the obtained tuning guideline optimal gain is chosen to be $K_{wd1} = 0.27$ and $K_{yd1} = 0.05$. Tuning parameters of G_{m1} is shown in Table 3.2.

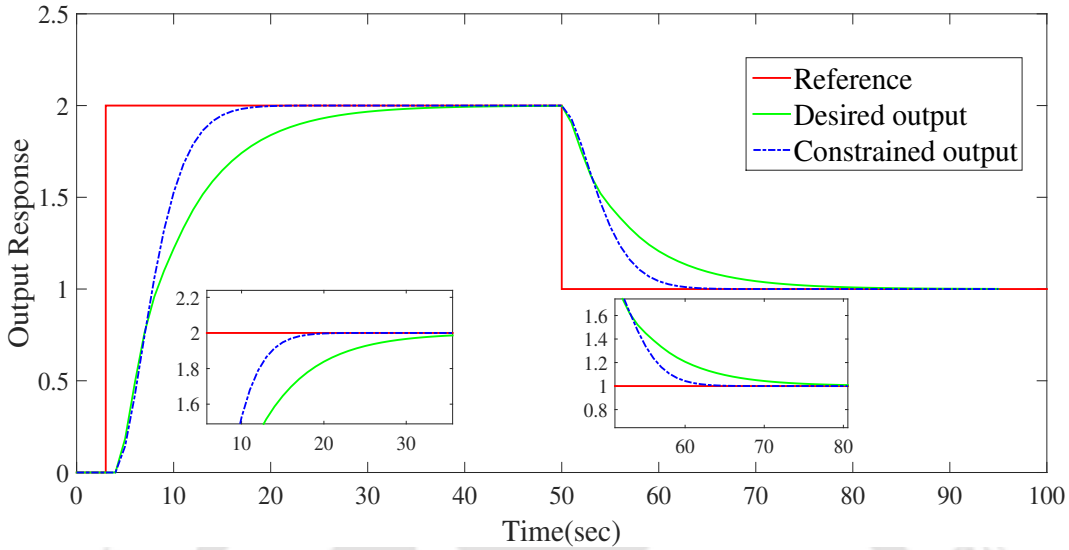

Figure 3.4: Closed-loop output response of G_{m2}

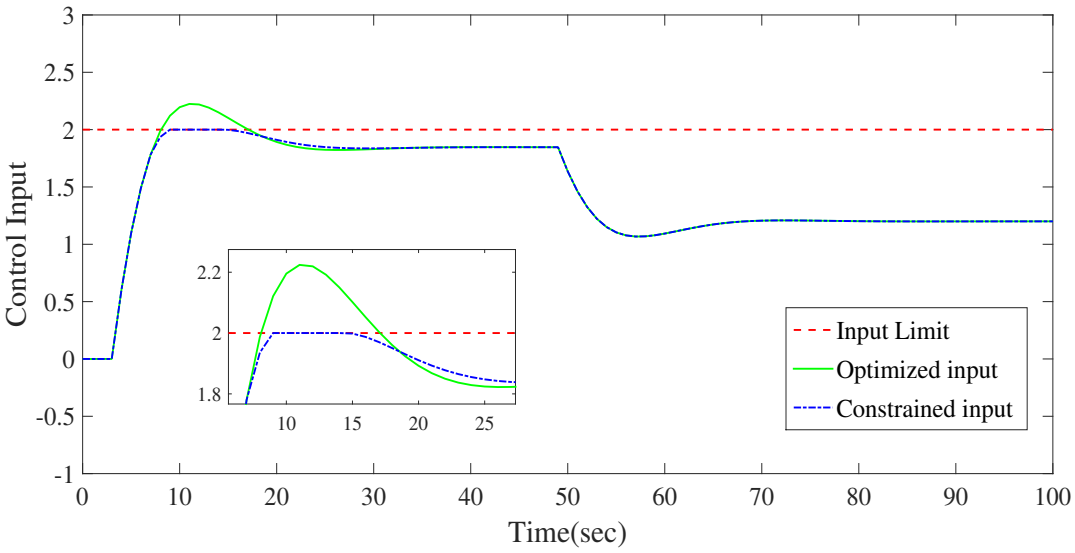

Figure 3.5: Optimized control input response of G_{m2}

Table 3.2: Tuning parameters for G_{m2}

Model	$M = 1$	$M = 2$
$G_{m2} = \dfrac{e^{-2s}}{(5s+1)(2s+1)}$	$q = 5.7$ $r = 101.02$	$Q_\lambda = \begin{bmatrix} 1070.1 & 0 \\ 0 & 831.5 \end{bmatrix}$ $Q_\delta = I_N$

3.6 Summary

GPC tuning formula for stable SISO FOPDT plant model is derived in this chapter. It is observed that a large value of control horizon increases the complexity as well as execution time of the controller without any significant improvement in the performance of the controlled system. From the simulation study it can be observed that, the proposed tuning formula is able to drive the closed-loop system to the specified time domain specifications. A generalized tuning expression for the weights of the cost function is derived in this chapter for a control horizon of one and two.

CHAPTER 4

PRE-COMPUTED GPC FOR DC-DC BUCK CONVERTER

4.1 Introduction

An advanced controller such as MPC or GPC is widely explored to control switching mode power supplies (SMPS) [66–70], because of its efficiency in increasing the overall plant performance and handling system complexities. However, a PI or a PID controller is recognized as the most commonly used control technique in the process control industry. The PID controller accounts for approximately 90% of all the available industrial controllers. However, plant model selection is the main limitation while designing a PI or PID controller. It is a well-known fact among control researchers that a PID controller's performance is compromised in the presence of plant dead time. For such closed-loop plant model, an appropriate measure is to inspect the performance of a satisfactory optimal control technique in place of the classical PID controller. Out of all the available advanced optimization-based control algorithm, GPC is gaining a lot more attention recently for its predictive nature of the controller since its introduction. However, the use of GPC is limited because of its complicated tuning guidelines and implementation cost. Typically,

the cost of an MPC or GPC constitutes around 70% of the total design cost of a system. SMPS operates in switching frequency range of kilohertz to megahertz is a challenging domain for GPC implementation. GPC was mainly preferred for slower dynamic plants, but faster processors overcame this barrier. It can be argued that the GPC might not be an appropriate choice for converter circuit as the controller designing complexity is much more than the plant complexity, but this is not justified as the converter is a fundamental building block of the electric vehicle, microgrid, and portable devices.

The cost function's online optimization is computationally intensive as GPC optimization process has to be executed at every sampling instant. Real-time computation of GPC has only been used till date in applications with relatively large time constants, e.g. petrochemical industry. As DC-DC converters can be modeled as linear systems, it is not necessary to solve the optimization online; therefore, the GPC algorithm can be implemented offline for the inactive constrained case. In this case, the cost function can be solved analytically producing a fixed linear control law, that can be implemented online. Because of this reason, pre-computed GPC is considered in this research work. Using an online optimization solver-based GPC increases the computation burden of evaluating the control law for each switching cycle. This time-consuming calculation is the main reason for less popularity of GPC in power converter. Although PID is not designed for optimal performance of the converter, a standard PID compensator is preferred because of its computational efficiency. Usually, compensator elements are tuned manually to set coefficients.

GPC design process follows a standard compensator design with optimized control law. Designing steps are as follows.

1. Selection of an accurate converter model.

2. Selection of the performance criteria of the plant.

3. Design of GPC compensator parameters.

4. Implementing the controller by using analog or digital components.

Block diagram of the designed GPC compensator is shown in Figure 4.1. Analog to digital converter (ADC) is required in the output feedback path to measure the converter output, which is compared with the reference signal to eliminate the closed-loop system's tracking error.

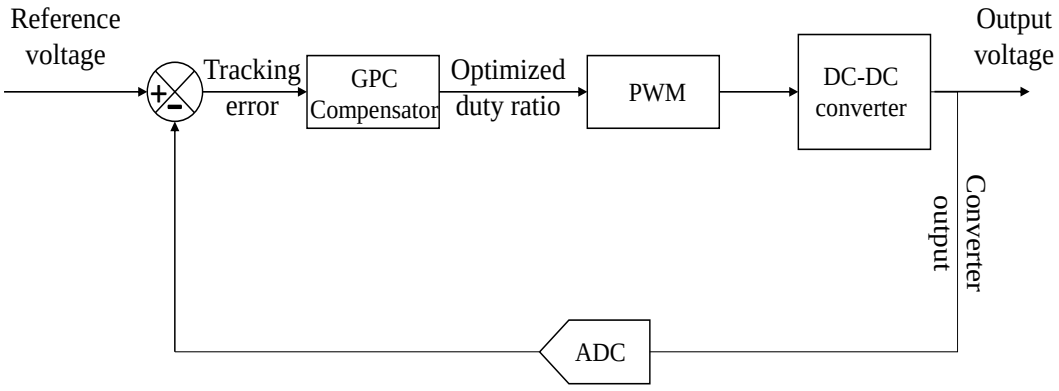

Figure 4.1: GPC compensator control loop for DC-DC buck converter

In this chapter, the performance of an unconstrained GPC is evaluated for a DC-DC buck converter in which the obtained control input is the duty ratio of the switch. Hence, this is essentially an input constrained control problem. Because of this reason, it is hard to stabilize the converter with a predefined feedback controller globally. Typically, control of converter is based on the measurement of inductor current and output voltage. Usually, a voltage measurement is more straightforward compared to the current measurement. The sensors used for the measurement of the inductor current is costlier than the voltage sensor. Hence, it is cost-effective to design an output-feedback controller for the converter voltage

mode control. The derived tuning algorithm for GPC is validated by conducting simulation and hardware experiment. During load and input variation, to eliminate the steady-state error, an outer PI loop is considered for the pre-computed GPC.

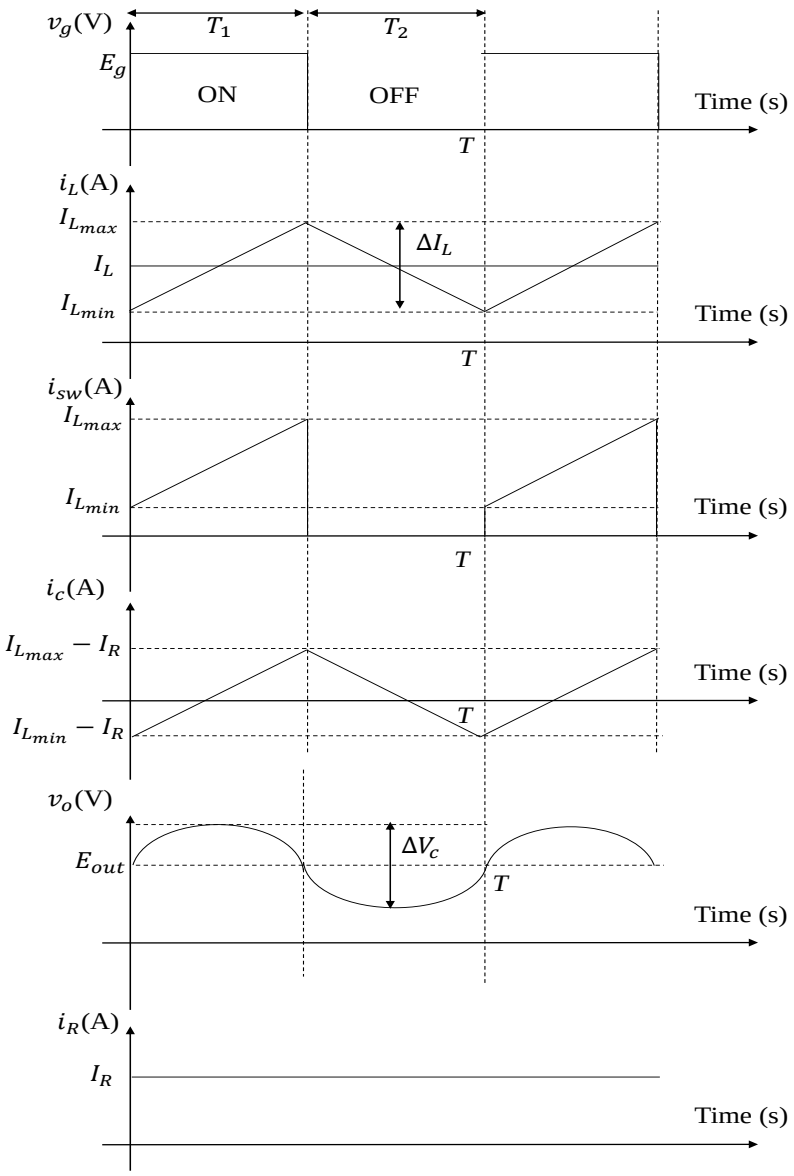

Figure 4.2: Switching cycle of SISO DC-DC buck converter

4.2 Operating principle

A brief introduction of the DC-DC buck converter is discussed in this section. While a buck converter is chosen to implement GPC, similarly, boost and buck-boost converter can also be chosen to design GPC as well. Switching cycle of the buck converter is shown in Figure 4.2. An ideal DC-DC buck converter circuit diagram is shown in Figure 4.3. From Figure 4.3, it can be observed that a buck converter consists of a DC source E_{in}, a switch S_w which is to be operated using a pulse width modulated (PWM) signal for a certain duty ratio (D_r), a freewheeling diode D, an inductor L, a capacitor C and a load. Here, it is considered that the load R is pure resistance in nature. In this circuit, output voltage across load R i.e. E_{out} is same as E_c which is voltage across capacitor C. Figure 4.4 and 4.5 are circuit diagrams of the buck converter when the switch is turned ON and OFF respectively. When the switch is ON, DC source supplies the input voltage and current flows through the inductor to the load. When the switch is turned OFF, the diode is in conduction mode as current does not change instantaneously in an inductor. Circuit parameters are obtained by solving circuit equations of the converter model using relevant electrical principles. The voltage drop across the inductor L is expressed as

$$E_L = L\frac{di_L}{dt} \tag{4.1}$$

When the switch is turned ON, inductor value increases from $I_{L_{min}}$ to $I_{L_{max}}$. From Figure 4.4, using Kirchhoff's voltage law, the voltage equation across L can be written as

$$E_{in} - E_{out} = L\frac{I_{L_{max}} - I_{L_{min}}}{T_1} = L\frac{\Delta I_L}{T_1} \tag{4.2}$$

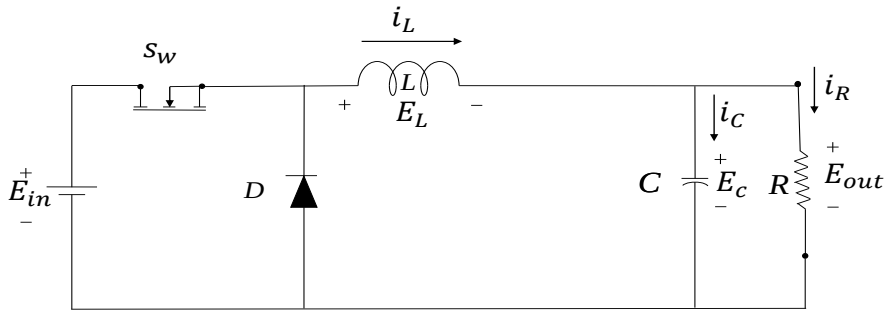

Figure 4.3: An ideal DC-DC buck converter circuit diagram for pure resistive load

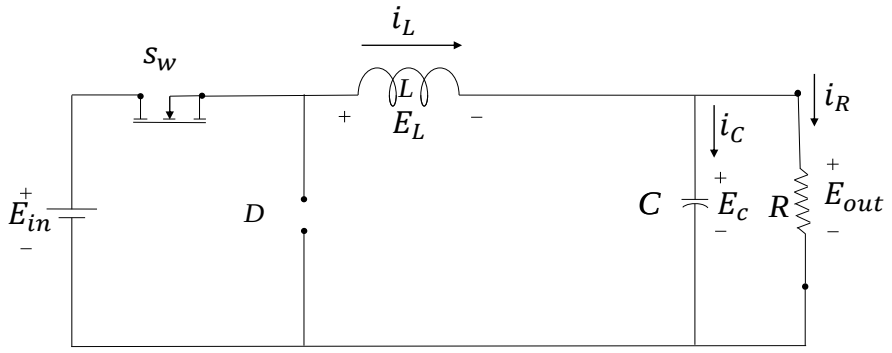

Figure 4.4: DC-DC buck converter circuit diagram when switch is ON

From (4.2), ON period T_1 is obtained as follows

$$T_1 = \frac{\Delta I_L L}{E_{in} - E_{out}} \tag{4.3}$$

Similarly, during OFF period voltage equation can be written as

$$E_{out} = L\frac{I_{L_{max}} - I_{L_{min}}}{T_2} = L\frac{\Delta I_L}{T_2} \tag{4.4}$$

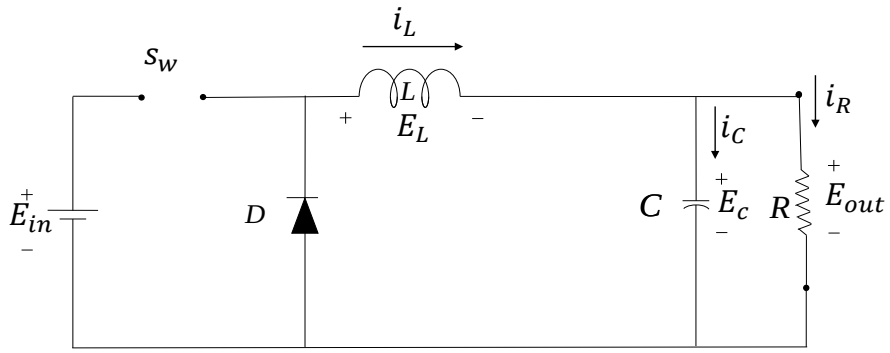

Figure 4.5: DC-DC buck converter circuit diagram when switch is OFF

and OFF period, T_2 can be expressed as

$$T_2 = \frac{\Delta I_L L}{E_{out}} \tag{4.5}$$

From (4.2) and (4.4), ripple current ΔI_L is evaluated as

$$\Delta I_L = \frac{(E_{in} - E_{out})T_1}{L} = \frac{E_{out}T_2}{L} \tag{4.6}$$

So, the ripple in inductor current can be minimized using high switching frequency and higher value of inductance. Using above equations, duty ratio of buck converter in CCM is obtained as

$$E_{out} = \frac{E_{in}T_1}{T} \Rightarrow D_r = \frac{E_{out}}{E_{in}} \tag{4.7}$$

Efficiency of the DC-DC buck converter is mainly dependent on design parameters of the circuit. Hence, inductor and capacitor critical values are chosen as per the following expressions, so that the converter operates in CCM

$$L_c = \frac{(E_{in} - E_{out})D_r}{2\Delta I_L f_{sw}} \tag{4.8}$$

$$C_c = \frac{\Delta I_L}{8\Delta E_c f_{sw}} \tag{4.9}$$

There are two ways by which the desired output voltage can be achieved. First one is by varying the duty ratio of the switch. The second one is by varying the input voltage, called the reference governance (RG) control. The method of varying the duty ratio using a closed-loop control mechanism by comparing with the reference voltage and output voltage is called the voltage mode control (VMC). In reference tracking, the target is to obtain optimal control by minimizing the error between the reference voltage and output voltage. Once the optimized control input is obtained, the desired PWM signal is generated by comparing with a carrier signal. Circuit elements of the converter are selected to operate in CCM with the desired amount of capacitor voltage ripple and inductor current ripple. Design parameters for the chosen converter are noted in Table 4.1. Inductor and capacitor equivalent series resistance (ESR) is also provided in the Table 4.1.

Table 4.1: Design parameter for the DC-DC buck converter

Parameter	Notation	Value
Input voltage	E_{in}	(8-17) V
Reference voltage	E_r	6 V
Switching frequency	f_{sw}	20 kHz
Inductor ESR	R_{el}	0.12 Ω
Capacitor ESR	R_{cl}	0.365 Ω
Capacitor	C	98 μF
Inductor value	L	560 μH
Load	R	10 Ω
Current ripple	ΔI_L	20%
Voltage ripple	ΔE_c	15%

4.3 Proposed tuning guidelines

The steps involved in designing the GPC are recalled as follows.

Step 1: To proceed for the controller designing procedure, a discretized transfer function model of the buck converter is first obtained. Since, the design procedure for any model-based controller performs better for a relatively exact identified model, transfer function model identified by Raman et al. [71] using relay feedback method is referred in this chapter. The buck converter's transfer function is identified in [71], which is an SOPDT system. The identified SOPDT model is expressed as in (4.10)

$$G_p(s) = \frac{6.8e^{-2.68\times10^{-4}s}}{8.6699 \times 10^{-7}s^2 + 0.0019s + 1} \tag{4.10}$$

The SOPDT model, $G_p(s)$ is approximated to an FOPDT model. To obtain the approximated FOPDT model, Skogestat approximation procedure is followed because this method is the simplest one, and it gives a relatively exact approximation of a higher-order system to FOPDT system. FOPDT approximation of the model is represented as

$$G_m(s) = \frac{6.8e^{-8.37\times10^{-4}s}}{1.331 \times 10^{-3}s + 1} \tag{4.11}$$

Root mean square error (RMSE) of 0.6576% is evaluated for the identified and the approximated converter model. Figure 4.6 shows that the modeling mismatch in the approximated plant model is mainly because of the delay for the approximated FOPDT model. Steady-state performance of the approximated model dynamics is similar with the identified converter dynamics. After approximation of SOPDT model to FOPDT model is obtained with a satisfactory fit with the original plant, the discretized FOPDT model is obtained as explained in Chapter 3.

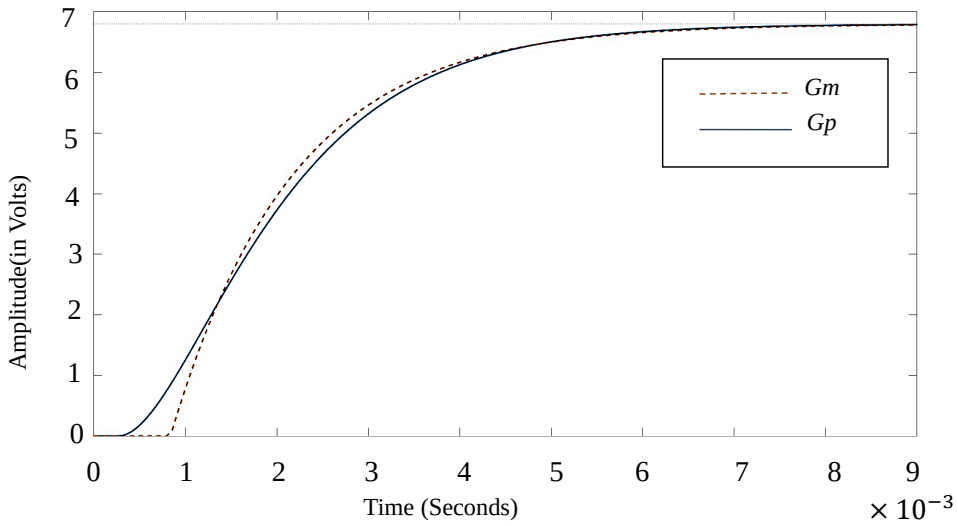

Figure 4.6: Comparison of approximated SOPDT and FOPDT model responses

Step 2: The next step is to predict the output model. For which prediction and control horizons are evaluated as per the tuning guideline proposed in Chapter 3. To evaluate tuning parameters, time domain specifications are considered. In general, settling time and overshoot are specified to determine the closed-loop transfer function of the plant. Required coefficient matrices are evaluated using (3.59) and (3.60) as follows

$$r_{aa} = \frac{(Y_{aa}X_{ab} - X_{aa}Y_{bb})(a - K_{y_1})}{aX_{ab}K_{w_1} - Y_{bb}K_{y_1}} \tag{4.12}$$

$$r_{bb} = \frac{(Y_{aa}X_{bb} - X_{ab}Y_{bb})(aK_{y_1} - K_{w_1})}{aX_{bb}K_{w_1} - Y_{11}K_{y_1}} \tag{4.13}$$

Step 3: After evaluating all the tuning parameters of GPC, output prediction is obtained by using (3.7). Once the predicted converter model is generated, the defined cost function (4.14) is optimized to obtain the linear feedback gain matrix.

$$J = \sum_{i=N_1}^{N_2} \delta(i)[\hat{y}(k+i|k) - w(k+i)]^2 + \sum_{i=0}^{M-1} \lambda(i)[\Delta u(k+i)]^2 \tag{4.14}$$

where N_1 and N_2 are the minimum and maximum prediction horizon obtained by the inequality criteria.

4.4 Simulation result

Simulation is performed for reference tracking of a predefined voltage. A reference voltage (E_r) of 6 V is tracked for the chosen buck converter. Optimal tuning parameter values as well as heuristically chosen values are noted in Table 4.2. In Figure 4.7, closed-loop output voltage response of DC-DC buck converter is shown for different values of GPC tuning parameters. It is observed that in the presence of disturbance in the load side, the proposed tuning algorithm is operating in an optimum condition. Whereas in Case I and II, transient response during disturbance is not desirable. The setting of the prediction horizon is typically based on the delay time and the settling time of the plant. To select the control horizon (M), a high value is avoided as it does not affect the overall controller performance. It is set at a value of 2. So, tuning of weights for control horizon of two is followed for transfer function (4.11). Evaluated weights are noted in Table 4.2. For these values of the controller parameter, the closed-loop output is response is simulated in MATLAB. As it can be observed from Figure 4.7, pre-computed GPC controller tracks the step reference of 6 V desirably in the absence of output disturbance, and during load disturbance, the tracking performance is compromised because of the modeling error which has not been considered. An overshoot of 3% is chosen as the design parameter for the buck converter. Load disturbance is considered in simulation in terms of step disturbance in the output

side. In hardware result, it is observed that there is an average error of 3%, which is the offset error present in the output voltage. The open-loop discrete transfer function is obtained to design the controller. After the controller design procedure is complete, the stability of the closed-loop system is analyzed by Jury's stability criteria.

Table 4.2: Design parameter of GPC

Parameter	**Notation**	**Optimal value**	**Case I**	**Case II**
Prediction Horizon(min)	N_1	10	10	30
Prediction Horizon(max)	N_2	20	20	50
Control Horizon	M	2	10	30
Control weight	r_{aa}	124.78	1	100
Control weight	r_{bb}	98.39	1	100
Error weight	q	10	100	1

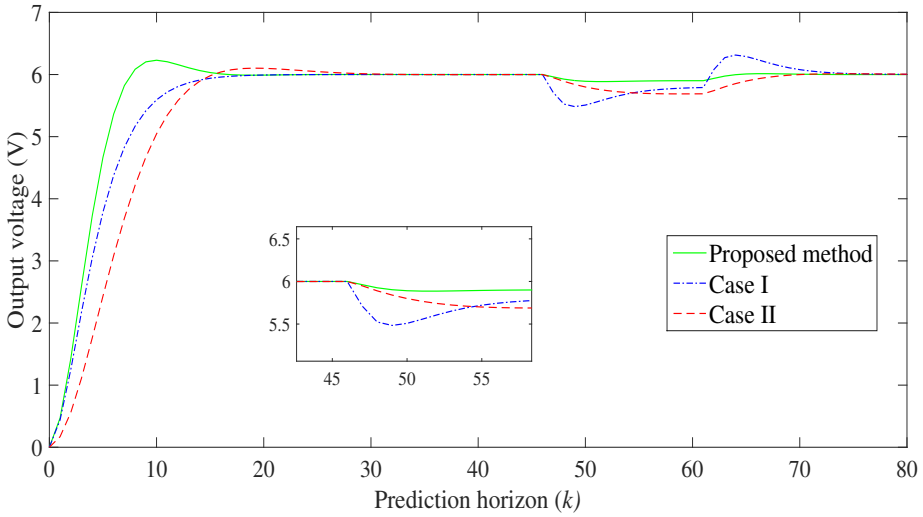

Figure 4.7: Closed-loop GPC response of a DC-DC buck converter for reference tracking voltage $E_r = 6$ V, when disturbance is present in terms of load variation in the load side.

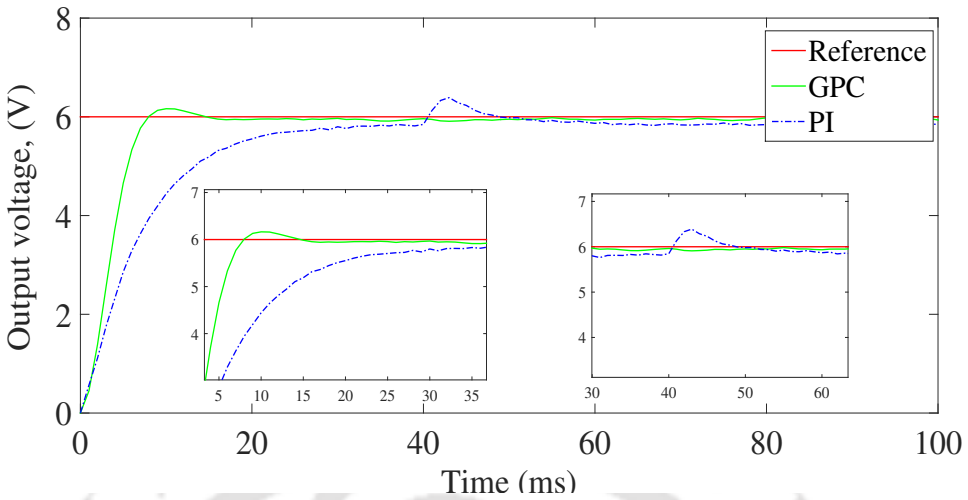

Figure 4.8: Output voltage response of GPC and PI control in presence of disturbance and noise

The overall closed-loop performance of the proposed GPC tuning algorithm is compared with PI control in Figure 4.8. The approximated FOPDT model is considered as the plant model for simulation. A PI control with gain adjustment [71] is having offset error as the plant model response is observed in presence of noise and disturbance. The PI controller structure is chosen as $K_p(1+\frac{1}{sT_i i})$. The PI controller parameters are obtained as $K_p = 1$, $T_i = 100^{-6}$. The reference value is set at 6 V. From the simulation result in Figure 4.8, it can be observed that output voltage response of the PI control is having tracking error due to load disturbance and added noise. The response speed of closed-loop PI controller is slower than the closed-loop GPC system. Finally the filtered output response is presented. While the gain adjustment of PI control gives usually a satisfactory result, but there is also known case of unsatisfactory behavior if PI controller when implemented for delayed system. Moreover, in presence of noise the performance of PI control degrades as the model behaves as a non-minimum phase system for a delayed plant model.

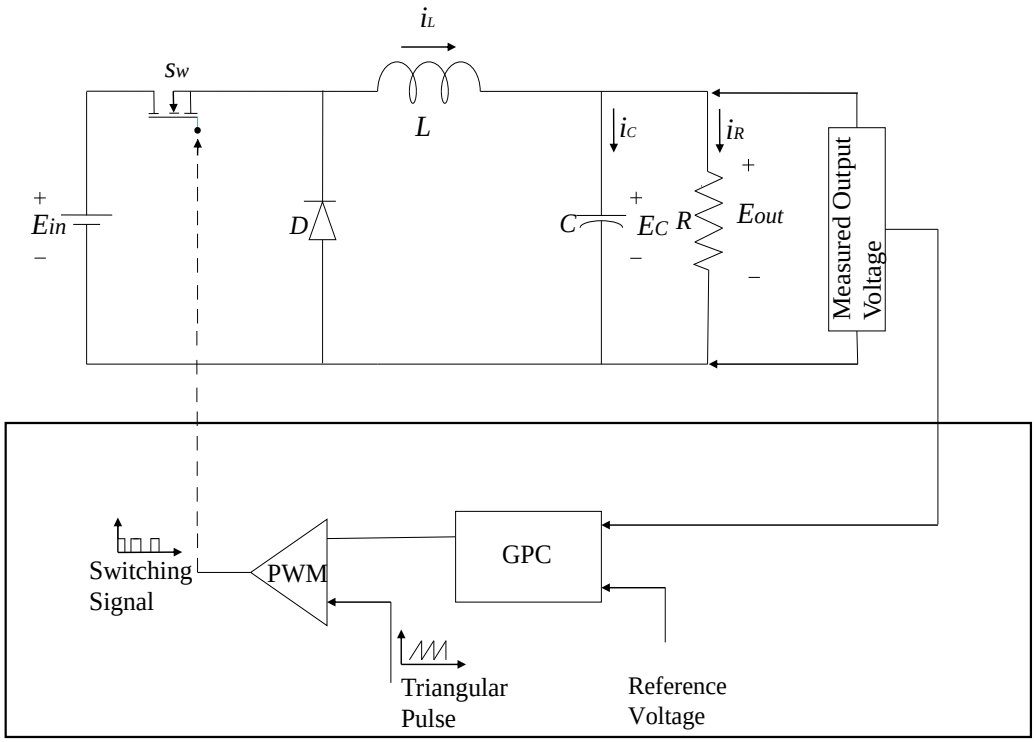

Figure 4.9: Closed-loop block diagram of the DC-DC buck converter

4.5 Experimental result and discussions

The GPC algorithm has been implemented to regulate buck converter output voltage by assembling the converter topology circuit elements in the hardware setup, as shown in Figure 4.10. The setup elements are chosen as follows: an n-channel MOSFET IRF540N is used for switching operation. To implement switching through MOSFET, a driver circuit is realized using IC HCPL 3120, which drives the low power PWM pulse obtained from the F28335 control card to a high power PWM signal. A fast Recovery Schottky diode NFK 03 is used

to minimize the ON-state voltage drop across the diode. Values of the converter circuit elements and controller design parameters are noted in Table 4.1 and 4.2 respectively. The first step is to model the desired controller in MATLAB/Simulink, as shown in Figure 4.9. After the modeling is done, code composer studio (CCS) interfacing software is used to implement the designed controller's generated code. Using CCS code is loaded in DSP TMS320F28335 C2000 micro-controller. The output voltage is down scaled to a low voltage as per the DSP board. The down scaled voltage is up scaled after passing through a 12-bit ADC on the DSP board. A reference voltage is set as explained in the design of GPC in Section 4.3, to control the voltage of the buck converter. Using the GPC code, the optimal control input is generated, which is compared with a triangular wave to obtain the designed PWM signal having a constant frequency of 20 kHz.

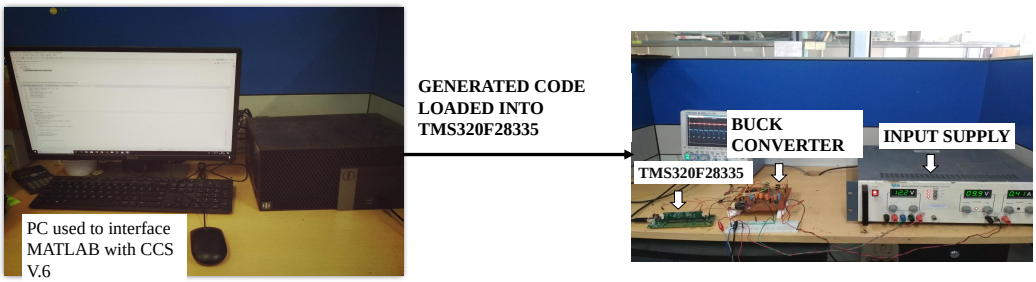

Figure 4.10: System used to implement the GPC algorithm

The output voltage waveform is observed in digital oscilloscope and the waveform for an input voltage of 12 V is shown in Figure 4.11. Reference voltage of 6 V is set for output tracking by the controller. As it can be observed in Figure 4.11 a gate of required duty ratio as evaluated by the error minimizing algorithm is generated to track the reference signal. Experimental result of transient response

of the closed-loop system is shown in Figure 4.12. To guarantee the stability and robustness of the implemented control algorithm a step change of 50% is injected at load side. Load value is changed from 10 Ω to 5 Ω suddenly and brought back to 10 Ω. Effect of sudden variation in load is shown in Figure 4.13. Similarly input voltage is also suddenly varied from 12 V to 10 V and the effect is shown in Figure 4.14. To observe the effect of controller tracking, input voltage is varied from 8 V-17 V and the percentage error noted for this range of voltage in Figure 4.15. It is observed that for the low value or high value of input error is relatively high. To remove the offset error which is shown in Figure 4.15, an integrator operator can be used prior to GPC for offset free reference tracking.

Figure 4.11: Gate pulse generated and steady state output of buck converter generated by hardware set up (voltage scale: 2.00 V/div, time scale: 10 μs/div)

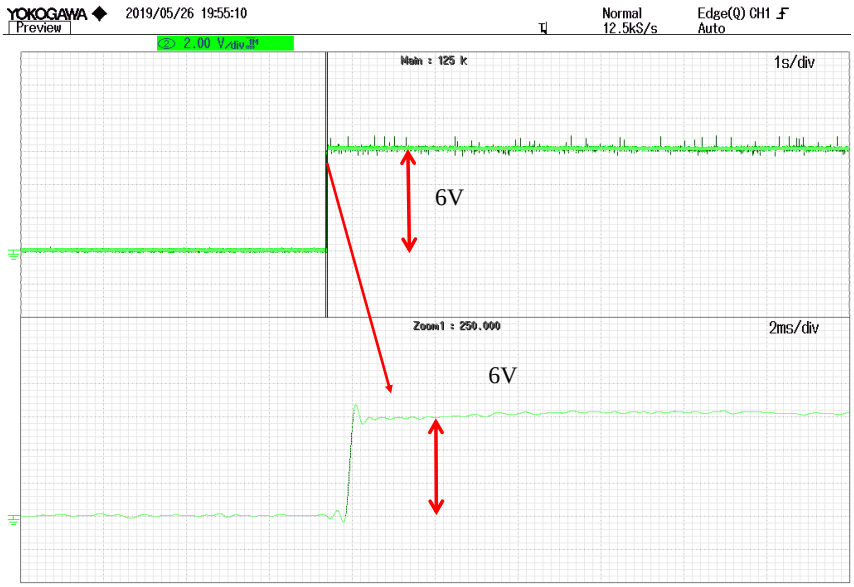

Figure 4.12: Reference tracking of the closed-loop plant model for E_r = 6V (voltage scale: 2.00 V/div, time scale: 1s/div)

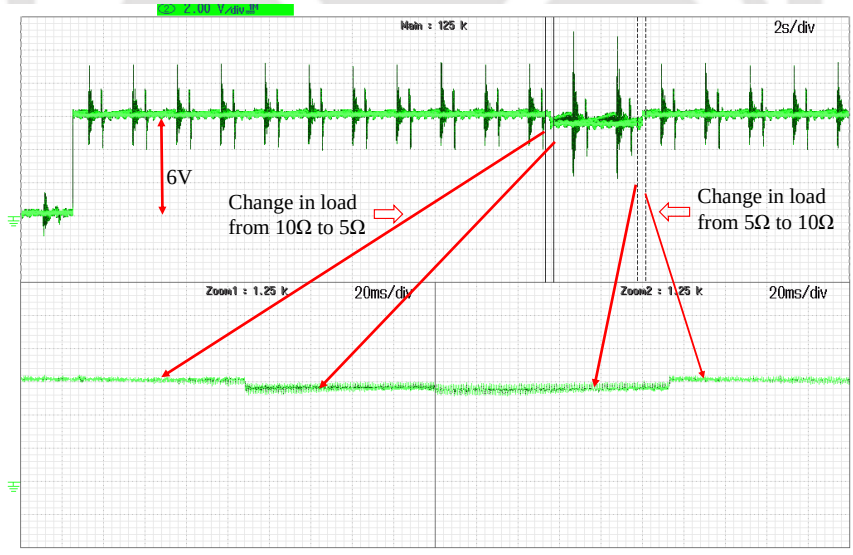

Figure 4.13: Hardware response of implemented control algorithm for output voltage due to a step change in load from 10 Ω to 5 Ω (voltage scale: 2.00 V/div, time scale: 2 s/div)

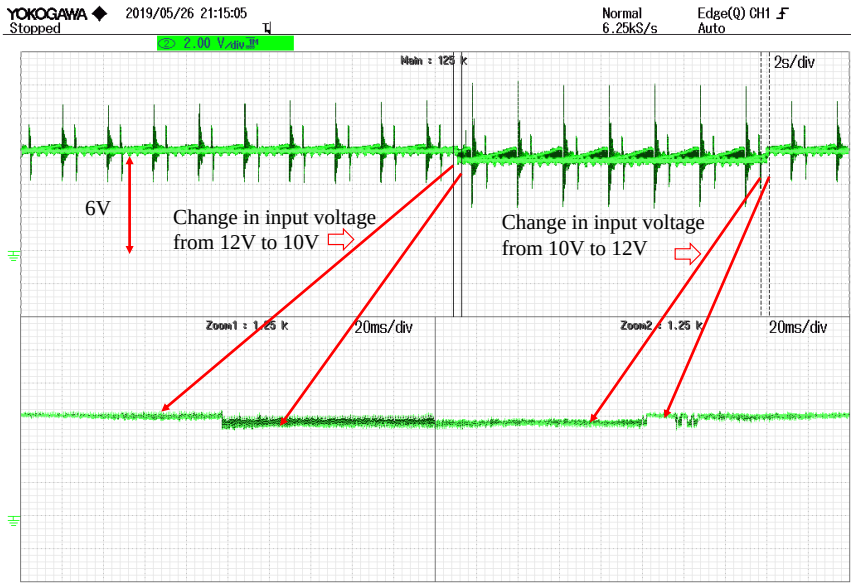

Figure 4.14: Hardware response of implemented control algorithm for output voltage due to a step change in E_{in} from 12 V to 10 V (voltage scale: 2.00 V/div, time scale: 2 s/div)

From the error plot it can be observed that for a low and high input voltage steady state error is increasing. This error is due to the offset, which can be minimized by using an integral operator $\left(\frac{1}{\Delta}\right)$ or a PI control. Steady state inductor current response of a load step change is shown in Figure 4.16. Main challenge while designing the GPC controller is the selection of prediction horizon and control horizon. Prediction horizon should be atleast more than the delay time for a proper design. Control horizon should not be very large because it increases the computational time without any significant improvement in the performance. The weights are calculated from the tuning formula derived in previous chapter.

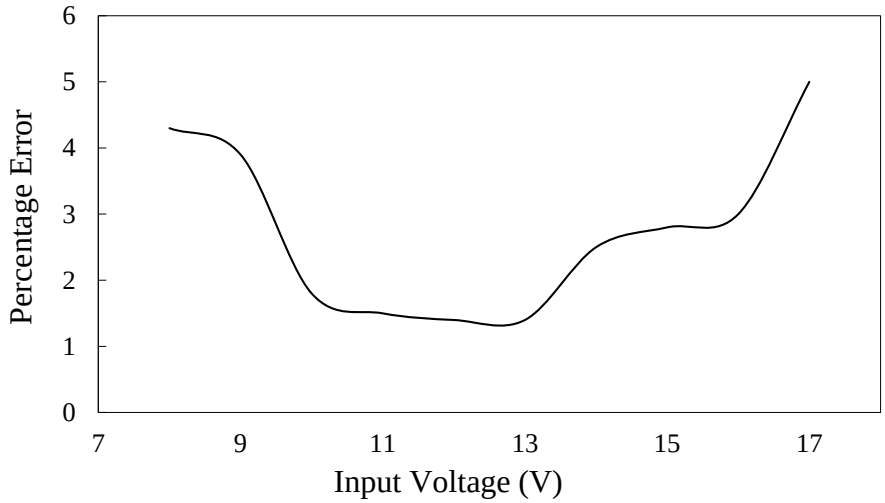

Figure 4.15: Tracking error vs input voltage for reference voltage of 6 V and load resistance variation of 50% (Load resistance is changed from 10 Ω to 5 Ω)

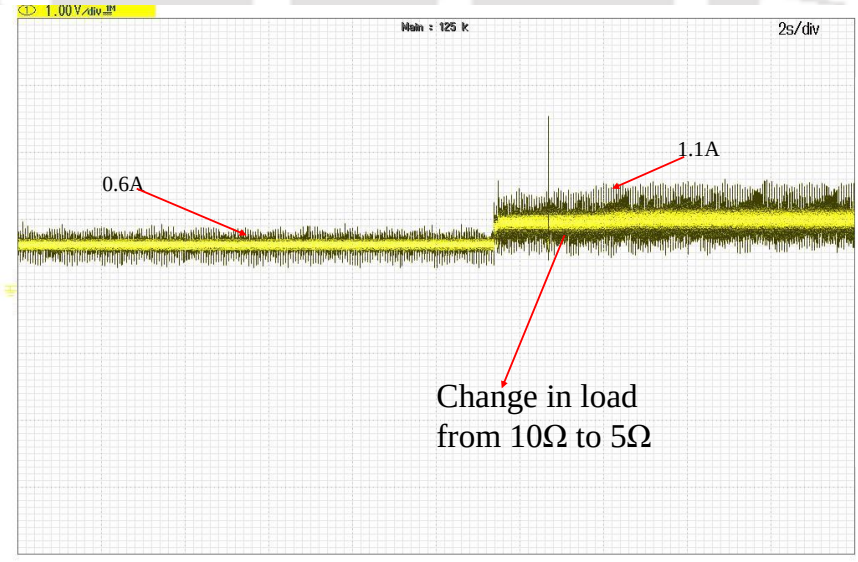

Figure 4.16: Hardware response of implemented control algorithm for steady state inductor current due to a step change in load from 10 Ω to 5 Ω (voltage scale: 1.00 V/div, time scale: 2 s/div)

4.6 Modified GPC for reference tracking

The proposed GPC feedback law can ensure that the output capacitor voltage regulation, when there is no plant-model mismatch. However, there always exist modeling error. A capacitor voltage offset error may occur in the real situation, which is the case in this designed buck converter. Several filtering capacitor and low efficient inductor resulted in offset capacitor voltage. In order to eliminate the offset error, an outer loop PI controller has been designed. The obtained pre-computed GPC results in a satisfactory performance of the buck converter voltage mode control but during load and input variation the tracking error is significant. Hence, to improve the reference tracking response during disturbance for a pre-computed GPC an outer loop PI control is designed, which ensure offset free reference tracking. The offset error during load variation is predominantly due to model mismatch during load variation in offline control mechanism because tuning parameters derived for a pre-computed GPC depends on the plant model. During load and input variation, plant model also varies, which is different from the considered model.

It is assumed that the the PI controller is represented as

$$y_k^{PI} = k_p(e_k) + k_I \sum_{i=0}^{k} (e_i) k_s \tag{4.15}$$

where y_k^{PI} is the output of the PI controller, $e_k = w_k - y_k$ and k_s is the sampling period. To achieve an offset free output voltage the output of the PI controller must be equal to the buck converter capacitor output voltage.

$$y_k^{PI} \simeq y_k \tag{4.16}$$

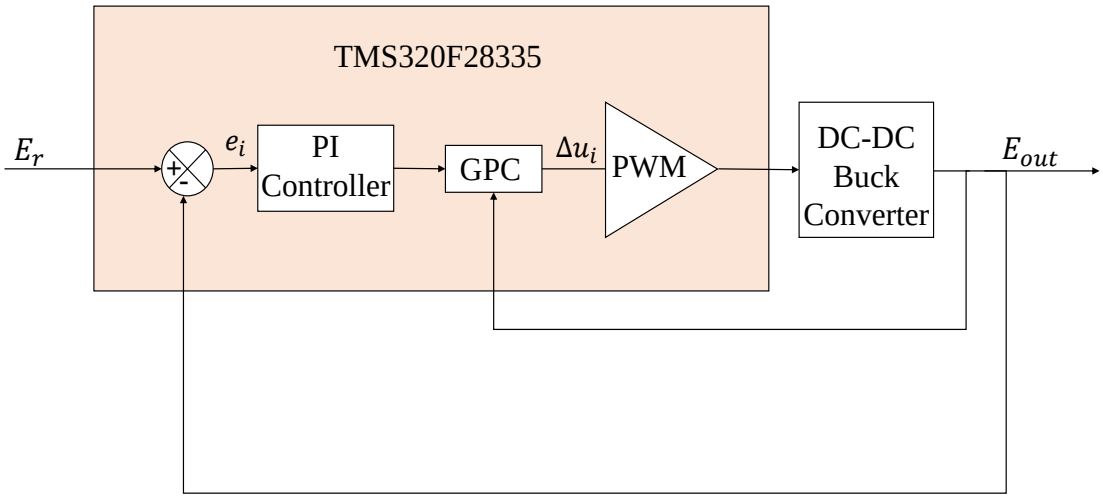

Figure 4.17: Block diagram of the dual loop control of buck converter

When we replace y_k in place of y_k^{PI} and follow eq. (4.15), it is expressed as,

$$y_k = k_p(w_k - y_k) + k_I \sum_{i=0}^{i} (w_k - y_i)k_s \tag{4.17}$$

$$e_{(k+1)} = \frac{1 + k_p}{1 + k_p + k_I k_s} e_k \tag{4.18}$$

Therefore the offset free tracking performance of the closed loop system i.e. $y_k = w_k$ can be achieved for $k_p \geq 0$ and $k_I \geq 0$ when the PI control is used in the outer loop along with an inner loop which is considerably fast. The PI controller values are chosen heuristically as $k_p = 10$, $k_I = 50$ and $k_s = 0.1ms$. Block diagram of the dual loop GPC for error free reference tracking is shown in Figure 4.17.

Tuning parameters of the GPC are set at $N = 20$, $M = 2$, $Q_\delta = diag\{10\}$, and $Q_\lambda = \begin{bmatrix} 85.62 & 0 \\ 0 & 74.27 \end{bmatrix}$. Simulation result of reference tracking is shown in Figure

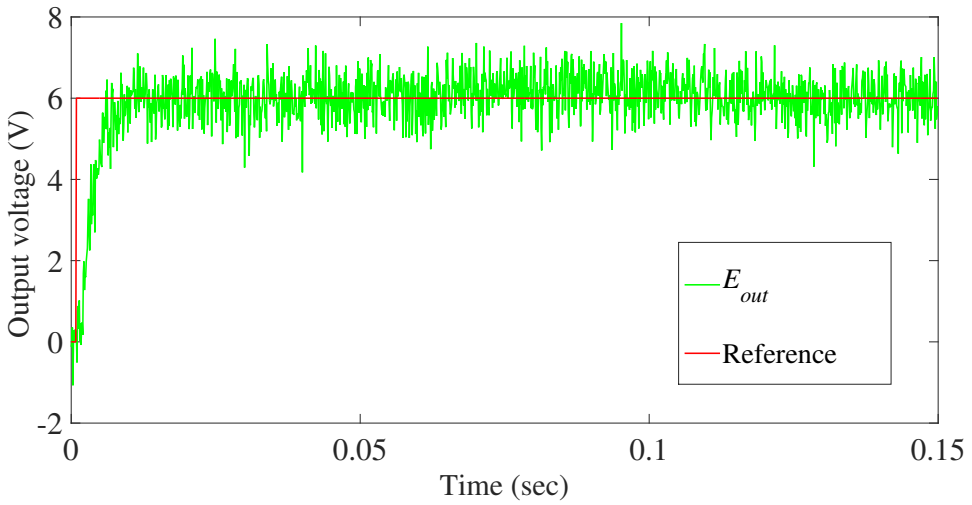

Figure 4.18: Voltage reference tracking of modified GPC

4.18. The simulation is performed by injecting a random noise of $SNR = 45.07$ dB. It can be observed that the proposed method is able to track the set output voltage within desired time limit. Hardware implementation result for modified GPC are shown in Figure 4.19 and 4.20. Figure 4.18 shows tracking response of the closed-loop model during 50% load variation. Similarly, Figure 4.19 shows tracking response of the closed-loop model during input variation of $\pm 2V$. The settling time for load and input variation is 10 $msec$. To observe the effect of load and input variation C and L are chosen to be a low value, which results in a high ripple at the output side. The converter is designed for voltage ripple of 15% and inductor current ripple of 20%. The outer loop PI controller has been tuned by conducting extensive numerical simulation of the closed-loop model in MATLAB. For a pre-computed GPC, during load and input variation, the tracking error increases due to the model mismatch and capacitor offset voltage. To improve the reference tracking response during disturbance for pre-computed GPC, an outer loop PI control is designed as shown in Figure 4.20, which ensure error free reference tracking. The designed dual loop controller has been experimentally

validated as shown in Fig. 4.19.

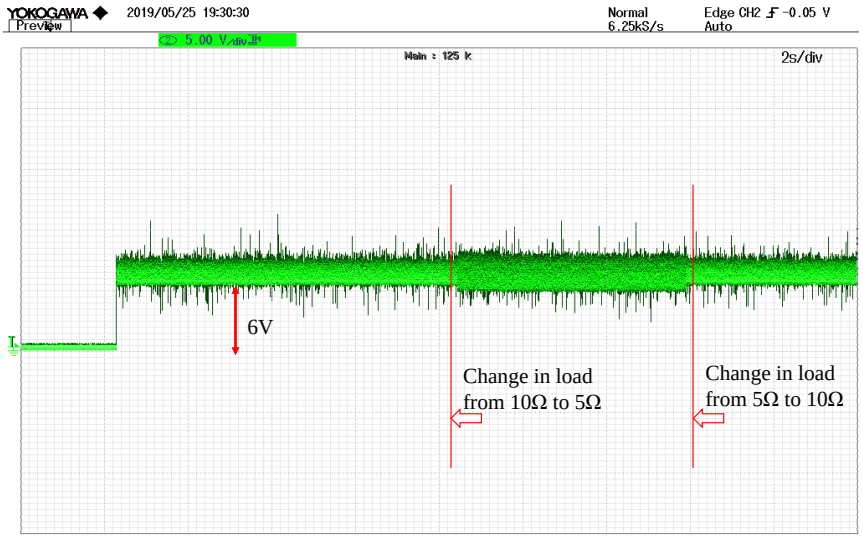

Figure 4.19: Hardware response of implemented modified GPC algorithm for output voltage due to a step change in load from 10 Ω to 5 Ω (voltage scale: 5.00 V/div, time scale: 2 s/div)

4.7 Summary

In this chapter, GPC is designed for VMC of DC-DC buck converter for reference tracking problem in presence of load disturbance in SISO case. Simulation results for different tuning parameters are presented and compared. There is a trade off between maximum overshoot and tracking error in presence of load disturbance. As this is a pre-computed optimization method, during load change buck converter model parameters change, hence resulting in modeling error. GPC offers benefit in DC-DC converters in terms of its clearly defined design process, time-domain performance criteria, simple tuning technique and guarantee of stability. To improve the tracking performance a modified pre-computed GPC tuning algorithm has been validated in simulation and experiment for a stable FOPDT plant model for

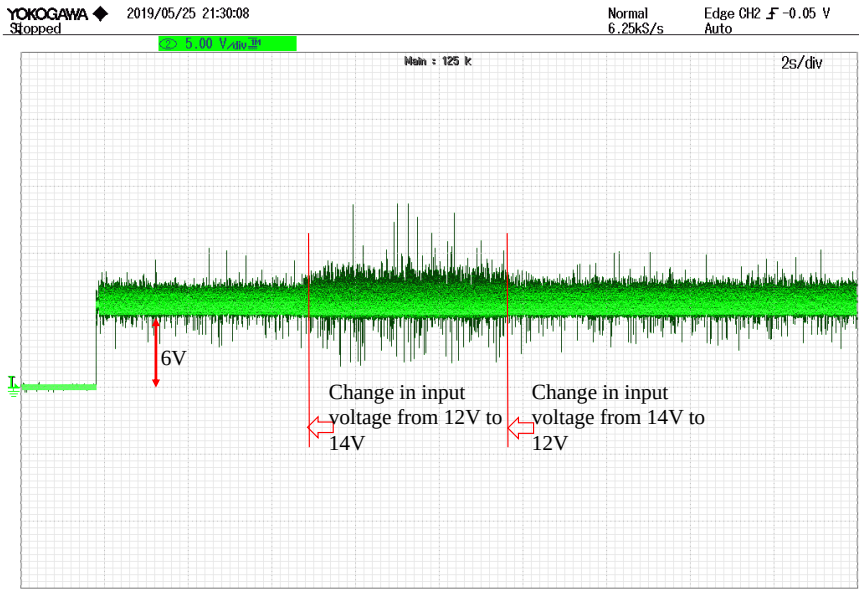

Figure 4.20: Hardware response of implemented modified GPC algorithm for output voltage due to a step change in E_{in} from 12 V to 10 V (voltage scale: 5.00 V/div, time scale: 2 s/div)

the DC-DC buck converter. The controller design procedure for reference tracking has been simplified by implementing the pre-computed GPC control input using a DSP micro-controller. Tracking error during load and input variation has been eliminated using a PI control at the outer-loop of the closed-loop pre-computed GPC. Although tracking error has been eliminated but the voltage ripple has been increased significantly.

CHAPTER 5

DESIGN OF GPC FOR MULTI-VARIABLE PLANT MDOEL

5.1 Introduction

Limiting power utilization in multi-processor frameworks requires utilization of numerous supplies with a wide range of multiple regulated output and input voltages. Since one inductor for each DC-DC converter is costly, there is an expanding interest in SIMO DC-DC converters. Portable devices such as cell phone, laptop, Bluetooth speaker and smart-watch, all work on battery input and multiple voltage levels for speaker, LCD screen and sensors. Use of low power portable device is increasing day by day, which is motivating researchers to develop an efficient control algorithm for these devices to achieve the desired output. Hence, the supply voltage must satisfy this demand for a heterogeneous input voltage requirement for several components of the device for efficient and desirable system performance. For component requiring multiple input supply to function, single-input multiple-output (SIMO) DC-DC converter [72] plays an important role. Recently, multi-output power converters have been researched widely due to its many advantages over single output converter [73–76]. A SIMO converter has a small volume

compared to a dual inductor system as it works using only a single inductor. SIMO DC-DC converter is preferred over multiple SISO converters due to its advantage of small volume, low cost and high efficiency for low power application. As the number of inductors required in a SIMO topology decreases, battery life and efficiency of the switching converter is improved. SIMO converter makes use of a single or a coupled inductor instead of numerous parallel converters. The issue of using multiple inductors is that, inductors are bulky and also it is challenging to switch in a synchronized manner. Due to a decrease in the number of components, the cost is reduced and efficiency is improved.

Mainly, these converters are used for low power application devices. However, these converters come with several design and regulation challenges. As it has only a single input supply, the output needs to be multiplexed. Multiplexing outputs ensure that the converter output is never short-circuited. To provide proper multiplexing, the inductor current is allowed to flow through each output for a particular switching time. The effect of output cross-coupling in the chosen plant dynamics is prominent when there is a change in either one of the output which affects the other output because of this reason the design of a control circuit is difficult for a SIMO converter. There have been many successful implementations of classical control techniques for the control of SIMO power converters. Still, due to complicated closed-loop system dynamics, the controller design procedure is very complicated. Usually, a controller is designed for the decoupled output voltages to minimize the cross-regulation [77]. A state feedback cross derivative is proposed in [78] to minimize the effect of load variation. Consequently, the regulated output of the converter is susceptible to the supply voltage variations. Design of a decoupler requires a detailed design strategy of the controller; otherwise, it might reduce the overall system stability. To resolve this issue of use decoupler, time multiplexing of output is considered [79] for each output, and the

SIMO converter is converted to an individual SISO converter. In this method, the system is wholly decoupled in nature, but inductor ripple current is heavily affected for load change. In another technique, the SIMO converter is operated in pseudo-CCM mode. In this method, the inductor is connected with a parallel switch which operates in the freewheeling interval. However, this configuration of an additional switch results in inductor current during the freewheeling switch break. Hence, loss in the converter is increased along with an increase in foot-print. A method proposed in [80] states that the current control loop is used to determine duty cycles of each output. However still, the output is affected by cross-regulation due to difference in operating bandwidth among the current inner loops. The predictive current control technique [81] is proposed to obtain required duty cycles for outputs to suppress cross-regulation, but the calculation complexity is very high compared to an analog controller. Loop shaping technique for open-loop plant transfer function is implemented to obtain the desire operating points by minimizing the second norm of the error between the desired open-loop dynamics and the actual plant model [82].

In this chapter, a dual output DC-DC buck converter is considered to show the design procedure of GPC in case of a SIMO converter. The model of the single inductor dual output (SIDO) DC-DC buck converter is considered for this purpose. The plant model is formulated in the transfer function matrix structure. An augmented states space model is obtained from the transfer function form, and output prediction model can be generated from one step ahead equation same as SISO case. A Luenberger-type observer [83] is designed to have an error-free reference tracking. Criteria to evaluate observer gains has also been derived in this chapter. Simulation results of an unconstrained optimization are presented. There are mainly two challenges in the control of a multi-port converter, namely cross-regulation and cross-coupling. Cross-regulation is defined as the effect on

output due to load variation in another output. In comparison, cross-coupling is defined as the effect of reference variation. Control of a dual output converter by the GPC strategy shows that the designed controller is robust to input and load variation.

5.2 Design of GPC

For a SISO system, prediction of output from transfer function is easy to compute by using traditional GPC transfer function model but it cannot be directly extrapolated for a MIMO plant model. Hence a state-space model is adopted for prediction model. Assuming l outputs, m inputs and n states the states-space model of a plant is represented as

$$\begin{aligned} x_m(k+1) &= A_m x_m(k) + B_m u(k) + B_\varsigma u_{dist}(k) \\ y_m(k) &= C_m x_m(k) \end{aligned} \tag{5.1}$$

where, x_m and y_m are the state equation and output equation respectively. It is also assumed that all the states of the chosen plant model are controllable. If number of states are less than number of outputs, then all outputs can not be controlled with zero steady state error independently. Input disturbance is incorporated as $u_{dist}(k)$, which is assumed to be zero mean integrated white noise. $u_{dist}(k)$ is written in difference equation as

$$u_{dist}(k) - u_{dist}(k-1) = \zeta(k) \tag{5.2}$$

where $\zeta(k)$ is the white noise. From (5.1) the following equation is written as

$$x_m(k) = A_m x_m(k-1) + B_m u(k-1) + B_\varsigma u_{dist}(k-1) \tag{5.3}$$

To remodel the state-space model in $\Delta u(k)$ as input variable, state vector $x_m(k)$ is replaced with $\Delta x_m(k)$ where $\Delta x_m(k) = x_m(k) - x_m(k-1)$. From (5.1) and (5.3), $\Delta x_m(k+1)$ can be expressed as

$$\Delta x_m(k+1) = A_m \Delta x_m(k) + B_m \Delta u(k) + B_\zeta \zeta(k) \tag{5.4}$$

Similarly, $\Delta y_m(k+1)$ is obtained as

$$\Delta y_m(k+1) = C_m \Delta x_m(k+1) \tag{5.5}$$

$$\Rightarrow \Delta y_m(k+1) = C_m A_m \Delta x_m(k) + C_m B_m \Delta u(k) + C_m B_\zeta \zeta(k) \tag{5.6}$$

This modified state model is obtained to include change in input $\Delta u(k)$ as a decision making variable in the cost function for optimization which is the core concept of GPC. New state vectors are chosen as $x_n(k) = \begin{bmatrix} \Delta x_m(k) & y_m(k) \end{bmatrix}$ for the augmented state plant model. Therefore, modified state-space model of the plant model is written as

$$\begin{bmatrix} \Delta x_m(k+1) \\ y_m(k) \end{bmatrix} = \begin{bmatrix} A_m & 0_m^T \\ C_m A_m & I \end{bmatrix} \begin{bmatrix} \Delta x_m(k) \\ y_m(k) \end{bmatrix} + \begin{bmatrix} B_m \\ C_m B_m \end{bmatrix} \Delta u(k) + \begin{bmatrix} B_\zeta \\ C_m B_\zeta \end{bmatrix} \zeta(k) \tag{5.7}$$

$$y_m(k) = \begin{bmatrix} O_m & I \end{bmatrix} \begin{bmatrix} \Delta x_m(k) \\ y_m(k) \end{bmatrix} \tag{5.8}$$

where I is Identity matrix of appropriate dimension and O_m is zero matrix. Output prediction equation is obtained by recursion of one step ahead state equation as

explained in Chapter 2. The augmented model in (5.7) and (5.8) is denoted as

$$x_n(k+1) = A_n x_n(k) + B_n \Delta u(k) + B_d \zeta(k) \tag{5.9}$$

$$y_n(k) = C_n x_n(k) \tag{5.10}$$

Prediction of the augmented state matrix is obtained to determine the output prediction model, expressed as

$$x_n(k+1|k) = A_n x_n(k|k) + B_n \Delta u(k|k) + B_d \zeta(k|k) \tag{5.11}$$

$$\begin{aligned} x_n(k+2|k) = A_n^2 x_n(k|k) + A_n B_n \Delta u(k|k) + A_n B_d \zeta(k|k) + B_n \Delta u(k+1|k) + \\ B_d \zeta(k+1|k) \end{aligned} \tag{5.12}$$

$$\vdots$$

$$\begin{aligned} x_n(k+N|k) = A_n^N x_n(k|k) + A_n^{N-1} B_n \Delta u(k|k) + A_n^{N-2} B_n \Delta u(k+1|k) + \cdots + \\ A_n^{N-M} B_n \Delta u(k+M-1|k) + A_n^{N-1} B_d \zeta(k|k) + A_n^{N-2} B_d \zeta(k+1|k) + \\ \cdots + B_d \zeta(k+N-1|k) \end{aligned} \tag{5.13}$$

The notation $x_n(k+i|k)$ denotes the i step ahead state variable evaluated at k instant sampled time. The predicted output is obtained as

$$y_m(k+1|k) = C_n A_n x_n(k|k) + C_n B_n \Delta u(k|k) + C_n B_d \zeta(k|k) \tag{5.14}$$

$$\begin{aligned} y_m(k+2|k) = C_n A_n^2 x_n(k|k) + C_n A_n B_n \Delta u(k|k) + C_n A_n B_d \zeta(k|k) + C_n B_n \Delta u(k+1|k) + \\ C_n B_d \zeta(k+1|k) \end{aligned} \tag{5.15}$$

$$\vdots$$

$$\begin{aligned} y_m(k+N|k) = C_n A_n^N x_n(k|k) + C_n A_n^{N-1} B_n \Delta u(k|k) + C_n A_n^{N-2} B_n \Delta u(k+1|k) + \cdots + \\ C_n A_n^{N-M} B_n \Delta u(k+M-1|k) + C_n A_n^{N-1} B_d \zeta(k|k) + C_n A_n^{N-2} B_d \zeta(k+1|k) + \\ \cdots + C_n B_d \zeta(k+N-1|k) \end{aligned} \tag{5.16}$$

where $\zeta(k|k)$ is assumed to be a zero-mean Gaussian noise at k discrete sample time, hence the predicted value of $\zeta(k+i|k)$ at future sample i is assumed to be zero. The prediction of state variable and output variable is calculated as the expected values of the respective variables, hence, the noise effect to the predicted values being zero. For notational simplicity in representation, the expectation operator is not used. New vectors of optimized control input and predicted output are defined as

$$\Delta U(k) = \begin{bmatrix} \Delta u(k|k) & \Delta u(k+1|k) & \dots & \Delta u(k+M-1|k) \end{bmatrix} \tag{5.17}$$

$$Y_p(k) = \begin{bmatrix} y_m(k+1|k) & y_m(k+2|k) & \dots & y_m(k+N|k) \end{bmatrix} \tag{5.18}$$

Predicted state-space model is written as

$$Y_p(k) = C_n x_n(k) \tag{5.19}$$

$$\Rightarrow Y_p(k) = F_p x_n(k) + Q_p \Delta U(k) \tag{5.20}$$

where dimension of the F_p and Q_p in output prediction equation (5.20) depends on the chosen prediction horizon and control horizon.

$$F_p = \begin{bmatrix} C_n A_n \\ C_n A_n^2 \\ \vdots \\ C_n A_n^N \end{bmatrix}, \quad Q_p = \begin{bmatrix} C_n B_n & 0 & \dots & 0 \\ C_n A_n B_n & C_n B_n & \dots & 0 \\ \vdots & \vdots & \vdots & \vdots \\ C_n A_n^{N-1} B_n & C_n A_n^{N-2} B_n & \dots & C_n A_n^{N-M} B_n \end{bmatrix} \tag{5.21}$$

The chosen cost function is expressed as

$$J = \mathbf{Q}\sum_{i=1}^{N} \|(W(k) - Y_p(k))\|_2^2 + \mathbf{R}\sum_{i=0}^{M} \|\Delta U(k)\|_2^2 \tag{5.22}$$

where $W(k)$ is the reference sequence and $\mathbf{Q}$ is the error weight matrix and $\mathbf{R}$ is the control weight matrix, which are chosen to be positive definite constant diagonal matrices. Current optimal control input is obtained by minimizing a cost function with respect to the control increment $\Delta U(k)$ i.e. $\dfrac{dJ}{d\,(\Delta U(k))} = 0$. According to receding horizon control principle, from the obtained optimized control input only the first row is considered to generate the feedback gain matrix K_{mpc}. Optimized control input is expressed as

$$\Delta u(k) = \begin{bmatrix} 1 & 0 & 0 & \dots & 0 \end{bmatrix} (Q_p^T \mathbf{Q} Q_p + \mathbf{R})^{-1} Q_p^T \mathbf{Q} (W(k) - F_p x_n(k)) \tag{5.23}$$

$$= K_{mpc}(W(k) - F_p x_n(k)) \tag{5.24}$$

$$= K_{w_1} W(k) - K_{y_1} x_n(k) \tag{5.25}$$

where K_{mpc} is denoted as K_{w_1} for the gain matrix of reference trajectory. Gain K_{w_1} is the first element of $(Q_p^T \mathbf{Q} Q_p + \mathbf{R})^{-1} Q_p^T \mathbf{Q}$ and K_{y_1} is the first element of $(Q_p^T \mathbf{Q} Q_p + \mathbf{R})^{-1} Q_p^T \mathbf{Q} F_p$. The modified state model for closed-loop system is written as

$$x_n(k+1) = (A_n - B_n K_{y_1})\, x_n(k) + B_n K_{w_1} W(k) \tag{5.26}$$

Hence, eigenvalues of $(A_n - B_n K_{y_1})$ determines the stability of the closed-loop system. When eigenvalues lie on the left half of the s-plane, the system is said to be stable one. If eigenvalues lie on the right half side of the s-plane, the system is said to unstable and if eigenvalues lie on the y-axis the system is said to be marginally stable.

5.3 Observer design for the state estimation

In this section, a Luenberger-type observer is designed for the state estimation of the GPC. To simplify the design procedure, the plant model is chosen to be without white noise. The observer model is represented as

$$\hat{x}_o(k+1) = A_n\hat{x}_o(k) + B_n\Delta u(k) + L_o\left(y_n(k) - C_n\hat{x}_o(k)\right) \quad \forall k \geq 0 \tag{5.27}$$

where $\hat{x}_o(k+1)$ is defined as the state estimation obtained by the Leunburger-type observer and the observer gain is defined as L_o. $\zeta(k)$ is assumed to be zero in the augmented state-space model. Defining $e(k) = x_n(k) - \hat{x}_o(k)\ \forall k \geq 0$, the error in observer estimation is obtained as

$$e(k+1) = \left(A_n - L_oC_n\right)e(k) \quad \forall k \geq 0 \tag{5.28}$$

$$= \tilde{A}_n e(k) \tag{5.29}$$

A Lyapunov function candidate is defined as

$$Z_o(e(k)) = e^T(k)Q_oe(k) \quad \forall k \geq 0 \tag{5.30}$$

Theorem 5.1 *Let Q_o be defined as a symmetric positive definite matrix, then there exist a Luenberger gain matrix L_o defined as*

$$L_o = Q_o^{-1}P_o \tag{5.31}$$

Proof:

It is defined that $Q_o = Q_o^T > 0$. The Lyapunov function is expressed as in

(5.30). Therefore $\Delta Z_o(e(k))$ is defined as

$$\Delta Z_o(e(k)) = Z_o(e(k+1)) - Z_o(e(k)) \tag{5.32}$$

$$= e^T(k+1)Q_o e(k+1) - e^T(k)Q_o e(k) \tag{5.33}$$

$$= e^T(k)\left(\tilde{A}_n^T Q_o \tilde{A}_n - Q_o\right) e(k) \tag{5.34}$$

From (5.34), it can be observed that for $\Delta Z_o(e(k)) < 0$

$$\tilde{A}_n^T Q_o \tilde{A}_n - Q_o < 0 \quad \forall k \geq 0 \tag{5.35}$$

Therefore, (5.35) can be expressed as a negative value and it is assumed that

$$\tilde{A}_n^T Q_o \tilde{A}_n - Q_o < -(1-\epsilon^2)Q_o \quad \forall k \geq 0 \tag{5.36}$$

Now, (5.36) is rearranged to

$$\tilde{A}_n^T Q_o \tilde{A}_n - Q_o + (1-\epsilon^2)Q_o < 0 \quad \forall k \geq 0 \tag{5.37}$$

$$= Q_o\epsilon^2 - \tilde{A}_n^T Q_o Q_o^{-1} Q_o \tilde{A}_n > 0 \quad \forall k \geq 0 \tag{5.38}$$

(5.38) can be expressed as a Schur compliment in (5.39)

$$\begin{bmatrix} Q_o & Q_o\tilde{A}_n \\ \tilde{A}_n^T Q_o & Q_o\epsilon^2 \end{bmatrix} > 0 \tag{5.39}$$

which can be expressed in observer gain matrix form as

$$\begin{bmatrix} Q_o & Q_o\left(A_n - L_o C_n\right) \\ \left(A_n - L_o C_n\right)^T Q_o & Q_o\epsilon^2 \end{bmatrix} > 0 \tag{5.40}$$

$L_o = Q_o^{-1} P_o$ is defined, hence (5.40) is represented as

$$\begin{bmatrix} Q_o & Q_o A_n - P_o C_n \\ A_n^T Q_o - C_n P_o^T & Q_o \epsilon^2 \end{bmatrix} > 0 \tag{5.41}$$

Therefore, it can be concluded that

$$\Delta Z_o(e(k) < -(1-\epsilon^2) e^T(k) Q_o(e(k)) < 0, \forall k \geq 0, \forall (p(0)) \neq 0$$

with this observer implementation, states of GPC optimized control $x_n(k)$ is replaced by the observer state.

$$\Delta u(k) = K_{w_1} W(k) - K_{y_1} x_o(k) \tag{5.42}$$

The closed-loop dynamics system equation can be formed as

$$x_n(k+1) = A_n x_n(k) - B_n K_{y_1} x_o(k) + B_n K_{w_1} W(k) \tag{5.43}$$

The observer tracking error is defined as $\bar{x}(k) = x_n(k) - \hat{x}_o(k)$. Model of the observer is expressed as

$$\bar{x}(k+1) = (A_n - L_o C_n)\, \bar{x}(k) \tag{5.44}$$

So, the rate at which error converges can be regulated by varying the state matrix in (5.44) . Smilarly, (5.43) can be written as

$$x_n(k+1) = (A_n - B_n K_{y_1})\, x_n(k) + B_n K_{y_1} \bar{x}(k) + B_n K_{w_1} W(k) \tag{5.45}$$

The closed-loop equation combining observer dynamics and the augmented equa-

tion can be written as

$$\begin{bmatrix} \bar{x}(k+1) \\ x_n(k+1) \end{bmatrix} = \begin{bmatrix} A_n - L_o C_n & \mathbf{0}_{n\times n} \\ B_n K_{y_1} & A_n - B_n K_{y_1} \end{bmatrix} \begin{bmatrix} \bar{x}(k) \\ x_n(k) \end{bmatrix} + \begin{bmatrix} \mathbf{0}_{n\times m} \\ B_n K_{w_1} \end{bmatrix} W(k) \quad (5.46)$$

$\mathbf{0}_{n\times n}$ is defined as a $n \times n$ zero matrix and $\mathbf{0}_{n\times m}$ is defined as a $n \times m$ zero matrix. From (5.47) it can be observed that the observer design and the controller design are independent of each other. The eigenvalues (e_g) of the closed-loop can be determined as the

$$\det \left[e_g - \begin{bmatrix} A_n - L_o C_n & \mathbf{0}_{n\times n} \\ B_n K_{y_1} & A_n - B_n K_{y_1} \end{bmatrix} \right] = 0 \quad (5.47)$$

From (5.47) it can be observed that the augmented system eigenvalues remains unchanged when the observer is designed for the system. Poles of the system and the observer are independent of each other as the state matrix is a lower diagonal matrix. The location of observer eigenvalues can be decided by varying the observer gain (L_o). Similarly, the location of eigenvalues of the system is decided from the gain matrix K_{y1} of the optimized control input obtained by the cost function minimization.

5.4 Stability analysis of the control law

Stability analysis of GPC is difficult for the case of active constraints in optimal control, the control law forms a nonlinear optimal control problem. Control input in GPC is obtained using RHC, subject to feasibility of imposed constraints if any. Therefore the optimization procedure is repeated until the desired trajectory is achieved. There are several methods available for the stability analysis of the GPC control law based on the cost function which involves rigorous mathematics. In

this chapter, to analyze the closed-loop system stability, an equality constraint on the terminal state is considered, which means that the error between reference and output tends to zero. For stability analysis purpose only, augmented state vectors can be formed as $x_n(k) = \begin{bmatrix} \Delta x_m(k+1) \\ W(k) - y_m(k) \end{bmatrix}$. $x_n(k+N) = 0$ is set as the terminal state obtained from optimizing control sequence $\Delta u(k) = K_{mpc} f(x_n(k))$. It is also assumed that there exists a solution K_{mpc} such that the chosen cost function is minimized subject to the satisfying of all feasibility conditions. Subject to these assumptions, the closed-loop model predictive control system is asymptotically stable.

Stability of the GPC augmented state space model has been analyzed by choosing the quadratic cost function as the Lyapunov as shown in Theorem 3.1. Optimum of the chosen finite horizon cost function ($J(\Delta u(k))$) is considered to be the Lyapunov function. Lyapunov function $z(f(x_n(k)))$ is positive definite, and it tends to a finite value if $x_n(k)$ tends to finite. To analyze the convergence of the obtained control law, quadratic cost function ($J(\Delta u)$) is chosen as the Lyapunov function candidate, $z(f(x_n(k)))$. Along with the positive definiteness of the chosen Lyapunov function second criteria, $\Delta v(f(x_n(k+1))) < 0, \forall k \geq 0$ also needs to be satisfied for the asymptotic stability of the control law.

$$\Delta z(f(x_n(k+1))) = z(f(x_n(k+1))) - z(f(x_n(k))) \tag{5.48}$$

To proceed further for the analysis, a relation between the Lyapunov function candidate at sample time $k+1$ and k needs to be derived. Assuming that the optimized solution $\Delta u(k)$ satisfies all constraints at sample instant k, a feasible solution of $f(x_n(k+1))$ for the receding horizon is given by $x_n(k+1)$, which is

represented by the prediction model

$$x_n(k+1) = A_n(k) + B\Delta u(k) \tag{5.49}$$

Obtained optimal solution $\Delta u(k+1)$ is a function of $f(x_n(k+1))$, it is observed that

$$z(f(x_n(k+1))) \leq \hat{z}(f(x_n(k+1))), \qquad \forall k \geq 0 \tag{5.50}$$

where $\hat{z}(f(x_n(k+1)))$ is the obtained control sequence which is a function of the sequence $x_n(1)$, $x_n(2)$,...,$x_n(k+N-1)$. $\Delta z(f(x_n(k+1)))$ is then bounded by

$$z(f(x_n(k+1))) - z(f(x_n(k))) \leq \hat{z}(x_n(k+1) - z(x_n(k)) \tag{5.51}$$

For the sample time $k+1$, $k+2$, ..., $k+N-1$ the difference between these two Lyapunov functions is obtained as

$$\begin{aligned}\Delta z(f(x_n(k+1))) = (x_n(k+N)|k)^T\mathbf{Q}(x_n(k+N)|k) - \\ x_n(k+1)^T\mathbf{Q}x_n(k+1) - \Delta u(k)^T\mathbf{R}\Delta u(k)\end{aligned} \tag{5.52}$$

From the assumption of final constraint, it can be stated that

$$\begin{aligned}\Delta z(f(x_n(k+1))) \leq -x_n(k+1)^T\mathbf{Q}x_n(k+1) - \Delta u(k)^T\mathbf{R}\Delta u(k) \\ \forall k \geq 0\end{aligned} \tag{5.53}$$

Hence, it has been proved that the first derivative of the chosen Lyapunov function yields a negative value. To show that $z(f(x(k))) = 0 \; \forall \; e(0) = 0$ and $\Delta u(0) = 0$ a new variable $v = [x_n(k)\Delta u(k)]^T$ is defined. It is assumed, $\exists v \neq 0$ for which

$z = v^T \begin{bmatrix} \mathbf{Q} & 0 \\ 0 & \mathbf{R} \end{bmatrix} v = 0$. $\mathbf{Q}$ and $\mathbf{R}$ are already assumed to be diagonal matrices of constant value hence z is positive definite as $\begin{bmatrix} \mathbf{Q} & 0 \\ 0 & \mathbf{R} \end{bmatrix}$ is positive definite. $z = 0$ when $v = 0$, which contradicts original assumption. Hence $\Delta z(f(x_n(k+1))) \leq -(1-\lambda^2)\left\|v(k)\right\|^2$. Hence, asymptotic stability of the control law is established. Assuming a terminal constraint does not always results in a stable control law as there is a possibility that the active constraints from the terminal-state could cause a linear dependence with other inequality constraints such as constraints on input and output signals. When this happens, the active constraints (including the terminal-state constraints) may not be satisfied. To ensure the stability of the GPC controller, a feedback control has to be defined which must not violate the active constraints defined while solving for the solution of the cost function. It can be observed from the obtained optimal control input is that, the control input is similar to an unconstrained LQR. The optimal control input for defined terminal state is same as the feedback control of LQR.

5.5 Description of operation

Circuit diagram of SIDO DC-DC buck converter is shown in Figure 5.1. A SIDO converter consists of an inductor L, two capacitors C_1 and C_2 , with two output voltages E_{oa} and E_{ob}, where $E_{oa} < E_{ob}$ and one input voltage E_{in}. Input power through the inductor is controlled by switch S_1 and freewheeling diode D. Distribution of power from input to each output is controlled by switches S_a and S_b. Output voltages are regulated by duty ratios D_1, D_a and D_b of switches S_1, S_a and S_b respectively. Operation of the converter duty cycle for different switching cycles are shown in Figure 5.2. To operate SIDO Buck converter in continuous conduc-

tion mode (CCM), D_a+D_b=1 is followed. The parameters of the system under consideration is given in Table 5.1. Assuming ideal case, DC gain of the considered system is obtained by using time averaging equivalent circuit approach [74]. The DC voltage gains and inductor current are formulated as

$$\frac{E_{oa}}{E_{in}} = \frac{D_1(1-D_b)R_1}{D_b^2R_2 + (1-D_b)^2R_1} \tag{5.54}$$

$$\frac{E_{ob}}{E_{in}} = \frac{D_1D_bR_2}{D_b^2R_2 + (1-D_b)^2R_1} \tag{5.55}$$

$$I_L = \frac{E_{oa}}{R_1} + \frac{E_{ob}}{R_2} \tag{5.56}$$

where $0 < D_1 < 1$ and $0 < D_a, D_b < 1$. Steady-state operation of SIDO CCM Buck converter under $D_1 < D_b$ is considered in this chapter. From (5.54) and (5.55) D_1 and D_b are obtained as

$$D_1 = \frac{E_{oa}[D_b^2R_2 + (1-D_b)^2R_1]}{(1-D_b)R_1E_{in}} \tag{5.57}$$

$$D_b = \frac{I_b}{I_a + I_b} \tag{5.58}$$

Table 5.1: Design parameter for the SIDO buck converter [82]

Parameters	Specification	Value
Input voltage	E_{in}	5 V
Reference output voltage 1	E_{r1}	1 V
Reference output voltage 2	E_{r2}	1.5 V
Switching frequency	f_{sw}	100 kHz
Inductor value	L	200 μH
Capacitor value of output 1	C_1	10 μF
Capacitor value of output 2	C_2	10 μF
Load of output 1	R_1	2 Ω
Load of output 1	R_2	3 Ω
Duty ratio of switch S_1	D_1	0.25
Duty ratio of switch S_b	D_b	0.5
Input Power	Pin	5 W

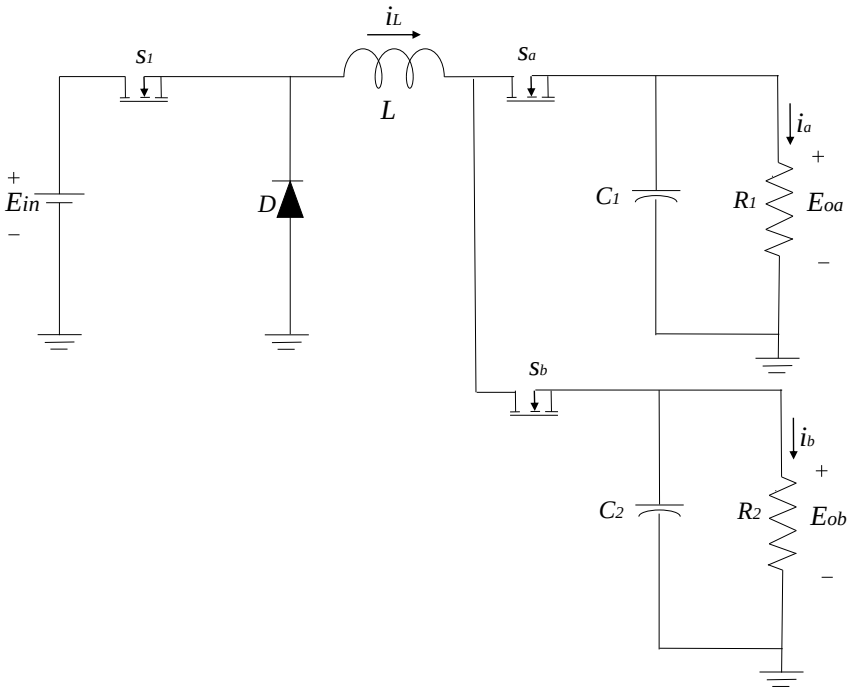

Figure 5.1: Circuit diagram of a SIDO DC-DC buck converter

Mode I:

There are three modes of operation in a switching cycle. In Mode I operation, switches S_1 and S_b are ON, switch S_a and freewheeling diode D are OFF, inductor current increases to a peak value of I_{L1} with a slope of $(E_{in} - E_{ob})/L$. The circuit diagram of this mode is shown in Figure 5.3.

Mode II:

In Mode II operation shown in Figure 5.4, switches S_1 and S_a are OFF, S_b and freewheeling diode D are ON hence inductor current decreases to a value of I_{L2} with a slope of $-E_{ob}/L$.

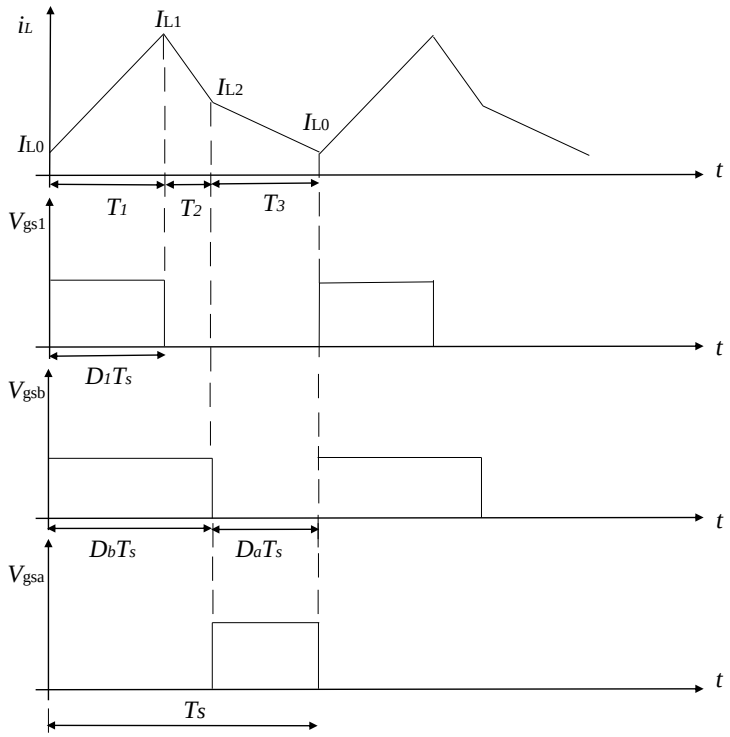

Figure 5.2: Switching cycle of SIDO Buck converter

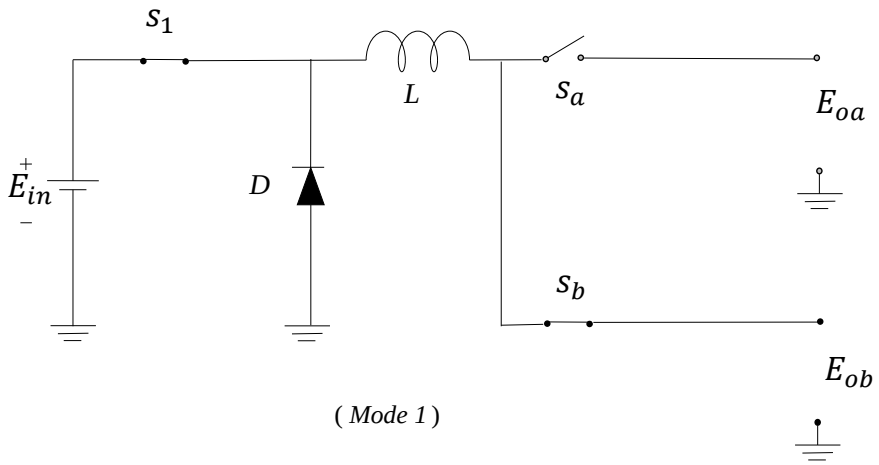

(*Mode 1*)

Figure 5.3: Mode I operation of SIDO Buck converter

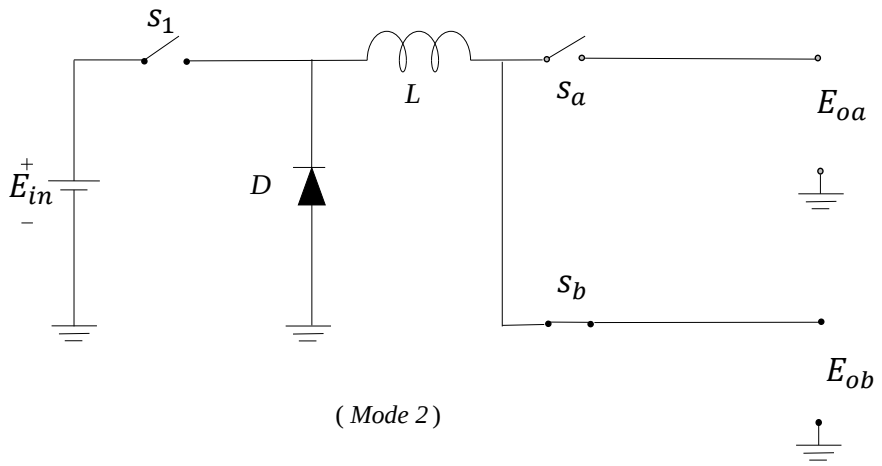

Figure 5.4: Mode II operation of SIDO Buck converter

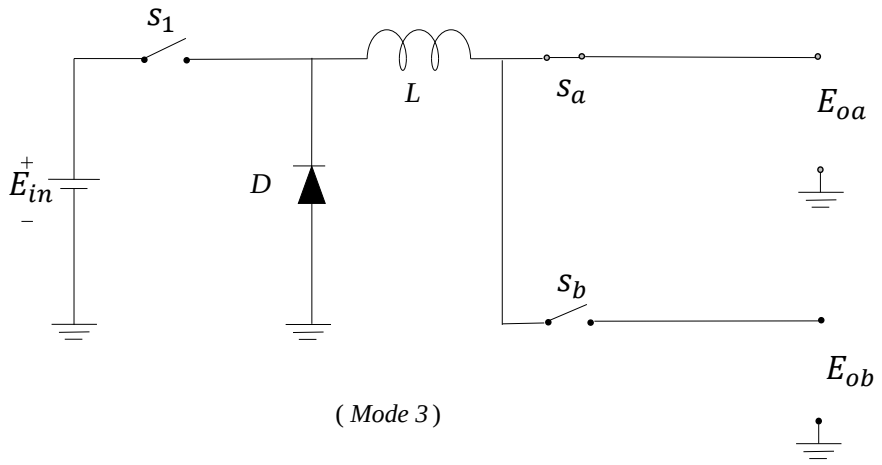

Figure 5.5: Mode III operation of SIDO Buck converter

Mode III:

Similarly, Mode III operation is shown in Figure 5.5, switches S_1 and S_b are operating at OFF state, while switch S_a and freewheeling diode D are ON which results in a decrease in inductor current to a value of I_{Lo} with a slope of $-E_{ob}/L$.

5.5.1 Transfer function matrix of SIDO DC-DC buck converter

Perturbation in duty ratios $\hat{d}_i(s)$ and $\hat{d}_b(s)$ of the SIDO CCM buck converter are chosen as system inputs which are obtained by the controller so that the closed-loop converter output voltage follows the set reference voltage. Similarly, the perturbation in two output voltages $\hat{e}_{oa}$ and $\hat{e}_{ob}(s)$ are chosen as the transfer function matrix outputs. Thus, a SIDO CCM Buck converter can be written as a two-input two-output (TITO) system. Detail derivation of the transfer functions is provided in Appendix A. According to the three modes of operations presented, the transfer functions of duty ratio to control outputs are represented from (5.59) to (5.62).

$$G_{d11}(s) = \frac{\hat{e}_{oa}(s)}{\hat{d}_1(s)} = \frac{E_{in}(1-D_b)R_{e1}(s)}{Z_{eq}} \tag{5.59}$$

$$G_{d12}(s) = \frac{\hat{e}_{ob}(s)}{\hat{d}_b(s)} = \frac{I_L R_{e2}(s)[sL + (1-D_b)R_{e1}(s)] + D_b R_{e2}(s)(E_{oa} - E_{ob})}{Z_{eq}} \tag{5.60}$$

$$G_{d22}(s) = \frac{\hat{e}_{oa}(s)}{\hat{d}_b(s)} = \frac{-I_L R_{e1}(s)[sL + D_b R_{e2}(s)] + (1-D_b)R_{e1}(s)(E_{oa} - E_{ob})}{Z_{eq}} \tag{5.61}$$

$$G_{d21}(s) = \frac{\hat{e}_{ob}(s)}{\hat{d}_1(s)} = \frac{E_{in} D_b R_{e2}(s)}{Z_{eq}} \tag{5.62}$$

where $R_{e1}(s) = 1/(\frac{1}{R_1} + sC_1)$, $R_{e2}(s) = 1/(\frac{1}{R_b} + sC_1)$ and $Z_{eq} = D_b^2 R_{e2}(s) + (1 - D_b)^2 R_{e1}(s) + sL$. E_{r1} and E_{r2} are the reference voltages which are desired to track by using GPC with minimized effect of variation in input and load, when there is a positive and negative step change in the signal. The transfer function matrix for open-loop SIDO buck converter in Figure 5.1 is derived and expressed as in

model (5.63).

$$\begin{bmatrix} \hat{e}_{oa}(s) \\ \hat{e}_{ob}(s) \end{bmatrix} = \begin{bmatrix} G_{d11}(s) & G_{d12}(s) \\ G_{d21}(s) & G_{d22}(s) \end{bmatrix} \begin{bmatrix} \hat{d}_1(s) \\ \hat{d}_b(s) \end{bmatrix} \tag{5.63}$$

5.6 Simulation result

The controller has been implemented and validated using numerical simulation in MATLAB. The transfer function matrix is converted to an augmented state-space model as described. The chosen converter circuit specifications are listed in Table 5.1. Simulation of the plant model has been performed for steady state performance, load variation and performance of the converter for observer based GPC. GPC parameters are chosen as $N = 20, M = 2, \mathbf{Q} = 10I_N, \mathbf{R} = 0.02I_M$, where I_N and I_M denotes identity matrices of appropriate dimension.

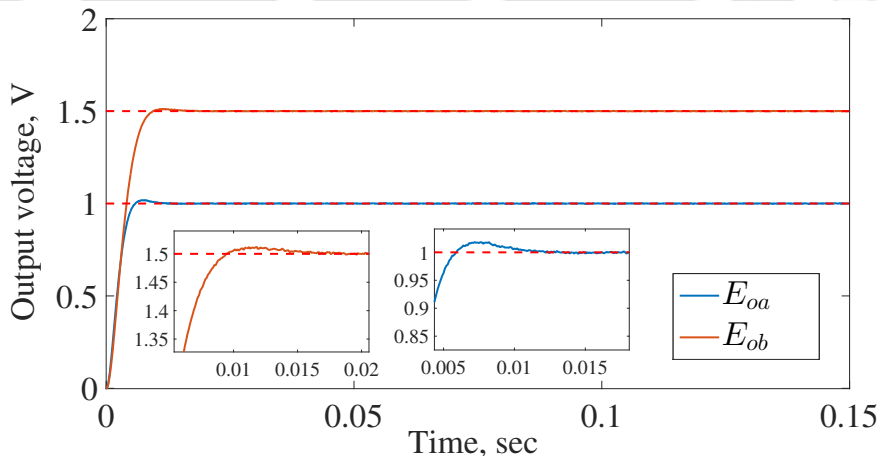

Figure 5.6: Reference tracking by GPC for SIDO buck converter

5.6.1 Steady state performance

Figure 5.6 shows reference tracking of set output voltages by GPC for a SIDO DC-DC buck converter without noise and disturbance. In Figure 5.7 and 5.8 the closed-loop model is simulated for step disturbance signal of magnitude 0.5 and noise signal of $SNR = 48.2\ dB$ for the obtained plant model.

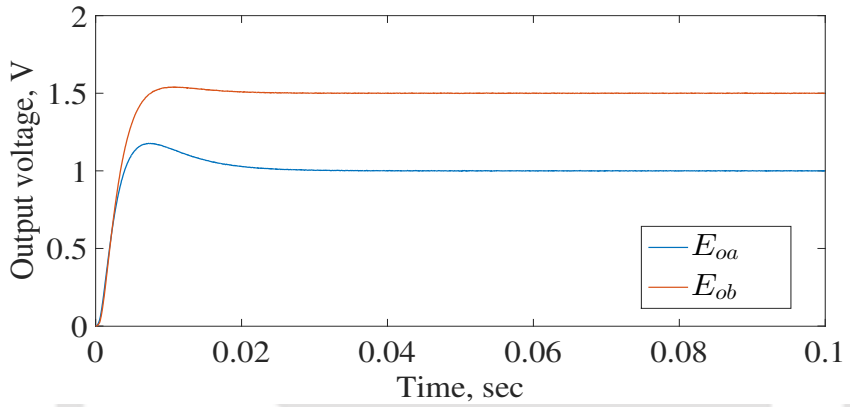

Figure 5.7: Output voltage responses in presence of step disturbance

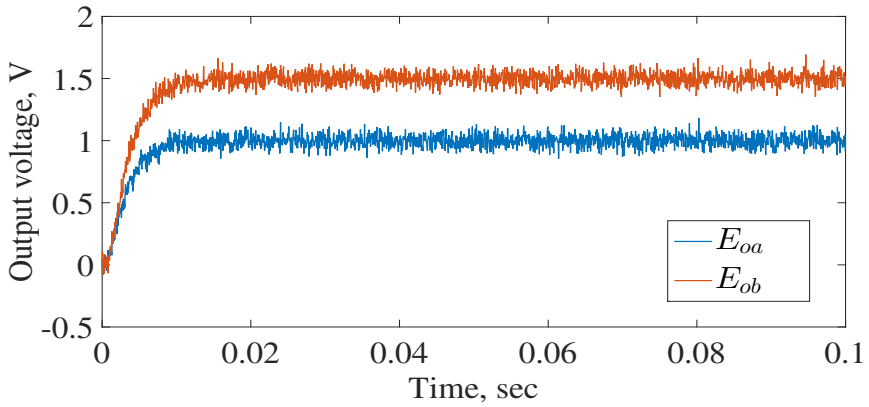

Figure 5.8: Output voltage responses for noisy signal

5.6.2 Performance during load variation

In this section the robustness of the GPC controller with respect to the 50% load variations is varified. The cross-regulation effect for the designed GPC without observer is shown in Figure 5.9 and 5.10. The effect of load variation has been minimized for the SIDO buck converter. Performance index (P. I.) of the controller can be evaluated by using the formula

$$\text{P. I.} = \left(\frac{\text{Overshoot of the observed signal due to load variation}}{\text{Actual voltage}}\right) \times \text{Load variation}(\%) \tag{5.64}$$

The numerical simulation is performed for a 50% load variation. Performance of GPC has been compared with other existing controller design methods for SIDO converter in Table 5.2.

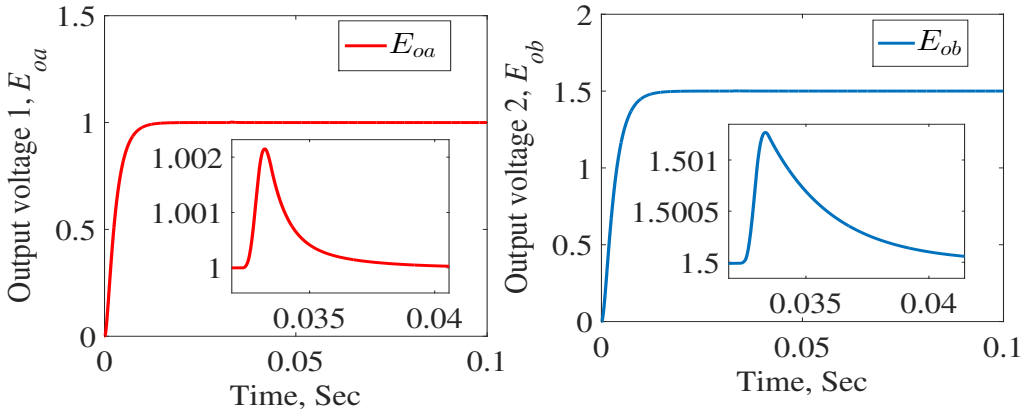

Figure 5.9: Output E_{oa} and E_{ob} responses during load variation at load 1

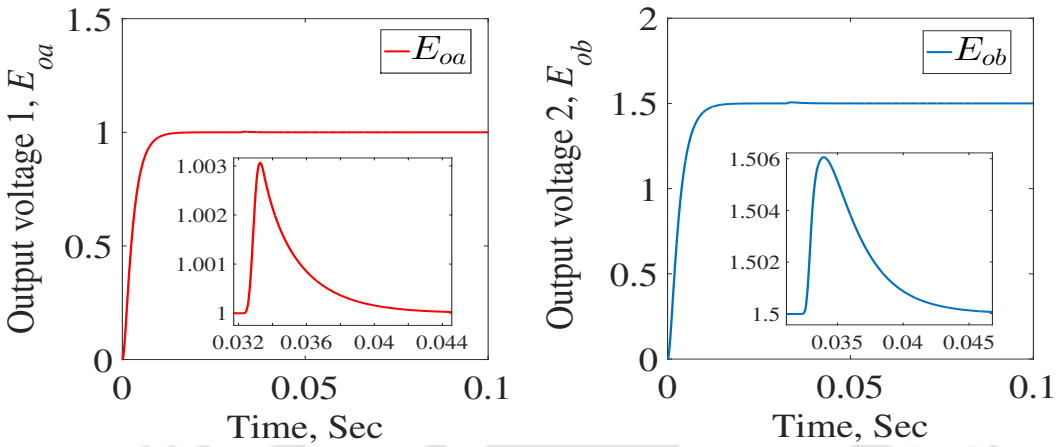

Figure 5.10: Output E_{oa} and E_{ob} responses during load variation at load 2

Table 5.2: Comparison of cross regulation minimization

Parameter	[80]	This work
Control method	FPGA	GPC
Input voltage	5 V	5 V
Output voltage	3.3 V, 2.5 V	1 V, 1.5V
Switching frequency	500kHz	100kHz
Inductor	4 μH	200 μH
Capacitors (C_1, C_2)	10 μF	10 μF
Load R_1	5 Ω	2 Ω
R_2	5 Ω	2 Ω
Settling time	50-100 ms	5-12 ms
P.I. 1 E_{oa}	0.25	0.15
E_{ob}	0.14	0.2
P.I. 2 E_{oa}	0.06	0.1
E_{ob}	0.02	0.03

5.6.3 Performance of the observer

Performance of GPC for reference tracking of set output voltage with and without observer is shown in Figure 5.11. Observer error convergence plot is shown in Figure 5.12. It can be observed from the observer error plot that, observer error is converging at a finite time.

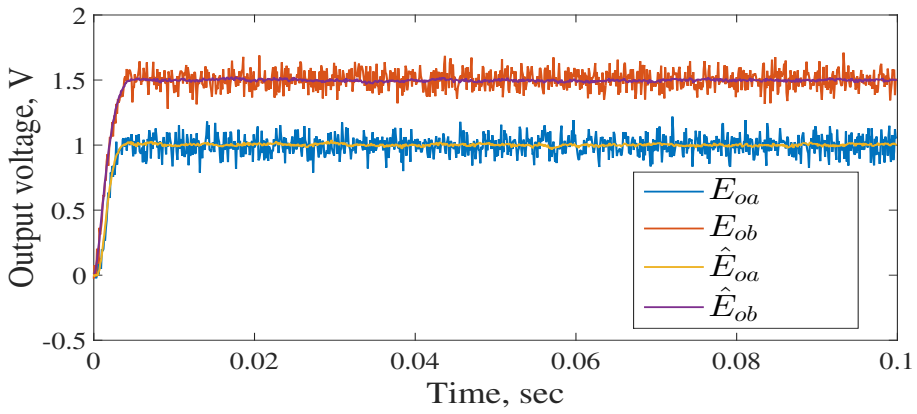

Figure 5.11: Comparison of output voltages E_{oa} and E_{ob} with and without observer design

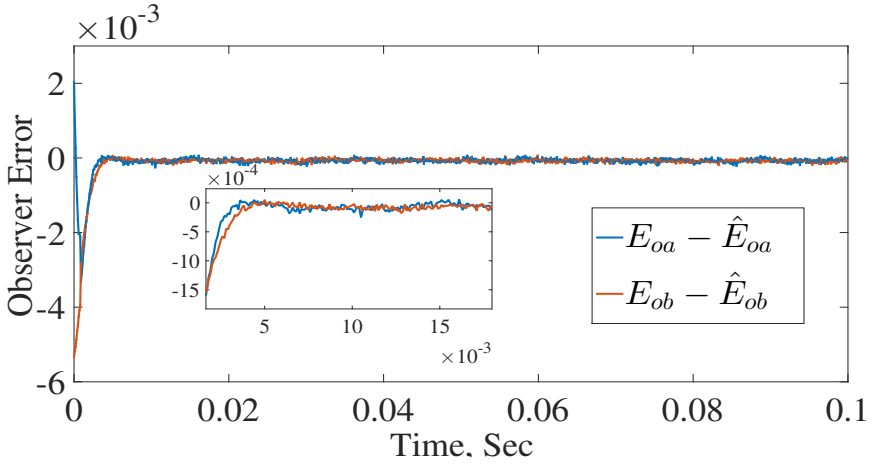

Figure 5.12: Observer estimation error for output reference voltage tracking

5.7 Summary

In this chapter, GPC is designed for a dual output system. Leunburger observer is designed and observer gain can be obtained by using Schur compliment method. Similarly, stability of the control law and convergence of the observer error is also established using Lyapunov function candidate. Controller is designed to minimize the cross regulation during load disturbance in numerical simulation platform using MATLAB. As the main focus is to design the GPC for reference tracking, i.e. the output voltage tracking using VMC and effect of perturbation in output voltage is considered.

CHAPTER 6

CONCLUSION

This thesis has provided a detailed understanding of GPC with the help of hardware embedded implementation and numerical simulation-based examples for GPC. A detailed mathematical preliminary is provided for the formulation of GPC control law. Hopefully, modeling and tuning guideline proposed in this thesis will help the reader in getting a better understanding of the controller. This thesis has laid a foundation for analytical tuning of plant first-order plant models for different types of delayed systems. The derived analytical expression of the tuning guideline is implemented for a SISO DC-DC buck converter system. Novel tuning guidelines for implemented buck converter has been presented in the thesis, which can be modified for boost or buck-boost converter accordingly by approximating to an FOPDT model. Although stability analysis is difficult for a predictive controller because of its complicated derivation of control law, a relatively more straightforward analysis is carried out for this purpose. A Lyapunov stability analysis is done by choosing the cost function of the optimization problem as the Lyapunov function. The overall conclusion of this thesis and recommendations for future work are presented in this chapter.

6.1 Scope for future work

The controller topic presented in this thesis is novel in many fields of research, particularly in power electronics and drives. Hence, various extension work for this research topic is possible.

1. Implementation of GPC by using analytical tuning expression for DC-DC buck converter is a starting point for this domain. This tuning analysis can also be performed for other converter topologies like boost, buck-boost converter or any complex circuit design in future research. As VMC mode of operation is implemented, current mode control (CMC) mode can also be implemented by formulating a current observer for this controller. As the first-order delayed system is taken into consideration to derive a general tuning expression similarly tuning expression for a second-order plant model can also be derived.

2. As optimal control is not a preferred control strategy in case of power converters because of its complicated control law derivation, there is always a resistance towards hardware implementation. So, if a complexity analysis of different controllers concerning the storage and time taken for the processor can be done, it would create much more impact on this domain.

3. There are many cases of plant dynamics available for which a feasible solution of the optimal control does not exist for active constraints. So, this area is not explored in this thesis only simulation results are presented as the plant chosen for implementation does not require constraints instead the main focus was given to the steady-state performance of the closed-loop model. A detailed analysis for active constraints case can be done for GPC to regulate a pre-compensated power converter, which is usually available in ready-made

hardware IC form is also an interesting topic to study further as it is not possible to remove or modified the hardware embedded primal controller. With this strategy, it is possible to improve the performance of the controller without discarding the primal regulator. This aspect is helpful when it is not possible to change the primal controller, and only the reference signal can be steered, or one of the controllers is preferred for lower frequency range and other for higher frequency range. While the stability of the controller has been established in this thesis, uniqueness of GPC control law is still an open topic to be researched.

APPENDIX A

SUPPLEMENTARY FILES

A.1 Small signal modeling of a SIDO buck converter

According to the time averaging equivalent circuit approach, switches S_1 and S_a can be replaced by the controlled voltage sources $\hat{e}_{s1}(s)$ and $\hat{e}_{sa}(s)$, while diode D and switch S_b can be replaced by the controlled current source $\hat{i}_D(s)$ and $\hat{i}_{sb}(s)$. Then the time averaging AC small signal equivalent circuit can be drawn as in A.1, where $\hat{e}_{s1}(s)$, $\hat{e}_{sa}(s)$, $\hat{i}_D(s)$ and $\hat{i}_{sb}(s)$ are given by:

$$\begin{cases} \hat{i}_D(s) = (1 - D_1)\hat{i}_L(s) - \hat{d}_1(s)I_L \\ \hat{e}_{s1}(s) = (1 - D_1)\hat{v}_{in}(s) - \hat{d}_1(s)E_{in} \\ \hat{i}_{sb}(s) = D_b\hat{i}_L(s) - \hat{d}_b(s)I_L \\ \hat{e}_{sa}(s) = D_b(\hat{e}_{oa}(s) - \hat{e}_{ob}(s)) + \hat{d}_b(s)(E_{oa} - E_{ob}) \end{cases} \tag{A.1}$$

From small signal equivalent circuit diagram as shown in Figure A.1, it can be

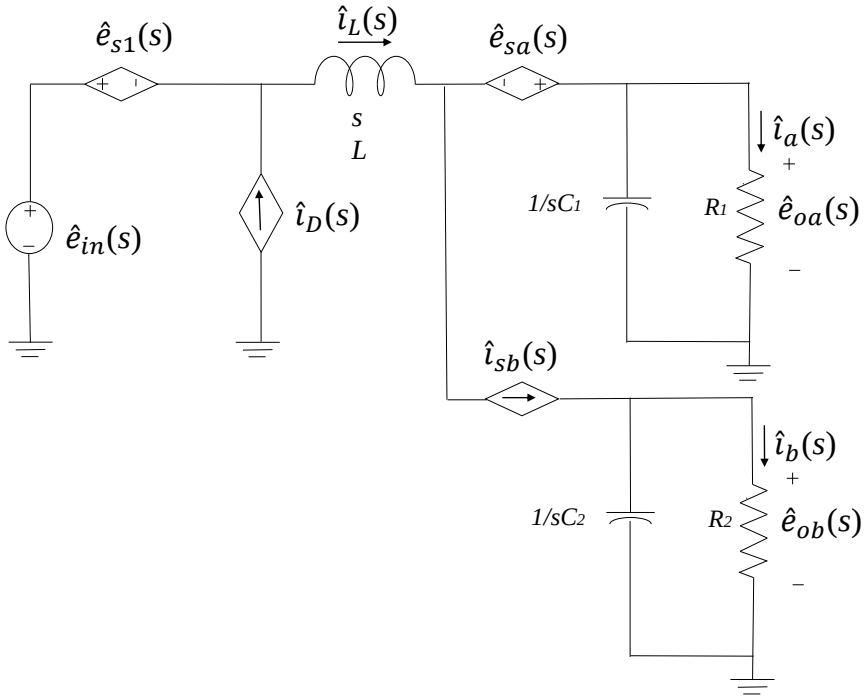

Figure A.1: Small signal equivalent circuit diagram of SIDO Buck converter

written as a small signal disturbance variable of the inductor current $\hat{i}_L(s)$ and input voltage $\hat{e}_{in}(s)$ as,

$$\hat{i}_L(s) = \frac{\hat{e}_{oa}(s)}{R_{e1}(s)} + \frac{\hat{e}_{ob}(s)}{R_{e2}(s)} \tag{A.2}$$

$$\hat{e}_{in}(s) = \hat{e}_{s1}(s) + sL\hat{i}_L(s) - \hat{e}_{sa}(s) + \hat{e}_{oa}(s) \tag{A.3}$$

where $R_{e1}(s) = 1/(\frac{1}{R_1} + sC_1)$ and $R_{e2}(s) = 1/(\frac{1}{R_b} + sC_1)$. Duty ratio control to output transfer functions are written as,

$$G_{d11}(s) = \left.\frac{\hat{e}_{oa}(s)}{\hat{d}_1(s)}\right|_{\hat{e}_{in}(s)=0,\hat{d}_b(s)=0} = \frac{E_{in}(1-D_b)R_{e1}(s)}{D_b^2 R_{e2}(s) + (1-D_b)^2 R_{e1}(s) + sL} \tag{A.4}$$

$$G_{d22}(s) = \left.\frac{\hat{e}_{ob}(s)}{\hat{d}_b(s)}\right|_{\hat{e}_{in}(s)=0,\hat{d}_i(s)=0} = \frac{I_L R_{e2}(s)[sL + (1-D_b)R_{e1}(s)] + D_b R_{e2}(s)(E_{oa} - E_{ob})}{D_b^2 R_{e2}(s) + (1-D_b)^2 R_{e1}(s) + sL} \tag{A.5}$$

As it can be observed from the Figure A.1, the cross regulation transfer functions are represented as,

$$G_{d21}(s) = \left.\frac{\hat{e}_{oa}(s)}{\hat{d}_b(s)}\right|_{\hat{e}_{in}(s)=0,\hat{d}_i(s)=0} = \frac{-I_L R_{e1}(s)[sL + D_b R_{e2}(s)] + (1-D_b)R_{e1}(s)(E_{oa} - E_{ob})}{D_b^2 R_{e2}(s) + (1-D_b)^2 R_{e1}(s) + sL} \tag{A.6}$$

$$G_{d22}(s) = \left.\frac{\hat{e}_{ob}(s)}{\hat{d}_i(s)}\right|_{\hat{e}_{in}(s)=0,\hat{d}_b(s)=0} = \frac{E_{in} D_b R_{e2}(s)}{D_b^2 R_{e2}(s) + (1-D_b)^2 R_{e1}(s) + sL} \tag{A.7}$$

Output current to output voltage transfer functions are written as,

$$Z_{i11}(s) = \left.\frac{\hat{e}_{oa}(s)}{\hat{i}_a(s)}\right|_{\hat{e}_{in}(s)=0,\hat{d}_i(s)=0,\hat{d}_b(s)=0} = \frac{D_b^2 R_{e1}(s)R_{e2}(s) + sLR_{e1}(s)}{D_b^2 R_{e2}(s) + (1-D_b)^2 R_{e1}(s) + sL} \tag{A.8}$$

$$Z_{i22}(s) = \left.\frac{\hat{e}_{ob}(s)}{\hat{i}_b(s)}\right|_{\hat{e}_{in}(s)=0,\hat{d}_i(s)=0,\hat{d}_b(s)=0} = \frac{D_a^2 R_{e1}(s)R_{e2}(s) + sLR_{e2}(s)}{D_b^2 R_{e2}(s) + (1-D_b)^2 R_{e1}(s) + sL} \tag{A.9}$$

The cross coupled transfer function are written as,

$$Z_{i21}(s) = \left.\frac{\hat{e}_{oa}(s)}{\hat{i}_b(s)}\right|_{\hat{e}_{in}(s)=0,\hat{d}_i(s)=0,\hat{d}_b(s)=0} \frac{-D_a D_b^2 R_{e1}(s)R_{e2}(s)}{D_b^2 R_{e2}(s) + (1-D_b)^2 R_{e1}(s) + sL} \tag{A.10}$$

$$Z_{i12}(s) = \left.\frac{\hat{e}_{ob}(s)}{\hat{i}_a(s)}\right|_{\hat{e}_{in}(s)=0,\hat{d}_i(s)=0,\hat{d}_b(s)=0} \frac{-D_a D_b^2 R_{e1}(s)R_{e2}(s)}{D_b^2 R_{e2}(s) + (1-D_b)^2 R_{e1}(s) + sL} \tag{A.11}$$

A.2 Jury's stability criteria [65]

Suppose a closed-loop transfer function is represented in a discrete time domain as

$$G(z) = \frac{C(z)}{1 + C(z)R(z)} = \frac{N(z)}{D(z)} \tag{A.12}$$

The closed-loop system is stable if all poles of the system lie inside the unit circle in a z - domain. The poles are defined as the roots of the the polynomial $D(z)$. Jury's stability criteria [65] is similar to Routh-Hurwitz stability criteria in continuous time domain, where a Routh table is prepared and from the elements of the table stability of the closed-loop system is determined. Similarly, for n order polynomial, characteristic polynomial is expressed as

$$D(z) = d_n z^n + d_{n-1} z^{n-1} + \cdots + d_2 Z^2 + d_1 z + d_0 \tag{A.13}$$

Following assumptions are made before proceeding for the Jury's table formation

1. Coefficients of polynomial $D(z)$ are all real numbers.
2. $d_n > 0$; which means degree of the polynomial is n.
3. $d_0 \neq 0$; which states that the polynomial does not have a root at the origin.
4. There are no roots on the unit circle for polynomial $D(z)$.

Table A.1: Jury's stability array

z^0	z^1	z^2	...	z^{n-1}	z^n
d_0	d_1	d_2	...	d_{n-1}	d_n
d_n	d_{n-1}	d_{n-2}	...	d_1	d_0
a_0	a_1	a_2	...	a_{n-1}	
a_{n-1}	a_{n-2}	a_{n-3}	...	a_0	
b_0	b_1	b_2	...	b_{n-2}	
b_{n-2}	b_{n-3}	b_{n-4}	...	b_0	
...	...	...	...		
...	...	...	...		
p_0	p_1	p_2			

where the elements of the odd numbered rows are reversed in even numbered rows. The elements of odd numbered rows are evaluated as

$$a_k = \begin{vmatrix} d_0 & d_{n-k} \\ d_n & d_k \end{vmatrix}, b_k = \begin{vmatrix} a_0 & d_{n-k-1} \\ d_{n-1} & d_k \end{vmatrix}, \ldots$$

For all the roots to lie inside the unit circle, necessary and sufficient conditions are given as

$$D(1) \geq 0; \tag{A.14}$$

$$(-1)^n D(-1) \geq 0; \tag{A.15}$$

$$|d_0| \leq d_n; \tag{A.16}$$

$$|a_0| \geq a_{n-1}; \tag{A.17}$$

$$|b_0| \leq b_{n-2}; \tag{A.18}$$

$$\vdots \tag{A.19}$$

$$|p_0| \leq p_2 \tag{A.20}$$

A.3 Property of symmetric positive definite matrix using Schur's compliment [84]

For a square matrix A defined in the form

$$\begin{bmatrix} X & Y \\ Y^T & Z \end{bmatrix} \tag{A.21}$$

where $X \in \mathbb{R}^{p\times p}$ and $Y \in \mathbb{R}^{p\times q}$ are symmetric matrices and $Z \in \mathbb{R}^{q\times q}$, the matrix A is positive definite when

$$Z > 0 \quad \text{and} \quad X - YZ^{-1}Y^T > 0 \tag{A.22}$$

$$X > 0 \quad \text{and} \quad Z - Y^T X^{-1} Y > 0 \tag{A.23}$$

Publications from this Thesis

Journal paper

- **K. Manjari** , S. Majhi and Kasi V. Ramana,"A Pre-Computed Generalized Predictive Control of DC-DC Buck Converter", *IET Circuits, Devices and Systems* , vol. 14, no. 1, pp. 41–47, 2019.

Book chapter

- **K. Manjari** and S. Majhi, "Reference Tracking by Designing State Estimation Observer for Generalized Predictive Control of a Single Inductor Dual Output Buck Converter", September 2021.

Conference paper

- **K. Manjari** and S. Majhi, " Model Predictive Control of Single-Inductor Dual-Output Buck Converter", in *Proceedings of International Conference on Power Electronics, Drives and Energy Systems (PEDES)*, pp. 1-6, Chennai, India, 18-21 December, 2018.

- **K. Manjari** and S. Majhi ,"Generalized Predictive Control Tuning for Desired Frequency Domain Specification", in *Proceedings of IEEE Region 10 Conference (TENCON)*, pp. 2245-2250, Kochi, India, 17-20 October, 2019.

- **K Manjari** and S. Majhi, " Generalized Predictive Control of Pre-Compensated DC-DC Buck Converter", *International Conference on Power Electronics, Drives and Energy Systems (PEDES)*, Jaipur, India, 16-19 December 2020.

Bibliography

[1] E. F. Camacho and C. Bordons, *Model Predictive Control*. Springer Science and Business Media, London, 2013.

[2] S. J. Qin and T. A. Badgwell, "A Survey of Industrial Model Predictive Control Technology," *Control Engineering Practice*, vol. 11, no. 7, pp. 733–764, 2003.

[3] C. Bordons, and E. F. Camacho, "A Generalized Predictive Controller for a Wide Class of Industrial Processes, " *IEEE Transactions on Control Systems Technology*, vol. 6, no. 3, pp. 372–387, 1998.

[4] D. W. Clarke, "Application of Generalized Predictive Control to Industrial Processes," *IEEE Control Systems Magazine*, vol. 8, no. 2, pp. 49–55, 1988.

[5] L. Zadeh and B. Whalen, "On Optimal Control and Linear Programming," *IRE Transactions on Automatic Control*, vol. 7, no. 4, pp. 45–46, 1962.

[6] A. Propoi, "Use of Linear Programming Methods for Synthesizing Sampled Data Automatic Systems," *Automation and Remote Control*, vol. 24, no. 7, pp. 837–844, 1963.

[7] E. G. Cho, K. A. Thoney, T. J. Hodgson, and R. E. King, "Supply Chain Planning: Rolling Horizon Scheduling of Multi-factory Supply Chains," in *Proceedings of Conference on Winter Simulation: Driving Innovation*, pp. 1409–1416, New Orleans, LA, USA, 7-10 December, 2003.

[8] R. Franz, M. Milam, and J. Hauser, "Applied Receding Horizon Control of The Caltech Ducted Fan," in *Proceedings of American Control Conference,* pp. 3735–3740, Anchorage, AK, USA, 8-10 May, 2002.

[9] M. J. West, C. M. Bingham, and N. Schofield, "Predictive Control for Energy Management in All/More Electric Vehicles with Multiple Energy Storage Units," in *Proceedings of IEEE International Electric Machines and Drives Conference,* pp. 222–228, Madison, WI, 1-4 June, 2003.

[10] G. Stewart and F. Borrelli, "A Model Predictive Control Framework for Industrial Turbo Diesel Engine Control" in *Proceedings of IEEE Conference on Decision and Control,* pp. 5704–5711, Cancun, Mexico, 9-11 December, 2008.

[11] S. Di Cairano, D. Yanakiev, A. Bemporad, I. V. Kolmanovsky, and D. Hrovat,"An MPC Design Flow for Automotive Control and Applications to Idle Speed Regulation," in *Proceedings of IEEE Conference on Decision and Control,* pp. 5686–5691, Cancun, Mexico, 9-11 December, 2008.

[12] P. Falcone, F. Borrelli, J. Asgari, E. H. Tseng, and D. Hrovat, "Predictive Active Steering Control for Autonomous Vehicle Systems," *IEEE Transaction on Control Systems Technology,* vol. 15, no. 3, pp. 566–580, 2007.

[13] J. Rodriguez and P. Cortes, *Predictive Control of Power Converters and Electrical Drives.* John Wiley and Sons, 2012.

[14] S. Kouro, P. Cortés, R. Vargas , U. Ammann , J. Rodríguez, " Model Predictive Control - A Simple and Powerful Method to Control Power Converters," *IEEE Transactions on Industrial Electronics*, vol. 56, no. 6, pp. 1826–38, 2008.

[15] D. Q. Mayne, J. B. Rawlings, C. V. Rao, and P. O. Scokaert, "Constrained Model Predictive Control: Stability and Optimality," *Automatica*, vol. 6, no. 6, pp. 789–814, 2000.

[16] W. H. Kwon, A. Bruckstein, and T. Kailath, "Stabilizing State-Feedback Design via The Moving Horizon Method," *International Journal of Control*, vol. 37, no. 3, pp. 631–643, 1983.

[17] S. Boyd, S. P. Boyd, and L. Vandenberghe, *Convex Optimization*. Cambridge university press, 2004.

[18] A. Bemporad, A. Casavola, and E. Mosca, " Nonlinear Control of Constrained Linear Systems via Predictive Reference Management," *IEEE Transactions on Automatic Control*, vol. 42, no. 3, pp. 340–349, 1997.

[19] D. Limon, A. Ferramosca, , I. Alvarado, and T. Alamo, " Nonlinear MPC for Tracking Piece-wise Constant Reference Signals," *IEEE Transactions on Automatic Control*, vol. 63, no. 11, pp. 3735-3750, 2018.

[20] J. Lee, W. Cho, and T. F. Edgar,"Multiloop PI Controller Tuning for Interacting Multivariable Processes," *Computers and Chemical Engineering,* vol. 22, no. 11, pp. 1711–1723, 1998.

[21] L. Rundqwist, "Anti-reset Windup for PID Controllers," in *IFAC Proceedings Volumes,* vol. 23, no. 8, pp. 453–458, 1990.

[22] L. S. Pontryagin, *Mathematical Theory of Optimal Processes*. Routledge, 2018.

[23] A. Bemporad, M. Morari, V. Dua, and E. N. Pistikopoulos,"The Explicit Linear Quadratic Regulator for Constrained Systems," *Automatica,* vol. 38, no. 1, pp. 3–20, 2002.

[24] C. R. Cutler and D. L. Ramaker, "Dynamic Matrix Control – A Computer Control Algorithm," in *Proceedings of Joint Automatic Control Conference*, San Francisco, USA, 13-15 August, 1980.

[25] J. Richalet, ,A. Rault, J. L. Testud, and J. Papon, "Model Predictive Heuristic Control," *Automatica* , vol. 14, no. 5, pp. 413–428, 1978.

[26] R. Rouhani and R. K. Mehra, "Model Algorithmic Control (MAC); Basic Theoretical Properties," *Automatica*, vol. 18, no. 4, pp. 401–414, 1982.

[27] D. W. Clarke, C. Mohtadi, and P. Tuffs, "Generalized Predictive Control - Part I. The Basic Algorithm," *Automatica*, vol. 23, no. 2, pp. 137–148, 1987.

[28] ——, "Generalized Predictive Control - Part II. Extensions and Interpretations," *Automatica*, vol. 23, no. 2, pp. 149–160, 1987.

[29] D. W. Clarke and P. J. Gawthrop, "Self-Tuning Controller," in *Proceedings of the Institution of Electrical Engineers*, vol. 122, pp. 929–934, 1975.

[30] W. K. Ho, C. C. Hang, and L. S. Cao, "Tuning of PID Controllers Based on Gain and Phase Margin Specifications," *Automatica,* vol. 31, no. 3, pp. 497–502, 1995.

[31] J. L. Garriga and M. Soroush, "Model Predictive Control Tuning Methods: A Review," *Industrial and Engineering Chemistry Research*, vol. 49, no. 8, pp. 3505–3515, 2010.

[32] R. Shridhar and D. J. Cooper, "A Tuning Strategy for Unconstrained SISO Model Predictive Control," *Industrial and Engineering Chemistry Research*, vol. 36, no. 3, pp. 729–746, 1997.

[33] ——, "A Tuning Strategy for Unconstrained Multi-Variable Model Predictive Control," *Industrial and Engineering Chemistry Research*, vol. 37, no. 10, pp. 4003–4016, 1998.

[34] A. R. Mcintosh, S. L. Shah, and D. G. Fisher, "Selection of Tuning Parameters for Adaptive Generalized Predictive Control," in *Proceedings of American Control Conference,* pp. 1846–1851, Pittsburgh, PA, USA, 21-23 June, 1989.

[35] ——, "Analysis and Tuning of Adaptive Generalized Predictive Control," *The Canadian Journal of Chemical Engineering*, vol. 69, no. 1, pp. 97–110, 1991.

[36] S. Di Cairano and A. Bemporad, "Model Predictive Control Tuning by Controller Matching," *IEEE Transactions on Automatic Control*, vol. 55, no. 1, pp. 185–190, 2009.

[37] E. N. Hartley and J. M. Maciejowski, "Designing Output-Feedback Predictive Controllers by Reverse Engineering Existing LTI Controllers," *IEEE Transactions on Automatic Control*, vol. 58, no. 11, pp. 2934–2939, 2013.

[38] Q. N. Tran, L. Özkan, and A. Backx, "Generalized Predictive Control Tuning by Controller Matching," *Journal of Process Control*, vol. 25, pp. 1–18, 2015.

[39] K. Tan, S. Huang, and T. Lee, "Development of a GPC Based PID Controller for Unstable Systems with Deadtime," *ISA Transactions*, vol. 39, no. 1, pp. 57–70, 2000.

[40] A. Ferramosca, D. Limón, I. Alvarado, T. Alamo, and E. F. Camacho, "MPC for Tracking with Optimal Closed-loop Performance," in *Proceedings of IEEE Conference on Decision and Control,* pp. 4055–4060, Cancun, Mexico, 9-11 December, 2008.

[41] W. H. Kwon, Y. I. Lee, and S. Noh, "Partition of GPC into A State Observer and A State Feedback Controller," in *Proceedings of American Control Conference,* pp. 2032–2036, Chicago, IL, USA, 24-26 June, 1992.

[42] D. Limón, T. Alamo, F. Salas, and E. F. Camacho, "Input to State Stability of Min–Max MPC Controllers for Nonlinear Systems with Bounded Uncertainties," *Automatica*, vol. 42, no. 5, pp. 797–803, 2006.

[43] D. Limón, T. Alamo, and E. Camacho, "Stable Constrained MPC without Terminal Constraint," in *Proceedings of American Control Conference,* pp. 4893–4898, Denver, CO, USA, 4-6 June, 2003.

[44] B. Picasso, D. Desiderio, and R. Scattolini, "Robust Stability Snalysis of Nonlinear Discrete Time Systems with Application to MPC," *IEEE Transactions on Automatic Control*, vol. 57, no. 1, pp. 185–191, 2011.

[45] X. Chen, M. Heidarinejad, J. Liu, and P. D. Christofides, "Composite Fast-slow MPC Design for Nonlinear Singularly Perturbed Systems: Stability Analysis," in *Proceedings of American Control Conference,* pp. 4136–4141, Montreal, Canada, 27-29 June, 2012.

[46] D. Limón, T. Alamo, F. Salas, and E. F. Camacho, "On the Stability of Constrained MPC Without Terminal Constraint," *IEEE Transactions on Automatic Control*, vol. 51, no. 5, pp. 832–836, 2006.

[47] A.-L. Elshafei, G. Dumont, and A. Elnaggar, "Perturbation Analysis of GPC with One-step Control Horizon," *Automatica*, vol. 27, no. 4, pp. 725–728, 1991.

[48] D. Q. Mayne, "Model Predictive Control: Recent Developments and Future Promise," *Automatica,* vol. 50, no. 12, pp. 2967–2986, 2014.

[49] J. Richalet, A. Rault, J. L. Testud, and J. Papon, "Model Predictive Heuristic Control," *Automatica* , vol. 14, no. 5, pp. 413–428, 1978.

[50] R. M. C. De Keyser and A. R. Van Cauwenberghe, "Extended Prediction Self-Adaptive Control," in *Proceedings of 7th IFAC Symposium on Identification and System Parameter Estimation*, York, UK, 3-7 July, 1985.

[51] J. Richalet, S. A. el Ata-Doss, C. Arber, H. B. Kuntze, A. Jacubasch, and W. Schill, " Predictive Functional Control - Application to Fast and Accurate Robots," in *Proceedings of 10th Triennial IFAC Congress on Automatic Control*, Munich, Germany, 27-31 July, 1987.

[52] J. M. Lemos and E. Mosca, "A Multipredictor-Based LQ Self-Tuning Controller,"in *Proceedings of 7th IFAC Symposium on Identification and System Parameter Estimation*, York, UK, 3-7 July, 1985

[53] Q. Bi, W. J. Cai, E. L. Lee, Q. G. Wang, C. C. Hang, and Y. Zhang, "Robust Identification of First-Order Plus Dead Time Model from Step Response," *Control Engineering Practice*, vol. 7, no. 1, pp. 71–77, 1999.

[54] K. Y. Rani and H. Unbehauen, "Study of Predictive Controller Tuning Methods,"*Automatica*, vol. 33, no. 12, pp. 2243–2248, 1997.

[55] C. Rowe and J. Maciejowski, "Tuning Robust Model Predictive Controllers using LQG/LTR," in *Proceedings of 14th IFAC World Congress*, pp. 1231-1236, Beijing, Chia, 5-9 July, 1999.

[56] ——, "Tuning MPC Using H_∞ Loop Shaping," in *Proceedings of American Control Conference*, pp. 1332–1336, Chicago, Illinois, USA, 28-30 June, 2000.

[57] W. Wojsznis, J. Gudaz, T. Blevins, and A. Mehta, "Practical Approach to Tuning MPC," *ISA Transactions*, vol. 42, no. 1, pp. 149–162, 2003.

[58] A. Neshasteriz, A. K. Sedigh, and H. Sadjadian, "Generalized Predictive Control and Tuning of Industrial Processes with Second-Order Plus Dead Time Models," *Journal of Process Control*, vol. 20, no. 1, pp. 63–72, 2010.

[59] P. Bagheri and A. Khaki-Sedigh, " Tuning of Dynamic Matrix Controller for FOPDT Models Using Analysis of Variance," in *Proceedings of 18th IFAC World Congress*, pp. 12319–12324, Milano, Italy, 28 August- 02 September, 2011.

[60] J. Lee and Z. Yu, "Tuning of Model Predictive Controllers for Robust Performance," *Computers and Chemical Engineering*, vol. 18, no. 1, pp. 15–37, 1994.

[61] G. Shah and S. Engell, "Tuning MPC for Desired Closed-Loop Performance for MIMO Systems," in *Proceedings of American Control Conference*, pp. 11331–11336, San Francisco, California, USA, 29 June - 01 July, 2011.

[62] A. Al Ghazzawi, E. Ali, A. Nouh, and E. Zafiriou, "On-Line Tuning Strategy for Model Predictive Controllers," *Journal of Process Control*, vol. 11, no. 3, pp. 265–284, 2001.

[63] J. Maciejowski, "Reverse Engineering Existing Controllers for MPC Design," in *Proceedings of 3rd IFAC Symposium on System Structure and Control*, pp. 436–441, Foz de Iguassu, Brazil, 17-19 October, 2007.

[64] E. N. Hartley and J. M. Maciejowski, "Initial Tuning of Predictive Controllers by Reverse Engineering," in *Proceedings of European Control Conference*, pp. 725–730, Budapest, Hungary, 23-26 August, 2009.

[65] E. I. Jury, *Theory and Application of the z-Transform Method,* John Wiley and Sons, New York, 1964.

[66] R. Cordero, T. Estrabis, E. A. Batista, C. Q. Andrea, and G. Gentil, "Ramp-Tracking Generalized Predictive Control System based on Second-Order Difference," *IEEE Trans-*

actions on Circuits and Systems II: Express Briefs, (Early Access) doi: 10.1109/TCSII.2020.3019028.

[67] S. Kouro, M. Perez, J. Rodriguez, A. Llor, and H. Young, "Model Predictive Control: MPC's Role in The Evolution of Power Electronics," *IEEE Industrial Electronics Magazine*, vol. 9, no. 4, pp. 8–21, 2015.

[68] C. Olalla, R. Leyva, A. El Aroudi and I. Queinnec, "Robust LQR Control for PWM Converters: An LMI Approach," *IEEE Transactions on Industrial Electronics*, vol. 56, no. 7, pp. 2548–2558, 2009.

[69] S. Vazquez, J. Leon, L. Franquelo, J. Rodriguez, H. Young, A. Marquez, and P. Zanchetta, "Model Predictive Control: A Review of Its Applications in Power Electronics," *IEEE Industrial Electronics Magazine*, vol. 8, no. 1, pp. 16–31, 2014.

[70] C. Bordons and C. Montero, "Basic Principles of MPC for Power Converters: Bridging the Gap Between Theory and Practice," *IEEE Industrial Electronics Magazine*, vol. 9, no. 3, pp. 31–43, 2015.

[71] K. V. Ramana, S. Majhi, and A. K. Gogoi, "Modeling and Estimation of DC–DC Buck Converter Dynamics Using Relay Feedback Output with Performance Evaluation," *IEEE Transactions on Circuits and Systems II: Express Briefs*, vol. 66, no. 3, pp. 427–431, 2018.

[72] D. Kwon and G. A. Rincon-Mora, "Single-Inductor Multiple-Output Switching DC-DC Converters," *IEEE Transactions on Circuits and Systems II: Express Briefs*, vol. 56, no. 8, pp. 614–618, 2009.

[73] K. -Y. Lin, C. -S. Huang, D. Chen, and K. H. Liu, "Modeling and Design of Feedback Loops for a Voltage Mode Single-Inductor Dual-Output Buck Converter," in *IEEE Power Electronics Specialists Conference,* Jun. 2008, pp. 3389–3395.

[74] C. Huang, D. Chen, C. Chen and K. H. Liu, "Mix-Voltage Conversion for Single-Inductor Dual-Output Buck Converters," *IEEE Transactions on Industrial Electronics*, vol. 25, no. 8, pp. 2106-2114, Aug. 2010

[75] J. Scoltock, T. Geyer, and U. K. Madawala, "Model Predictive Direct Power Control for Grid-Connected NPC Converters," *IEEE Transactions on Industrial Electronics*, vol. 62, no. 9, pp. 5319–5328, 2015.

[76] R. J. Wai and K. H. Jheng, "High Efficiency Single-Inductor Multiple-Output DC-DC Converter," *IEEE Transactions on Power Electronics*, vol. 28, no. 2, pp. 886-898, 2012.

[77] B. F. Wang, V. R. K. Kanamarlapudi, L. Xian, X. Y. Peng, K. T. Tan, and P. L. So, "Model Predictive Voltage Control for Single-Inductor Multiple-Output DC-DC Converter with Reduced Cross Regulation," *IEEE Transactions on Industrial Electronics*, vol. 63, no. 7, pp. 4187–4196, Jul. 2016.

[78] P. Patra, J. Ghosh, and A. Patra, "Control Scheme for Reduced Cross Regulation in Single-Inductor Multiple-Output DC-DC Converters," *IEEE Transactions on Industrial Electronics*, vol. 60, no. 11, pp. 5095–5104, Nov. 2013.

[79] D. Ma, W. -H. Ki, C. -Y. Tusi, and P. Mok, "Single-Inductor Multiple-Output Switching Converters with Time-Multiplexing Control in Discontinuous mode," *IEEE Journal of Solid-State Circuits*, vol. 38, no. 1, pp. 89–100, 2003.

[80] A. Pizzutelli and M. Ghioni, "Novel Control Technique for Single-Inductor Multiple-Output Converters Operating in CCM with Reduced Cross regulation," in *Proceedings of 23rd Annual IEEE Applied Power Electronics Conference and Exposition*, pp. 1502-1507, Austin, TX, USA, 24-28 February, 2008.

[81] Z. Shen, X. Chang, W. Wang, X. Tan, N. Yan, and H. Min, "Predictive Digital Current Control of Single-Inductor Multiple-Output Converters in CCM with Low Cross Regulation," *IEEE Transactions on Power Electronics*, vol. 27, no. 4, pp. 1917–1925, 2012.

[82] J. D. Dasika, B. Bahrani, M. Saeedifard, A. Karimi and A. Rufer, "Multi-Variable Control of Single-Inductor Dual-Output Buck Converters," *IEEE Transactions on Power Electronics*, vol. 29, no. 4, pp. 2061–2070, 2014.

[83] D. G. Luenberger, "An Introduction to Observers", *IEEE Transactions on Automatic Control*, vol. 16, no. 6, pp. 596-602, 1971.

[84] J. Gallier,"The Schur Complement and Symmetric Positive Semidefinite (and Definite) Matrices", *Penn Engineering*, 2019.